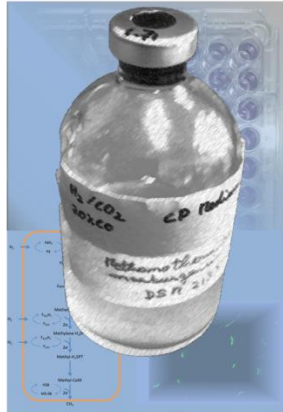




**TÉCNICO**  
LISBOA



# **Adaptation Studies and Proteomic Analysis of Carboxidotrophic Methanogens**

Ricardo Afonso Gonçalves Pereira

Thesis to obtain the Master of Science Degree in

## **Biological Engineering**

Supervisors: Prof. Diana Zita Machado de Sousa

Prof. Miguel Nobre Parreira Cacho Teixeira

## **Examination Committee**

Chairperson: Prof. Arsénio do Carmo Sales Mendes Fialho

Supervisor: Prof. Miguel Nobre Parreira Cacho Teixeira

Members of the Committee: Prof. Nuno Gonçalo Pereira Mira

**December 2014**



## Abstract

Carbon monoxide (CO) is generated by a variety of natural and anthropogenic processes. Nevertheless, CO is only present at trace amounts in the atmosphere, which is partly due to its utilisation by a wide range of diverse prokaryotes, both aerobic and anaerobic. Organisms able to autotrophically grow on CO, i.e. to use CO as carbon and electron source, are designated carboxydotrophs. Anaerobic carboxydotrophs are particularly interesting for biotechnological applications because they can produce added-value compounds, such as hydrogen, methane, fatty-acids and alcohols. CO is one of the main compounds of synthesis gas (or syngas) - product resulting from the gasification of carbonaceous sources (e.g. lignocellulosic biomass and wastes). In this way, syngas can be used by carboxydotrophs as a sustainable source for the production of chemicals and/or biofuels.

The present thesis focused on the study of methanogens for the production of methane from CO and CO/H<sub>2</sub> mixtures as sole substrate/electron donor. Several methanogenic species were tested for their ability to metabolise CO and/or CO/H<sub>2</sub> and the mechanisms and requirements for CO tolerance and oxidation were studied. The physiological response of these archaea to the presence of CO was detailed and the previously unreported carboxidotrophic ability for *Methanothermobacter marburgensis* was demonstrated. Furthermore, proteomic analysis of the CO-metabolizing capability of this organism was performed.

**Keywords:** Carbon Monoxide; Synthesis Gas; Methanogenesis; Adaptation; Proteomics; *Methanothermobacter marburgensis*

## Resumo

O monóxido de carbono (CO) é produzido por uma variedade de processos naturais e antropogénicos, estando, no entanto, presente em quantidades vestigiais na atmosfera, o que é em parte devido à sua utilização por uma ampla gama de diversos procariontes, tanto aeróbios como anaeróbios. Os organismos capazes de crescer autotroficamente em CO, *i.e.* de usá-lo como fonte de carbono e electrões, são designados carboxidotróficos. Os carboxidotróficos anaeróbios possuem especial interesse em aplicações biotecnológicas devido ao seu potencial de produção de compostos com valor acrescentado, tais como hidrogénio, metano, ácidos gordos e álcoois. O CO é um dos principais compostos do gás de síntese (ou syngas) - produto resultante da gasificação de fontes carboníferas (e.g. biomassa lignocelulósica e resíduos) e, deste modo, pode ser usado por carboxidotróficos como uma fonte sustentável para a produção de químicos e/ou biocombustíveis.

O foco da presente tese é o estudo de metanogénicos para a produção de metano a partir de CO e misturas de CO/H<sub>2</sub> como único substrato/dador de electrões. Várias espécies metanogénicas foram testadas quanto à sua capacidade de metabolizar CO e/ou CO/H<sub>2</sub> e os mecanismos e requisitos necessários à tolerância e oxidação de CO foram também estudados. A resposta fisiológica destes archaea à presença de CO foi detalhada e foi pela primeira vez demonstrada a capacidade carboxidotrófica de *Methanothermobacter marburgensis*. Além disso, foi efetuada a análise proteómica da capacidade metabolizante de CO deste organismo.

**Palavras-Chave:** Monóxido de Carbono; Gas de Síntese; Metanogénese; Adaptação; Proteómica; *Methanothermobacter marburgensis*

## Aknowledgements

First and foremost I'd like to offer my gratitude to Prof. Diana Sousa and Prof. Fons Stans for giving me the opportunity to perform this work at the Microbial Physiology group in the Microbiology Department of Wageningen University. Their invaluable guidance tempered by the willingness to allow me to venture out on my own, made for a great learning experience. I'd particularly like to thank Diana for her kind words and incentive in the rougher moments of my stay.

I'd also like to give a special acknowledgement to Ana Luísa Pereira who patiently taught me the basics of anaerobic culturing and shared a lot of great moments in the lab in the first few months.

Other special thanks go to the ever present technicians, particularly Ton van Gelder, whose teachings and concern for my safety at all times I will not forget.

In my office I had a wonderful environment of support and friendship in Ahmad Khadem, Anna Florentino, Lara Paulo and Vicente Nunez. Thank you for all for your sage advice and friendship. As we would say: "thanks for listening".

I also cannot forget the wonderful talks (scientific and otherwise) with my co-workers. Particularly Irene Sanchez-Andrea, Peer Timmers, Michael Visser and Martijn Diender were always available to discuss my scientific troubles which I appreciated.

Finally I'd like to thank the entire MicFys group for making me feel welcomed and a part of the family.

This study has been funded by FEDER, through the Operational Programme Thematic Factors of Competitiveness - COMPETE, and by Portuguese funds, through the Portuguese Foundation for Science and Technology (FCT), in the frame of the project FCOMP-01-0124-FEDER-027894 - "SYN2value - Syngas bio-upgrading to fuels and chemicals".



# Contents

|   |      |
|---|------|
| Abstract .....  | iii  |
| Resumo.....   | iv   |
| Aknowledgements.....  | v    |
| Contents .....  | vii  |
| List of Figures.....  | x    |
| List of Equations .....   | xi   |
| List of Tables .....  | xii  |
| List of Acronyms .....  | xiii |
| 1 Introduction.....   | 1    |
| 1.1 Research motivation and background.....   | 1    |
| 1.2 Syngas and microbial routes for syngas/CO conversion to fuels and chemicals ..... | 2    |
| 1.3 Other applications of CO-oxidizing microorganisms .....                           | 5    |
| 1.4 Microbial metabolism of carbon monoxide .....                                     | 6    |
| 1.4.1 Hydrogenogenic CO-oxidizers .....   | 10   |
| 1.4.2 Acetogenic bacteria.....  | 11   |
| 1.4.3 Sulphate-reducing bacteria .....  | 12   |
| 1.4.4 Methanogens .....   | 13   |
| 1.5 CO toxicity towards microorganisms.....   | 16   |
| 1.6 Biochemistry of CO oxidation.....   | 17   |
| 1.7 Genomic and proteomic insights .....  | 18   |
| 1.7.1 Genomics.....   | 18   |
| 1.7.2 Transcriptomics .....   | 19   |
| 1.7.3 Proteomics .....  | 19   |
| 2 Materials and methods .....   | 21   |
| 2.1 Comparative genomic analysys for selection of candidates .....                    | 21   |
| 2.2 Source of microorganisms.....   | 21   |

|       |   |    |
|-------|---|----|
| 2.3   | Medium composition and cultivation .....  | 21 |
| 2.4   | Adaptation studies .....  | 23 |
| 2.5   | Microscopy .....  | 23 |
| 2.6   | Analytical techniques .....   | 24 |
| 2.6.1 | GC measurements .....   | 24 |
| 2.6.2 | HPLC measurements .....   | 24 |
| 2.7   | Protein Extraction for LC-MS/MS analysis.....   | 24 |
| 2.8   | LC-MS/MS analysis .....   | 25 |
| 3     | Results and Discussion .....  | 26 |
| 3.1   | Selection of methanogenic candidates .....  | 27 |
| 3.1.1 | Genomic comparison of methanogens for potential carboxidotrophic abilities .                            | 27 |
| 3.1.2 | Further selection by literature search.....   | 29 |
| 3.1.3 | Final candidate list for physiological tests .....  | 30 |
| 3.2   | Growth characteristics of selected methanogens in the presence of CO.....                               | 34 |
| 3.3   | Physiological observations/effects of CO.....   | 35 |
| 3.3.1 | Inhibition by carbon monoxide .....   | 35 |
| 3.3.2 | Cellular CO release in methanogenic carboxidotrophic strains growing on H <sub>2</sub> /CO <sub>2</sub> |    |
|       | 37  |    |
| 3.4   | Adaptation studies to CO .....  | 39 |
| 3.4.1 | Consumption of CO by methanogenic strains.....  | 40 |
| 3.5   | Carboxidotrophic growth .....   | 44 |
| 3.5.1 | Presence of hydrogen in headspace .....   | 46 |
| 3.5.2 | Visual observations .....   | 47 |
| 3.6   | Proteomic studies of carboxidotrophic cultures .....  | 49 |
| 3.6.1 | Optimization of protein extraction and quantification protocols.....                                    | 49 |
| 3.6.2 | Proteomic analysis .....  | 50 |
| 4     | Conclusions and Future Work .....   | 52 |
| 5     | References.....   | 54 |

Annex I..... |

Annex II..... |

## List of Figures

|   |    |
|---|----|
| Figure 1 - Composition of syngas mixture depending on the source used for gasification (Sipma <i>et al.</i> 2006). .....  | 2  |
| Figure 2 - Possible routes for the chemical and microbial conversion of syngas to fuels and chemicals.....  | 3  |
| Figure 3 - Proposed pathways of electricity production from CO and syngas in an MFC (Mehta <i>et al.</i> 2010). (1) CO conversion to acetate by acetogenic carboxydrotrophs; (2) CO conversion to H <sub>2</sub> by hydrogenogenic carboxydrotrophs; (3) H <sub>2</sub> conversion to acetate by homoacetogens; (4, 5) acetate and H <sub>2</sub> consumption by electricigenic microorganisms; and (6) CO consumption by electricigenic carboxydrotrophs (hypothesized). ..... | 4  |
| Figure 4 – Terminal electron acceptors in anaerobic carboxydrotrophy. ....  | 7  |
| Figure 5 – Phylogenetic tree of anaerobic carboxidotrophic bacterial species. 16S rRNA gene sequenced-based tree was constructed using neighbor-joining methods. Branch length with 10% dissimilarity is represented in the scale bar. Known carboxydrotrophs are indicated in bold. ....   | 8  |
| Figure 6 – Phylogenetic tree of anaerobic carboxidotrophic archeal species. 16S rRNA gene sequenced-based tree was constructed using neighbor-joining methods. Branch length with 10% dissimilarity is represented in the scale bar. Known carboxydrotrophs are indicated in bold. * indicates information obtained in this thesis. Arrows evidence strains tested during this work. ....   | 9  |
| Figure 7 – Example of CO uptake in phototrophic bacteria as determined for <i>R. rubrum</i> (Ensign and Ludden 1991) .....  | 11 |
| Figure 8 – Metabolism of CO oxidation in acetogenic bacteria.....   | 12 |
| Figure 9 – Methanogenesis pathway in <i>M. thermoautotrophicus</i> for growth with H <sub>2</sub> as electron donor. Putative pathway changes for growth on CO are indicated. ....  | 14 |
| Figure 10 – Proposed pathway for CO-dependent methanogenesis in <i>M. barkeri</i> (left) and <i>M. acetivorans</i> (right) according to (Ferry and Lessner 2008). ....  | 15 |
| Figure 11 – Genomic, transcriptomic, proteomic and metabolomic approaches that can be used for the study of microbial metabolism.....   | 18 |
| Figure 12 – Schematic of adaptation protocol.....   | 23 |
| Figure 13 – Tree based on the CODH catalytic subunit in methanogens. ....   | 28 |
| Figure 14 – Gene topology of CODH/ACS alpha subunit neighbourhood for selected strains. Aligned CODH catalytic subunit coding genes are marked in red. ....   | 31 |
| Figure 15 – Overview of the presence of possible genes involved in the putative pathway for carboxidotrophic methanogenesis in selective strains .....  | 33 |
| Figure 16 - Effects of inhibition in the production of methane with increasing concentrations of CO for different tested strains.....   | 36 |
| Figure 17 - Effects of inhibition in the production of methane with a fixed concentrations of CO (15%) for <i>M. marburgensis</i> .....   | 37 |
| Figure 18 – Carbon monoxide formation from CO <sub>2</sub> and H <sub>2</sub> in <i>M. jannaschii</i> at 10% of CO (0.3 bar) .....  | 38 |

|   |    |
|---|----|
| Figure 19 – Representation of equilibrium between bound and dissolved CO in the CODH/ACS complex. ....  | 38 |
| Figure 20 - Heat map of consumption. Black symbolizes untested parameters, green colour intensity corresponds to rate of H <sub>2</sub> consumption (increasing rates from light green to dark green) and blue tone to % of CO consumed (increasing rates from light to dark blue)..... | 39 |
| Figure 21 – Dependency of solubility of H <sub>2</sub> and CO on temperature. ....  | 41 |
| Figure 22 - Result with phosphate buffer vs bicarbonate buffer at CO concentrations of 20% 43   |    |
| Figure 23 – Concentrations of gases in headspace for cultures growing on CO in the first transfer serie where carboxidotrophic growth was observed. ....  | 44 |
| Figure 24 – Adaptation of cultures to CO in the transfer series. ....   | 45 |
| Figure 25 – Production of H <sub>2</sub> in cultures growing carboxidotrophically .....   | 46 |
| Figure 26 – Microscopic observation of <i>M. marburgensis</i> cultures using different combinations of electron donors.....   | 47 |
| Figure 27– Microscopic observations of cells grown with CO during lysis with sonication. From left to right: before sonication, 18 cycles and 30 cycles. ....   | 49 |
| Figure 28 - Microscopic observations of cells subjected to 30 cycles of sonication. From left to right: cells grown on H <sub>2</sub> +CO before sonication; cells grown on CO. ....  | 49 |
| Figure 29 – Expected pathway for <i>M. thermautotrophicus</i> and <i>M. marbugensis</i> . Proteins whose expression is expected to increase in the presence of CO are marked in green. Those whose expression is expected to decrease are marked in blue. ....                          | 51 |

## List of Equations

|  |    |
|--|----|
| Equation 1 .....                       | 10 |
| Equation 2 .....                       | 11 |
| Equation 3 .....                       | 12 |
| Equation 4 .....                       | 13 |
| Equation 5 .....                       | 14 |
| Equation 6 .....                       | 17 |
| Equation 7 .....                       | 37 |
| Equation 8 - Henry's law equation..... | 41 |
| Equation 9 .....                       | 47 |
| Equation 10 .....                      | 47 |
| Equation 11 .....                      | 47 |
| Equation 12 .....                      | 47 |
| Equation 13 .....                      | 47 |

## List of Tables

|   |    |
|---|----|
| Table 1 – Potential products obtained from CO or H <sub>2</sub> /CO mixture.....  | 4  |
| Table 2 - Methanogenic microorganisms used in this work .....   | 21 |
| Table 3 – Operational conditions.....   | 22 |
| Table 4 – Selected candidates for testing and their physiological characteristics .....   | 30 |
| Table 5 – Overview of growth success with CO in the headspace for the cultures tested .....   | 34 |
| Table 6 - Inhibition by carbon monoxide on the production of methane for tested strains .....   | 35 |
| Table 7 - Henry's law constants dependency on temperature .....   | 41 |
| Table 8 - Sequence alignment results for putative CODH gene coding results in reference to the CODH of <i>M. methanothermobacter thermoautotrophicus</i> .....                                      | I  |
| Table 9 – Protein detected by LC-MS/MS for <i>Methanothermobacter thermautotrophicus</i> for high and low availability of H <sub>2</sub> as electron donor (data from {Farhoud, 2011 #3614}). ..... | I  |

## List of Acronyms

### Compounds

|                                  |                               |
|----------------------------------|-------------------------------|
| CO <sub>2</sub>                  | Carbon Dioxide                |
| CO                               | Carbon Monoxide               |
| H <sub>2</sub>                   | Hydrogen                      |
| H <sub>2</sub> S                 | Hydrogen Sulphide             |
| CH <sub>4</sub>                  | Methane                       |
| N <sub>2</sub>                   | Nitrogen                      |
| O <sub>2</sub>                   | Oxygen                        |
| CH <sub>3</sub> COO <sup>-</sup> | Acetate                       |
| AQDS                             | Anthraquinone-2,6-disulfonate |

### Enzymes

|                    |  |
|--------------------|--|
| ACS                | Acetyl-CoA Synthase                                      |
| CODH               | Carbon Monoxide Dehydrogenase                            |
| Eha                | Energy converting [Ni,Fe]-hydrogenase                    |
| Fd                 | Ferredoxin   |
| Ftr                | Formylmethanofuran: H <sub>4</sub> MPT formyltransferase |
| Fwd                | Formyl-MFR dehydrogenase                                 |
| H <sub>4</sub> MPT | Tetrahydromethanopterin                                  |
| Hdr                | Heterodisulfide reductase                                |
| Mch                | Methenyl- H <sub>4</sub> MPT cyclohydrolase              |
| Mcr                | Methyl-coenzyme M reductase isoenzyme I                  |
| Mfr                | Methanofuran   |
| Mvh                | F <sub>420</sub> -non reducing [Ni,Fe]-hydrogenase       |



# 1 Introduction

## 1.1 Research motivation and background

Rapid growth of world population, coupled with the emergence of developing countries, results in an ever increasing need for energy and fuel sources. Furthermore, limited availability and price fluctuations of fossil fuels have driven the energy market towards the search for renewable alternatives. In this context, biofuels offer an appealing opportunity for quenching these requirements in the near future.

Biofuels can be divided into first-generation and second-generation sources. Whilst first generation biofuels have recently received ample criticism for their often direct competition with food stocks placing their sustainability into question, second-generation biofuels are mostly attained from non-food lignocellulosic biomass and have no such drawbacks, making them a far more attractive solution for biofuel production (Mohammadi *et al.* 2011).

Lignocellulosic biomass is one of the most abundant sources for biofuels. It consists mainly of cellulose, hemicellulose and lignin and is a general term for describing the non-starch based fibrous plant material. However, the high availability is counterbalanced by the poor degradability of lignin by biological processes. Consequently, microbial conversion of materials where lignin is abundant, such as straw and wood, to fuels is challenging. Pre-treatment of the biomass to separate lignin can be achieved through steam-explosion and acid hydrolysis but such methods are not economically feasible (Carere *et al.* 2008).

A cost-effective and promising alternative to circumvent this hurdle is gasification of the biomass in order to generate syngas, a gas mixture composed predominantly of carbon monoxide (CO), hydrogen (H<sub>2</sub>) and carbon dioxide (CO<sub>2</sub>). Syngas can be further converted, both by chemical or microbial processes, to several added-value compounds. Bioconversion processes have several advantages over catalytic processes: i) milder temperatures and pressures can be used, ii) no requisite of a fixed CO/H<sub>2</sub> ratio, iii) less susceptibility to impurities in the feed gas, and iv) no need for costly pre-treatment of the feed gas or expensive metal catalysts (Henstra *et al.* 2007, Abubackar *et al.* 2011).

## 1.2 Syngas and microbial routes for syngas/CO conversion to fuels and chemicals

Gasification consists of a partial oxidation of the carbonaceous materials at elevated temperatures (700-1000 °C) with a controlled amount of oxygen and/or steam. Substrates for gasification include a wide array of carbon containing sources, such as coal, cokes, sewage sludge, municipal wastes, lignocellulosic biomass, and reformed natural gas. Syngas is mainly composed by CO, H<sub>2</sub> and CO<sub>2</sub>, but relative amounts of these compounds depend greatly both on the carbonaceous source used during gasification (vide Figure 1), as well as in the process parameters (e.g. gasifying agent, type of gasifier, etc). Syngas often contains minor amounts of other gases such as methane (CH<sub>4</sub>), nitrogen (N<sub>2</sub>) and hydrogen sulphide (H<sub>2</sub>S) (Henstra *et al.* 2007).

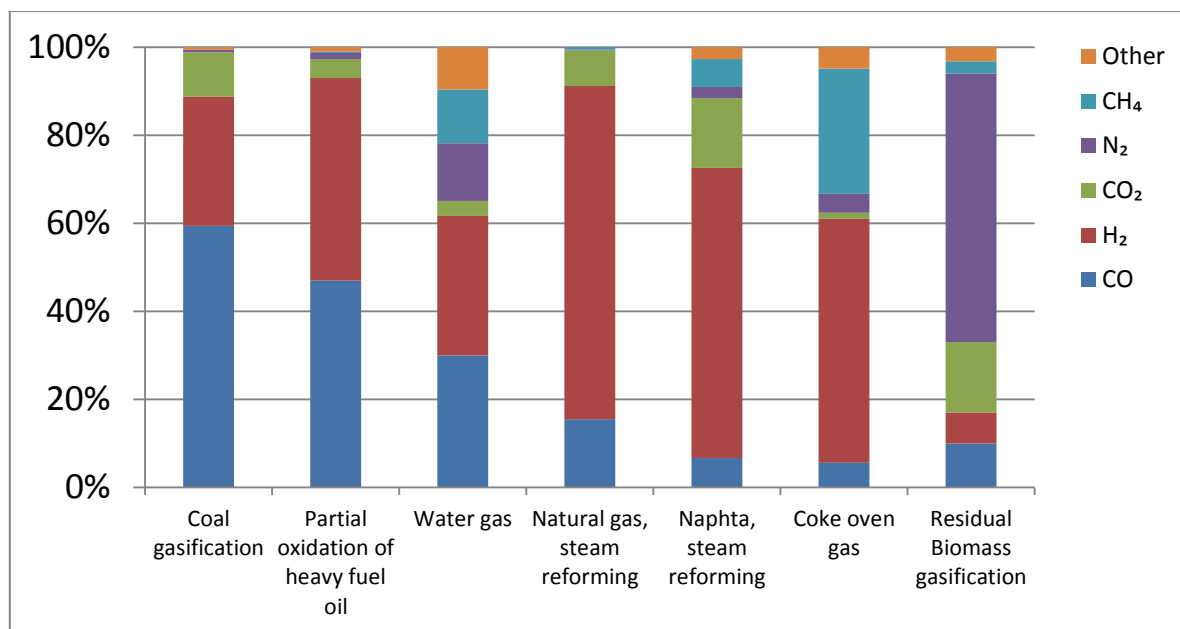


Figure 1 - Composition of syngas mixture depending on the source used for gasification (Sipma *et al.* 2006).

As can be expected, these variations in the composition of syngas are of major importance to determine its subsequent use. The presence of contaminants, such as H<sub>2</sub>S can be hazardous to the chemical processes used in the downstreaming of gasification, even at trace amounts. Carbon monoxide, in particular, provides a technological obstacle due to its toxicity towards biological reductive processes and poisoning of chemical catalysts (Sipma *et al.* 2006).

While chemical methods to reduce CO levels in the syngas mixture have been developed (e.g. the water-gas-shift reaction), these typically occur at extremely high temperatures and require a relatively homogenous feed, thwarting the economic feasibility and therefore the attractiveness of the entire process.

Microbiological conversion of CO by carboxidotrophic organisms could thus offer a potential alternative route to circumvent these problems. Fermentation of syngas/CO into several of the same

compounds attained by chemical processes have been reported (*vide* Figure 2). Fermentative processes are less sensitive to the contaminants often present in syngas and to variations in its composition. This allows for the use of low grade synthesis gas coming from a wider array of feed sources.

Methane in particular offers an interesting route as a final end product of biological conversion of syngas. Methanogenesis can be performed with a variety of substrates including some of the products from other biological conversions of syngas (such as acetate, ethanol and hydrogen). This ability could be useful to metabolize remaining compounds that could not be extracted from previous conversions of syngas mixture. Consequently, biogas, a denser and less toxic gas mixture, can be easily derived from syngas. This biomethanation process can thus be particularly useful in aiding the transportation and usability of syngas (Techtmann *et al.* 2009).

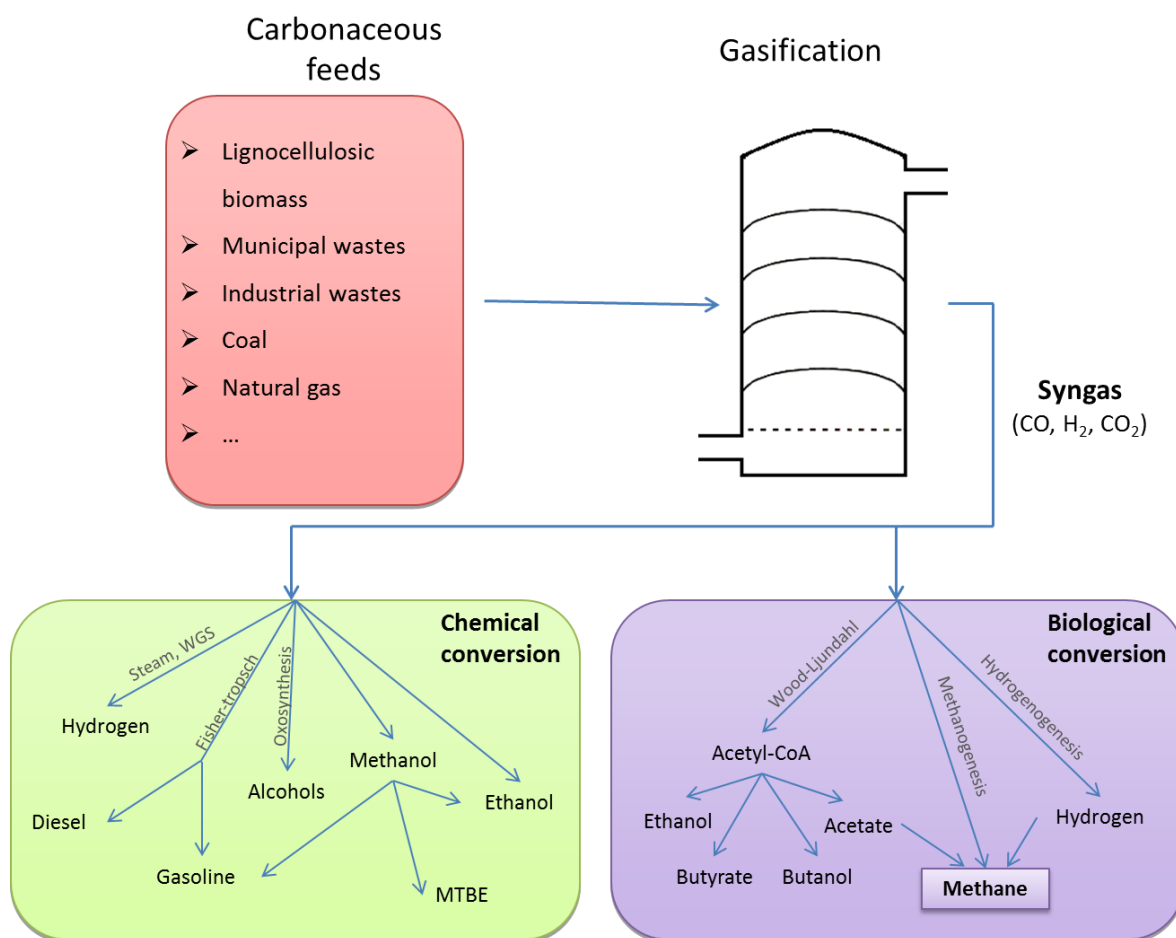


**Figure 2 - Possible routes for the chemical and microbial conversion of syngas to fuels and chemicals.**

Table 1 – Potential products obtained from CO or H<sub>2</sub>/CO mixture

| Product                                | Reaction  | $\Delta G^{or}$<br>kJ mol CO <sup>-1</sup> |
|--|---|--|
| <b>Reactions from CO</b>               |   |  |
| <b>Methane</b>                         | <b>4CO + 2H<sub>2</sub>O → CH<sub>4</sub> + 3CO<sub>2</sub></b>   | <b>-53</b>                                 |
| Acetate                                | 4CO + 2H <sub>2</sub> O → CH <sub>3</sub> COO <sup>-</sup> + H <sup>+</sup> + 2CO <sub>2</sub>                                  | -44  |
| Butyrate                               | 10CO + 4H <sub>2</sub> O → CH <sub>3</sub> (CH <sub>2</sub> ) <sub>2</sub> COO <sup>-</sup> + H <sup>+</sup> + 6CO <sub>2</sub> | -44  |
| Ethanol                                | 6CO + 3H <sub>2</sub> O → CH <sub>3</sub> CH <sub>2</sub> OH + 4CO <sub>2</sub>   | -37  |
| Formate                                | CO + H <sub>2</sub> O → HCOO <sup>-</sup> + H <sup>+</sup>  | -16  |
| Hydrogen                               | CO + H <sub>2</sub> O → H <sub>2</sub> + CO <sub>2</sub>  | -20  |
| n-Butanol                              | 12CO + 5H <sub>2</sub> O → CH <sub>3</sub> (CH <sub>2</sub> ) <sub>3</sub> OH + 8CO <sub>2</sub>                                | -40  |
| <b>Reactions from H<sub>2</sub>/CO</b> |   |  |
| <b>Methane</b>                         | <b>CO + 3H<sub>2</sub> → CH<sub>4</sub> + H<sub>2</sub>O</b>  | <b>-151</b>                                |
| Acetate                                | 2CO + 2H <sub>2</sub> → CH <sub>3</sub> COO <sup>-</sup> + H <sup>+</sup>   | -67  |
| Butyrate                               | 4CO + 6H <sub>2</sub> → CH <sub>3</sub> (CH <sub>2</sub> ) <sub>2</sub> COO <sup>-</sup> + H <sup>+</sup> + 2H <sub>2</sub> O   | -80  |
| Ethanol                                | 2CO + 4H <sub>2</sub> → CH <sub>3</sub> CH <sub>2</sub> OH + H <sub>2</sub> O   | -72  |
| Methanol                               | CO + 2H <sub>2</sub> → CH <sub>3</sub> OH   | -39  |
| n-Butanol                              | 4CO + 8H <sub>2</sub> → CH <sub>3</sub> (CH <sub>2</sub> ) <sub>3</sub> OH + 3H <sub>2</sub> O                                  | -81  |

An emerging biotechnological solution for the production of electricity from biomass is the microbial fuel cell (MFC). This device harnesses the electrons and protons generated during oxidation of an electron donor (e.g. CO) in order to produce electrical current. Coupling of this technology to feeds of syngas and CO has been demonstrated in several studies (Kim and Chang 2009, Mehta *et al.* 2010, Hussain *et al.* 2011).

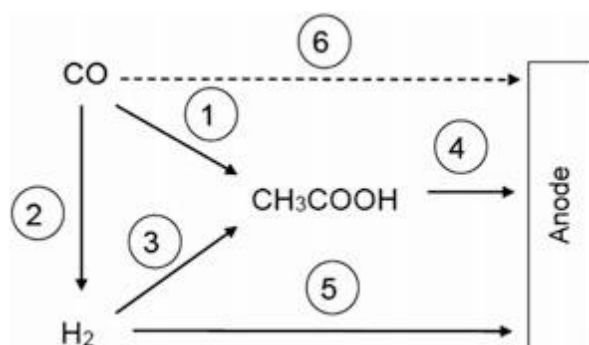


Figure 3 - Proposed pathways of electricity production from CO and syngas in an MFC (Mehta *et al.* 2010). (1) CO conversion to acetate by acetogenic carboxydrotrophs; (2) CO conversion to H<sub>2</sub> by hydrogenogenic carboxydrotrophs; (3) H<sub>2</sub> conversion to acetate by homoacetogens; (4, 5) acetate and H<sub>2</sub> consumption by electricigenic microorganisms; and (6) CO consumption by electricigenic carboxydrotrophs (hypothesized).

### 1.3 Other applications of CO-oxidizing microorganisms

While the previously mentioned applications in the processing of gasification products towards biofuel and organic acids are one of the most promising and the driving force for the development of this dissertation, it should be mentioned that CO-utilizing microorganisms have also raised interest in other fields.

A promising prospect is the potential for bioremediation by other means than the aforementioned route of conversion of waste products through gasification. In theory, purified CO-converting enzymes could be used in bio-filters for reducing CO levels in heavily polluted areas. This would be particularly useful in enclosed areas such as underground car parks. Furthermore, due to the close relation of CO to CO<sub>2</sub>, the methods of CO removal could, in theory be applied for removal of the CO<sub>2</sub> from the atmosphere where it acts as a greenhouse gas that is relatively inert (Ragsdale 2004). CO conversion mechanisms have also been associated to reductive dehalogenation and dechlorination being a potential basis for degradation of toxic compounds (Tiquia-Arashiro 2014).

Development of gas biosensors is another field of study where these organisms can play a pivotal role. Considering the overall toxicity of the gas towards several targets (*vide* section 1.5), reliable and efficient methods for its detection have considerable commercial interest. Currently, many CO detectors lack the specificity/accuracy required often resulting in false alarms or readings. Potential uses for CO biosensors include detection in confined spaces where CO is generated (mines, underground car parks, road tunnels, and industrial settings), as a control system for combustion (either in industrial setting or general fire alarms). (Colby *et al.* 1985).

## 1.4 Microbial metabolism of carbon monoxide

The first indications of microbial capability of metabolizing CO into cell material goes as far back as 1903 when thin films of bacteria were documented as growing in mineral media with coal gas mixture (mainly H<sub>2</sub> and CO) as potential carbon source. (Beijerinck and van Delden 1903)

In the following years, some studies were conducted that showed aerobic bacterial growth of isolated strains (*Actinobacillus oligocarbophilus*, *Actinobacillus paulotrophus* and *Actinomyces oligocarbophilus*) in the presence of CO but a rigorous confirmation for CO oxidation was lacking until 1953 in the work of Kistner with *Hydrogenomonas carboxydovorans* (Beijerinck and van Delden 1914, Lantzsch 1922, Mörsdorf *et al.* 1992).

While the number of organisms documented as capable of growth on CO as a sole carbon and electron source has grown substantially since, it is likely that the extent of carboxydotrophs is still grossly underestimated in literature. Use of this substrate often goes untested in growth studies and, due to initial inhibition imparted by CO, carboxidotrophic potential can be easily overlooked (Alves 2013).

The term carboxydotroph was first used in 1983 to describe utilization of CO as sole carbon and electron source during the study of chemolithoautotrophic aerobic respiratory organisms (Meyer and Schlegel 1983). Aerobic carboxydotrophy uses O<sub>2</sub> as a terminal electron acceptor. This type of CO-metabolism merely yields CO<sub>2</sub> and biomass which makes it less interesting from a biotechnological standpoint. Nevertheless, CO-utilizing microorganisms are taxonomically diverse, including also anaerobic bacteria and archaea (Figure 5 and Figure 6). Anaerobic CO conversion, can be coupled to a wider variety of acceptors (CO<sub>2</sub>, sulphate, sulphur, thiosulphate and protons). These anaerobic respiration processes can thus be divided into hydrogenogenesis, desulfurication, acetogenesis, iron-reduction and methanogenesis (Figure 4) (Oelgeschlager and Rother 2008).

For carboxydotrophy to be accomplished, the organisms have to be able to perform 3 necessary steps: oxidation of CO into CO<sub>2</sub>, utilization of the electrons derived from the previous oxidation for growth, incorporation of CO<sub>2</sub> into cell carbon. In addition, the microbe has to have the capacity for withstanding inhibition by CO.

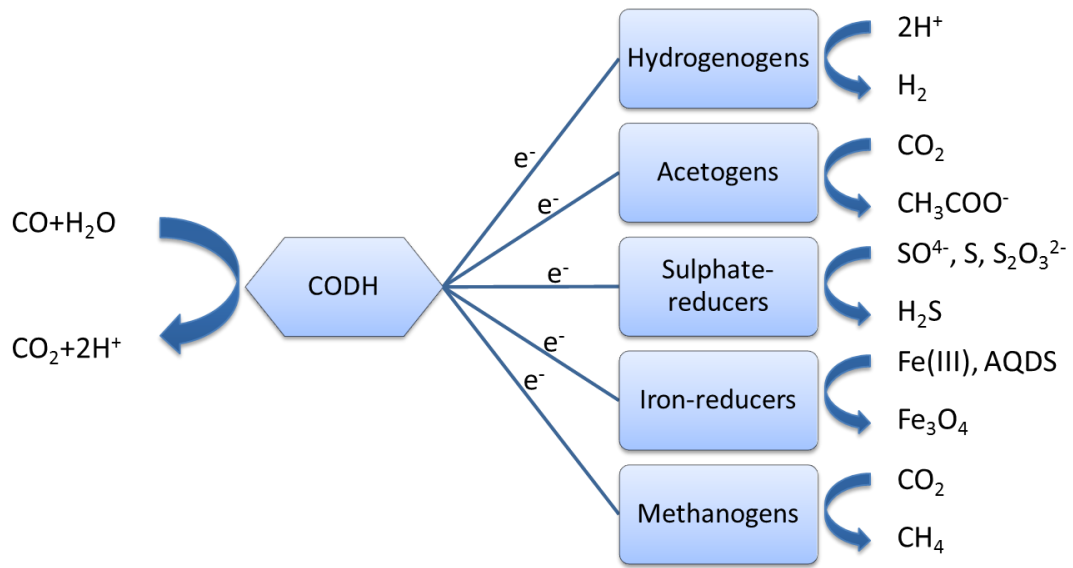


Figure 4 – Terminal electron acceptors in anaerobic carboxydutrophy.

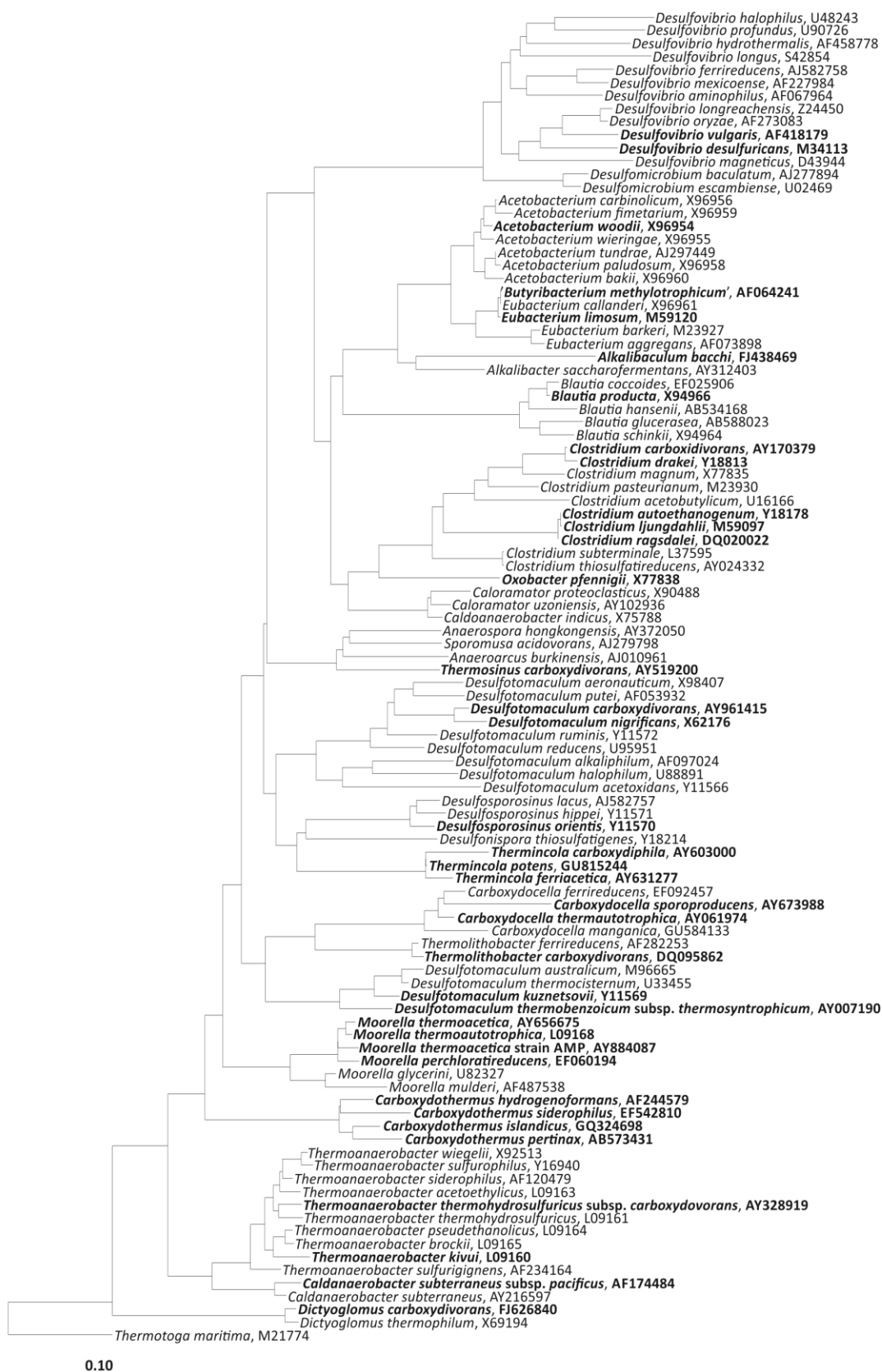


Figure 5 – Phylogenetic tree of anaerobic carboxidotrophic bacterial species. 16S rRNA gene sequenced-based tree was constructed using neighbor-joining methods. Branch length with 10% dissimilarity is represented in the scale bar. Known carboxydrotrophs are indicated in bold.

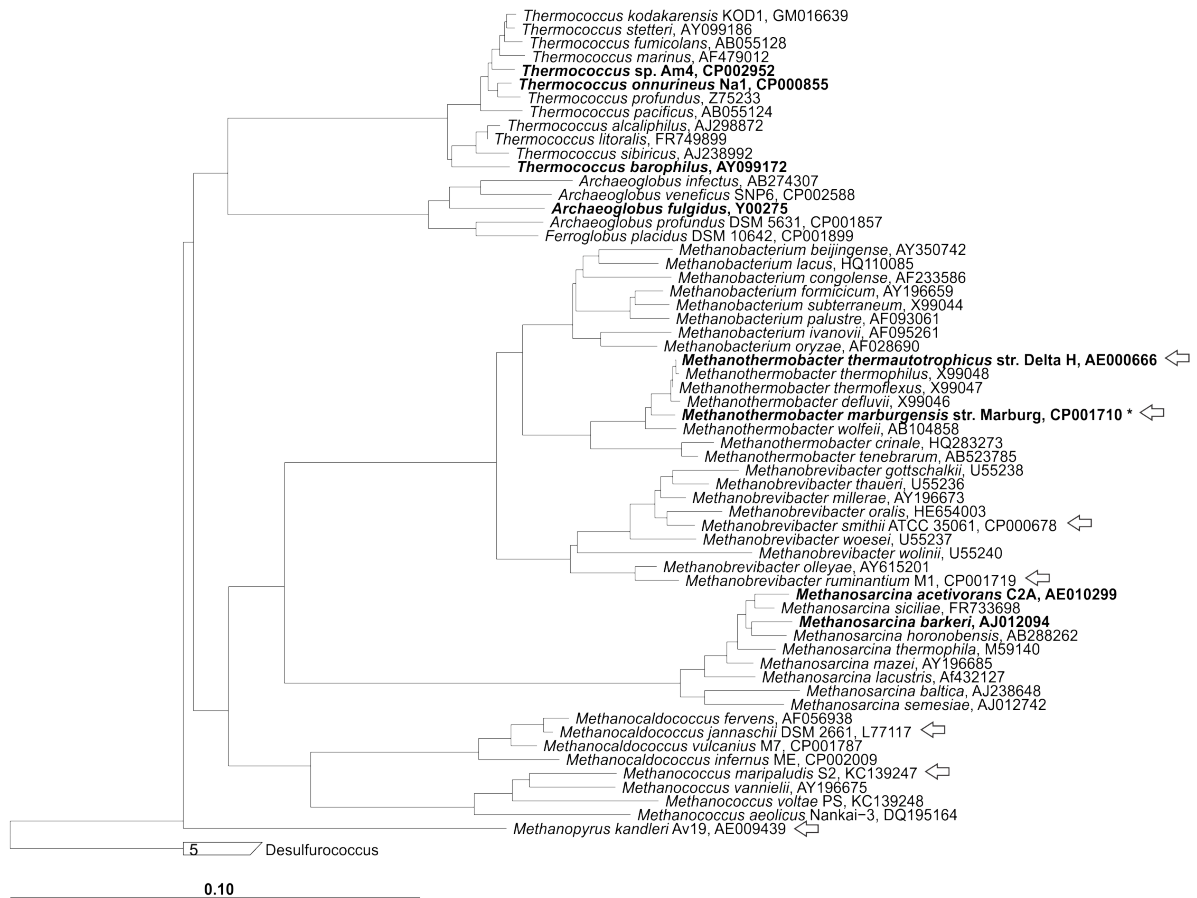
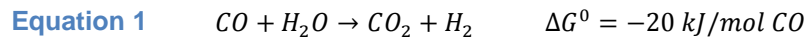


Figure 6 – Phylogenetic tree of anaerobic carboxidotrophic archeal species. 16S rRNA gene sequenced-based tree was constructed using neighbor-joining methods. Branch length with 10% dissimilarity is represented in the scale bar. Known carboxidotrophs are indicated in bold. \* indicates information obtained in this thesis. Arrows evidence strains tested during this work.

#### 1.4.1 Hydrogenogenic CO-oxidizers

The term hydrogenogenic was proposed by Svetlitchnyi to denominate organisms capable of producing H<sub>2</sub> from CO (Svetlitchnyi *et al.* 2001). This process occurs by oxidation of CO with protons derived from H<sub>2</sub>O to form H<sub>2</sub> and CO<sub>2</sub> according to the following stoichiometry:



Such reaction is the biological analogue of the water-gas-shift reaction used to chemically lower CO percentages in gas mixtures. The CO<sub>2</sub> generated is then partly processed into cell carbon by way of the Calvin Cycle (Dashekvicz and Uffen 1979).

This type of CO metabolism is shared by a wide array of phylogenetically diverse prokaryotes. However, analysis of the genes coding for CODH revealed a close similarity amongst the hydrogenogens suggesting that the ability for this type of carboxydrotrophy was propagated through lateral gene transfer (Techtmann *et al.* 2009, Techtmann *et al.* 2012).

A prominent hydrogenogen is *Carboxydotherrnus hydrogenoformans*. This hydrogenogenic bacterium was first described in 1991 as an obligate carboxydrotroph (Svetlichny *et al.* 1991) but has since been shown to be capable of utilizing a number of electron donors and acceptors (Henstra and Stams 2004). It can grow in the presence of 100% (v/v) CO and the robust growth presented by this organism in the gaseous substrate has made it one of the most well studied carboxydrotrophs (Gonzalez and Robb 2000, Henstra and Stams 2004, Zhao *et al.* 2011, Wang *et al.* 2013).

A particular subset of hydrogenogens is composed by phototrophic bacteria. Members of this group of facultative anaerobes have been shown as capable to utilize CO in the dark. While phototrophic bacteria's tolerance for CO was known (Hirsch 1968) it was not until the work of Uffen that their use of CO as a sole carbon and energy source in the dark was detailed. *Rubrivivax* (formerly *Rhodocyclus*) *gelatinosus* was shown as capable of growth in 100% CO (v/v) (Uffen 1976). Later, *Rhodospirillum rubrum* was also identified as capable of metabolizing CO into cellular material and energy. (Uffen 1981). Typically exhibiting low growth rates on CO, this group requires light to achieve optimum cell growth. For some strains, such as *Rhodopseudomonas palustris*, growth ceases in the dark even though hydrogenogenic CO-oxidation is occurring. This was interpreted as the cells only receiving maintenance energy in these conditions (Jung *et al.* 1999).

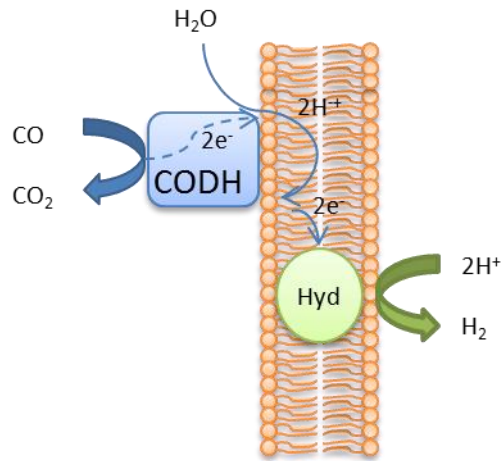


Figure 7 – Example of CO uptake in phototrophic bacteria as determined for *R. rubrum* (Ensign and Ludden 1991)

#### 1.4.2 Acetogenic bacteria

Acetogenic bacteria are obligate anaerobes capable of producing acetate through a variety of sources, including CO<sub>2</sub> through the Wood-Ljungdahl pathway. In this well-studied pathway, CO<sub>2</sub> molecules are combined with Co-enzyme A to form acetyl Co-A by the CODH/ACS enzyme complex. It has also been observed that some acetogens can use CO directly in this pathway (Kerby *et al.* 1983, Ljungdahl 1986, Wood 1991).



The first acetogens shown to oxidise CO were *Clostridium thermoaceticum* and *Clostridium formicoaceticum* (Diekert and Thauer 1978). The more recently studied *Clostridium carboxidovorans* can also produce substantial amounts of ethanol, butyrate and butanol from CO (Liou *et al.* 2005).

Other acetogenic bacteria include *Moorella thermoacetica* and *Moorella thermoautotrophica* that can grow on CO as sole energy source (Savage *et al.* 1987; Daniel *et al.* 1990).

The ability of acetogens to produce added-value compounds has made it one of the most promising for chemical and fuel production from syngas/CO.

Besides these *Clostridium* strains, *Acetogenium kivui* was discovered as being unable to utilise CO as electron donor but could use it as carbon source under the presence of H<sub>2</sub> (Daniel *et al.* 1990, Yang and Drake 1990).

However the record for highest tolerance and fastest growth belongs to *Peptostreptococcus productus* strains that have been reported as tolerating CO concentrations (v/v) of 90% (Lorowitz and Bryant 1984).

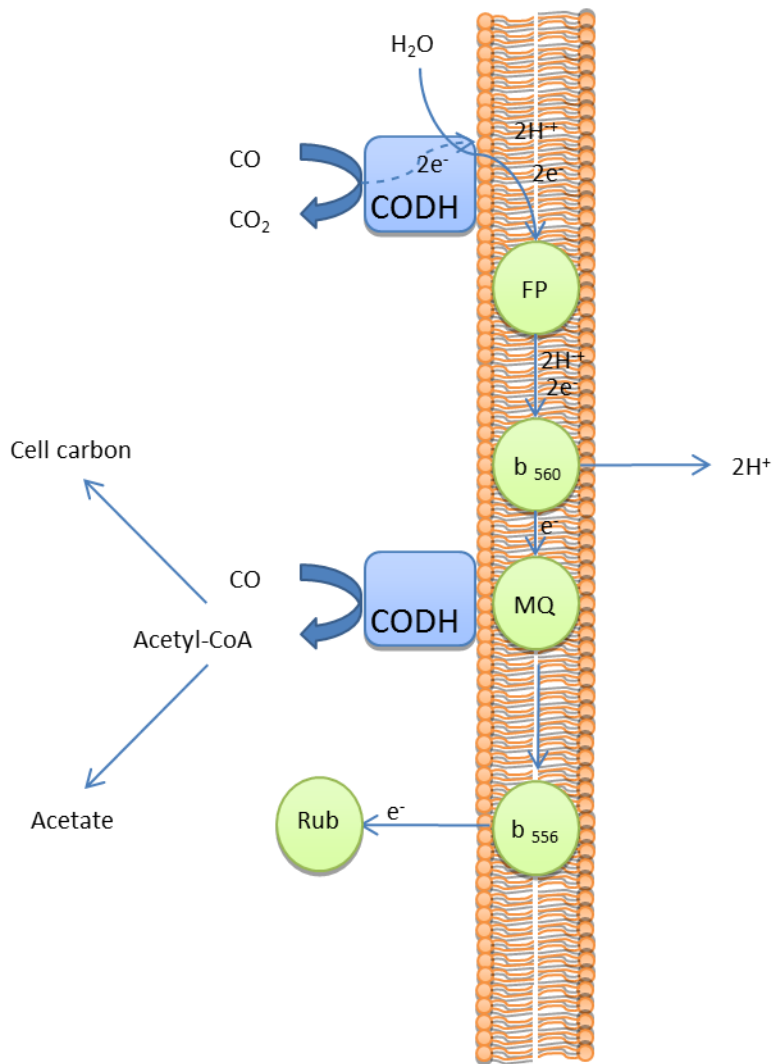
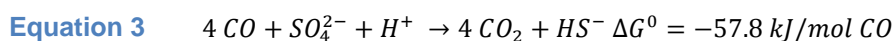


Figure 8 – Metabolism of CO oxidation in acetogenic bacteria.

### 1.4.3 Sulphate-reducing bacteria

Also counted within the obligate anaerobic bacteria are sulphate reducing bacteria (SRB). They can utilize this compound as an electron acceptor and that ability is spread through the SRB in phylogenetically diverse members.

Use of CO as a carbon source for this group was first recounted in 1958 by Yagi with the reaction being accomplished through the following stoichiometry (Yagi 1958, Yagi 1959, Yagi and Tamiya 1962, Thauer *et al.* 1977):



Later, in 1985, CODH from *Desulfovibrio desulfuricans* was characterized and a pathway for acetate degradation that involved CODH/acetyl-CoA synthase, which was demonstrated in

*Desulfobacterium autotrophicum*, was proposed shortly afterwards (Meyer and Fiebig 1985, Schauder *et al.* 1989).

*Desulfovibrio barsii* grew on formate and CO<sub>2</sub> in the presence of 1.5% (v/v) CO with removal of 15% of CO towards amino acid production (Jansen *et al.* 1984, Techtmann *et al.* 2009).

Furthermore, *Desulfovibrio vulgaris* (strain Madison) was shown to be capable of utilizing CO as electron donor when this gas was present in concentrations of up to 4% (v/v). This consumption of CO was followed by production of H<sub>2</sub> which was then consumed. However, concentrations above 4.5% were inhibitory (Lupton *et al.* 1984).

Similarly, growth on CO as only energy source at concentrations ranging between 5-20% was observed in *Desulfotomaculum orientis* and *D. nigrificans* with higher concentrations resulting in inhibition (Klemps *et al.* 1985).

Amongst the sulphate reducing microorganisms, *Desulfotomaculum carboxydvorans* is of particular importance since it can not only grow with a gas phase of 100% CO, but is also capable of growth without sulfate, essentially acting as a hydrogenogen (Parshina *et al.* 2005).

Other sulfate reducers, such as *Desulfotomaculum thermobenzoicum* and *Desulfotomaculum kuznetsovii*, not only produce H<sub>2</sub> (as an intermediary) but also acetate (Parshina *et al.* 2005).

Besides sulphate, elemental sulphur, dimethylsulfoxide and thiosulfate were shown to be reduced with CO in *Sulfospirillum carboxydvorans* (Jensen and Finster 2005).

#### 1.4.4 Methanogens

Study on the CO as a substrate for this archaea group has not only trailed behind other substrates for methane production but also the current knowledge on other non-methanogenic species (Ferry 2010).

For methanogens, the first indication of their ability to metabolize CO can be found in the work of Fischer with sewage sludge that described the formation of methane from carbon monoxide with carbon dioxide being proposed as an intermediary. However the co-culture nature of the experiment meant that a syntrophic mechanism could not be discarded with other anaerobes producing methanogenic substrates from CO (Fischer *et al.* 1931, Fischer *et al.* 1932).

Stephenson and Stickland reported in 1933 reduction of CO to CH<sub>4</sub> by a pure culture in the presence of hydrogen according to Equation 4. This work was confirmed in 1947 with cell suspensions converting CO to CH<sub>4</sub> with H<sub>2</sub> as intermediary (Stephenson and Stickland 1933, Kluyver and Schnellen 1947).

#### Equation 4



Decades later, in 1977, several methanogens were tested for their ability to remove CO from the headspace with the first report of a methanogen capable of using the gas as a sole carbon and energy source. In this study, a hydrogenotrophic methanogen (*Methanothermobacter*

*thermautotrophicus* strain ΔH) was described as converting CO to CO<sub>2</sub> and CH<sub>4</sub> as well as being capable of acting as electron donor to reduce F420. It was also noted that, despite its ability to grow on the gas, high concentrations of CO were inhibitory (with growth ceasing at concentrations above 60% (v/v)). Furthermore, even at the optimum concentrations of CO tested (30%), growth occurred at 100 times lower rates than with H<sub>2</sub>. H<sub>2</sub>-dependent growth was also highly affected at 40% CO suggesting inhibition of hydrogenases (Daniels *et al.* 1977).

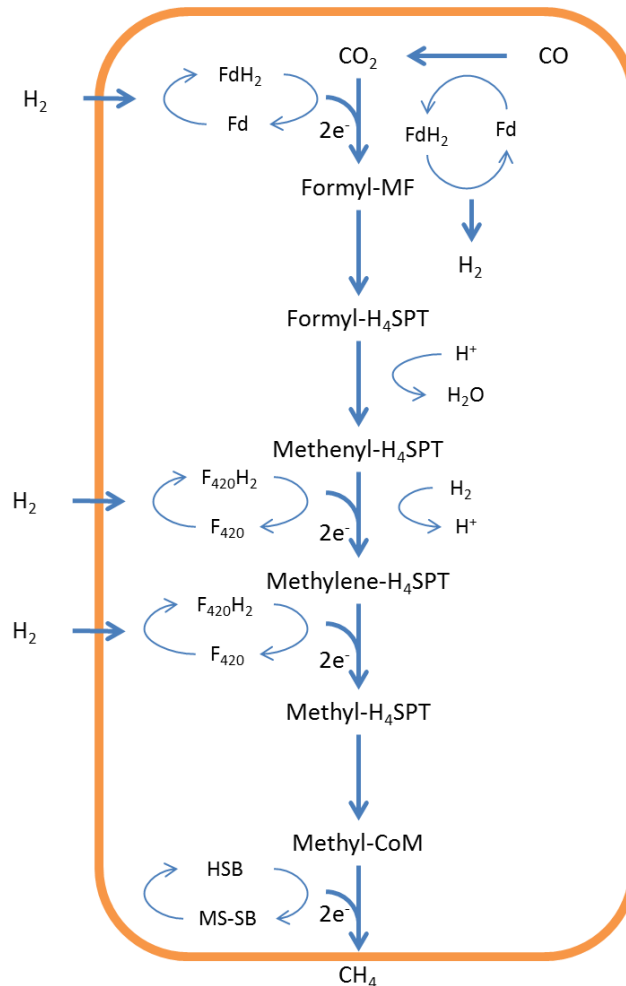
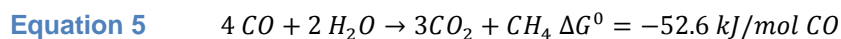


**Figure 9 – Methanogenesis pathway in *M. thermautotrophicus* for growth with H<sub>2</sub> as electron donor. Putative pathway changes for growth on CO are indicated.**

The proposed stoichiometry of the process followed equation Equation 5 (Daniels *et al.* 1977):



In 1984, *Methanosarcina barkeri* strain MS, a methanogen isolated in 1966, was shown to be able to grow on an atmosphere of 50% CO using the gas as a source of energy and carbon. It was observed that H<sub>2</sub> began being detectable when the CO percentage was above 20% supporting the

idea of H<sub>2</sub> being formed as an intermediary in the reduction of CO to CH<sub>4</sub> with the hydrogenases being inhibited by high CO partial pressures in the headspace (Bryant and Boone 1987).

For this acetoclastic species, CO oxidation to CO<sub>2</sub> and H<sub>2</sub> is coupled with production of ATP with ferredoxin mediating electron flow from CODH to membrane bound hydrogenases. O'Brien *et al.* also detailed that *M. barkeri* was inhibited by the presence of high concentrations of CO (O'Brien *et al.* 1984, Bott *et al.* 1986).

It was, however, fairly recently that a *Methanosarcina* species was observed to grow on CO under conditions suitable for proliferation in the natural environment. The marine isolate, *M. acetivorans* was sequestered from sediments rich in decaying kelp in an environment containing up to 10% CO. The generation time is lower than in other methanogens and growth occurs at CO partial pressures above 1 atm. These attributes have made this *Methanosarcina*, the most well studied methanogen for carboxidotrophic growth (Sowers *et al.* 1984, Lessner *et al.* 2006, Rother *et al.* 2007).

Extensive proteomic analysis of CO metabolism in *M. acetivorans*, indicated a previously unknown pathway for CO-dependent methanogenesis. In the CO reduction pathway evidenced, H<sub>2</sub> does not function as an intermediate in the methanogenesis process which falls in line with the notion of the intolerance to CO observed being connected to the inhibition of hydrogenases (O'Brien *et al.* 1984, Lessner *et al.* 2006).

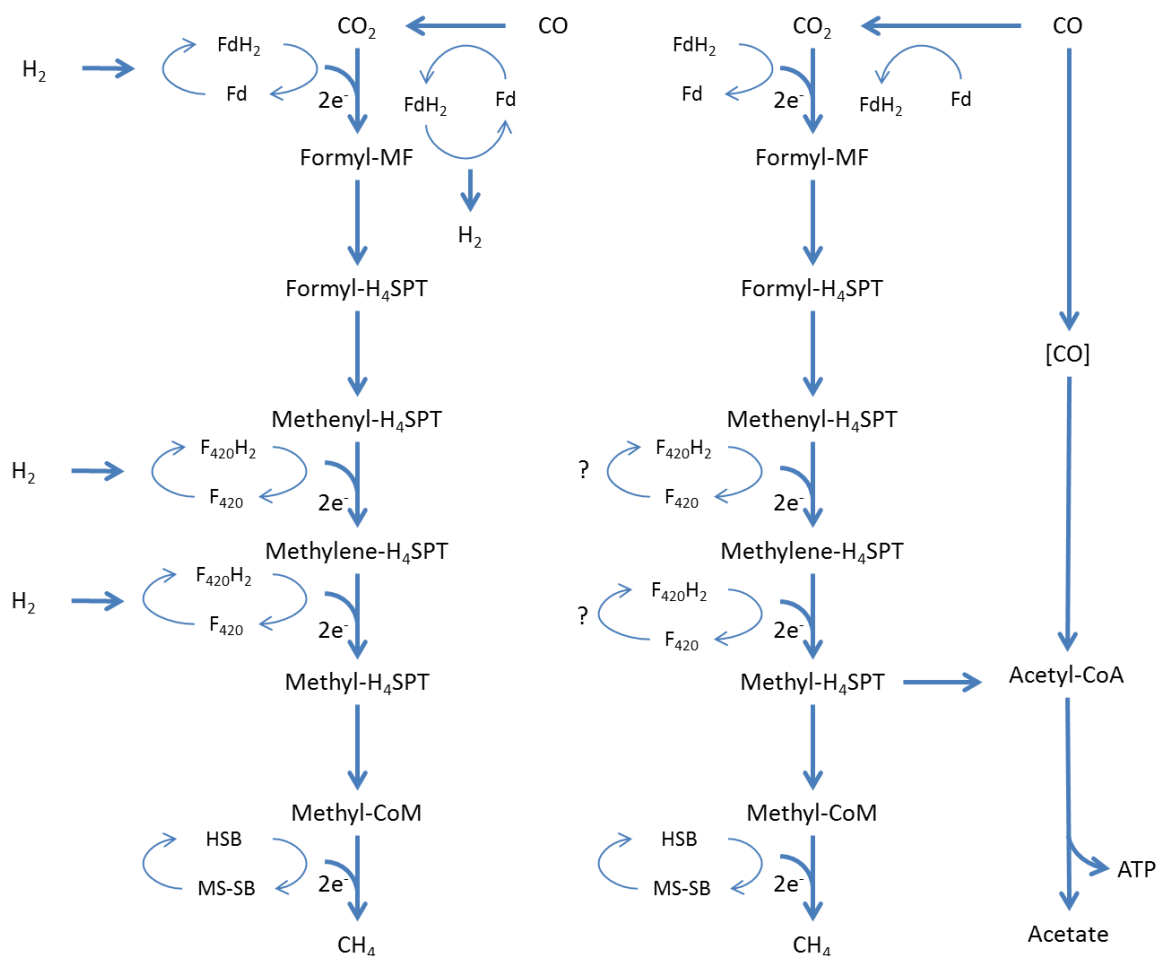


Figure 10 – Proposed pathway for CO-dependent methanogenesis in *M. barkeri* (left) and *M. acetivorans* (right) according to (Ferry and Lessner 2008).

## 1.5 CO toxicity towards microorganisms

Although CO functions as a metabolite in all three domains of life, it also possesses inherent toxic characteristics. As mentioned previously, CO can form stable complexes with the low valent states of the metal sites in metalloproteins. It is this property that makes it such a strong inhibitor of metalloenzymes such as hydrogenases and heme proteins and explains its toxicity towards such a wide range of organisms (Ragsdale 2004).

In humans, it is produced as a neural signalling molecule during heme metabolism (Verma *et al.* 1993). It was also found that it has a role as a transcriptional regulator that controls human circadian rhythms (Dioum *et al.* 2002). However, by binding to heme proteins, it can severely affect oxygen transport, causing several detrimental effects.

For bacteria, it is often present since it is produced in a number of metabolisms, such as amino acid synthesis (Ragsdale 2004).

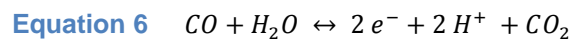
In the Wood-Ljungdahl pathway, which can occur in both archaea and bacteria, CO functions as an intermediate metabolite (Ragsdale 2004).

According to a prominent hypothesis, at the time of the origin of life, the CO presence in the Earth atmosphere was quite significant. This might help explain the diverse range of organisms found that possess CO metabolizing capabilities.

## 1.6 Biochemistry of CO oxidation

As previously discussed, several phylogenetically diverse organisms developed the ability to use CO as a metabolic building block.

Common to all different pathways mentioned is the presence of a specific enzyme, CO dehydrogenase (CODH). CODH allows for the interconversion of CO and CO<sub>2</sub>, accompanied by the generation of high energy electrons according to Equation 6. CODH is capable of using several different electron acceptors (e.g ferredoxin, flavodoxin, cytochromes)



Such an enzyme was first proposed by Yagi with it being identified in acetogenic bacteria and purified later to homogeneity (Yagi 1959, Diekert and Thauer 1978, Ragsdale *et al.* 1983).

These metalloenzymes are the basis of CO metabolism focused in this study. The reaction allows the CO to be used as a carbon source by means of one of the CO<sub>2</sub> fixing pathways.

With regards to the metal present in the active site of CODH, two types can be distinguished, molybdenum containing CODHs (Mo-CODH) and nickel-iron containing CODHs ([Ni,Fe]-CODH).

Mo-CODHs are not oxygen sensitive and are characteristic of aerobic carboxydrotrophy. They are characterized by having high Michaelis constant (K<sub>m</sub>) values but low turnover rates when compared to the CODH found in anaerobes. This makes them quite capable of uptake of CO for detoxification purposes, even at trace levels, but not extremely efficient at growth in the substrate (Ragsdale 2004).

On the other hand, [Ni,Fe]-CODHs are the backbone of anaerobic CO-oxidation focused in this dissertation. Analysis of currently available genomic sequence databases reveals their presence in a substantial number of bacterial and archaeal genomes (upwards of 6% percent). Furthermore, several carboxydrotrophs display multiple CODH coding genes with *Carboxydotherrmus hydrogenoformans* and *Methanosarcina acetivorans* topping the list with 5 occurrences (Techtmann *et al.* 2009, Techtmann *et al.* 2012).

Often coupled to CODH, acetyl-CoA synthase (ACS) also plays a key role by combining either free or molecular bound CO with a methyl group and Co-enzyme A to form acetyl CoA, a noteworthy base molecule in cell metabolism originating both cell material and ATP. The association of CODH with ACS in one structure, allows for the generation and consumption of CO in active sites that are in close proximity (70 Å) thus potentially reducing the effects of CO toxicity. This multi-enzyme complex organisation is commonly found in certain groups of prokaryotes including methanogens (Ragsdale 2004, Techtmann *et al.* 2012).

## 1.7 Genomic and proteomic insights

With the expansion of the knowledge base regarding molecular phenomena behind cell life of microorganisms, increasing amounts of information can be derived from sources beyond physiological observations of cultured organisms.

Molecular biology of microorganisms starts at the DNA level which encompasses the sum of all genetic directives for cell function. These molecules can be transcribed into messenger RNA, that in turn is translated into proteins. The latter are then responsible for most cellular functions including the synthesis of base components for the aforementioned biomolecules (Figure 11).

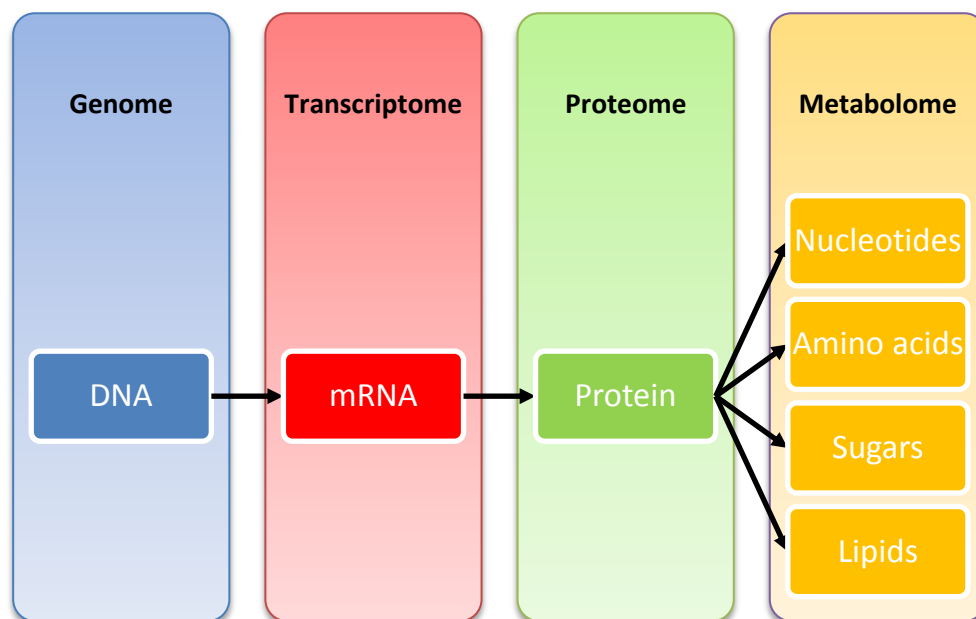


**Figure 11 – Genomic, transcriptomic, proteomic and metabolomic approaches that can be used for the study of microbial metabolism.**

### 1.7.1 Genomics

Genomic approaches to the study of microorganisms can be a valuable tool for acquiring a full overview of their functional potential. A significant amount of information can be derived from the detailed analysis of the genome of specific organisms such as the ability to metabolize previously untested substrates. Furthermore, comparison of gene sequences are the basis of the construction of phylogenetic trees.

The first archaeon with a fully sequenced genome was *M. jannaschii* in 1996 (Bult *et al.* 1996). Since then, a considerable number of archaeal species have had their genome sequenced.

Analysis of microbial genomes have demonstrated that CODH is ubiquitous amongst both bacterial and archaeal species. Extensive comparative genomic examination of the CODH coding sequences and their neighbourhood has allowed for some interesting insights into this protein complex

phylogeny bringing evidence of evolution of CODH by both vertical transmission and horizontal gene transfer (Techtmann *et al.* 2012).

### 1.7.2 Transcriptomics

Transcriptomic analyses consist in the observation of the expression level of genes in a given environment. It can provide crucial insight into the response mechanisms of a given organism since only expressed genes are being analysed.

Studies conducted for the transcriptome of several species subjected to the presence of CO have given information on gene clusters induced by this substrate. Unsurprisingly, these include the *cox* and *cdh* operons coding for Mo-CODH and Ni,Fe-CODH respectively (Santiago *et al.* 1999, Matschiavelli *et al.* 2012). In addition, transcriptomic data performed on methanogens have shown differences of the induction of genes related to methanogenesis (Lessner *et al.* 2006, Zhou *et al.* 2013).

Furthermore, comparative observation of the transcriptome under high and low levels of H<sub>2</sub>, such as the study conducted for *M. thermotrophicus*, provide clues about alternative pathways that can be used under H<sub>2</sub>-independent growth (de Poorter *et al.* 2007).

### 1.7.3 Proteomics

Despite all the data that can be derived from the transcriptome, mRNA molecules are relatively unstable when compared to proteins and not all are necessarily transcribed. Furthermore, post-translational modifications can occur and protein abundance levels are not necessarily strictly paralleled by the amount of corresponding mRNA present. These characteristics limit the usefulness of this approach for accurate determination of the current functions displayed by the cell in response to specific stimuli. Within that context, proteomic analysis can be of paramount importance to further expand the current understanding of cell biology.

Traditionally, proteomic analysis is conducted through protein separation by two-dimensional gel electrophoresis, a technique first demonstrated in 1975 (O'Farrell 1975). High-efficiency chromatographic peptide separation, together with mass spectrometry has advanced significantly this field of study allowing for better protein identification. Together with the development of robust bioinformatics tools, this method allows for a more reliable, less labour intensive and higher throughput analysis (Maron *et al.* 2007).

In relation to the known carboxidotrophic methanogens, adequate proteomic analysis comparing growth on CO to other substrates has only been performed for *M. acetivorans*. These studies evidence a novel pathway for methanogenesis in CO-grown cells (Rother *et al.* 2007).

Molecular biology techniques are being developed at an accelerated rate. These methods combined with potent bioinformatics tools provide previously unworkable approaches to understand cell life. Consequently, analysis of the genome and proteome are now routinely used to provide further insights in functions and interactions within microbial communities and to predict environmental responses. Moreover, the combination of the different approaches have the potential for further elucidating complex biological phenomena and reveal previously unidentified connections between biochemical processes and biological functions.

## 2 Materials and methods

### 2.1 Comparative genomic analysis for selection of candidates

Comparative genomic analysis for selection of candidates was performed using the tools available at the IMG/JGI website (Markowitz *et al.* 2014)

### 2.2 Source of microorganisms

Microorganisms used in this work (Table 1) were obtained from the Leibniz Institute DSMZ – German collection of Microorganisms and Cell Cultures.

Table 2 - Methanogenic microorganisms used in this work

| Code | Name   | DSM Id   | pH <sub>opt</sub> | t <sub>d</sub><br>(h) | T <sub>opt</sub><br>(°C) |
|------|--|----------|-------------------|-----------------------|--------------------------|
| mja  | <i>Methanocaldococcus jannaschii</i>             | DSM2661  | 6.0               | 0.433                 | 85                       |
| mka  | <i>Methanopyrus kandleri</i> AV19                | DSM6324  | 6.5               | 0.83                  | 98                       |
| mmg  | <i>Methanothermobacter marburgensis</i>          | DSM2133  | 6.8-7.4           | ----                  | 65                       |
| mth  | <i>Methanothermobacter thermautotrophicus</i> ΔH | DSM1053  | 7.2-7.6           | 1.486                 | 65                       |
| mmp  | <i>Methanococcus maripaludis</i> S2              | DSM14266 | 6.8               | 0.667                 | 37                       |
| msi  | <i>Methanobrevibacter smithii</i> PS             | DSM861   | 6.9-7.4           | -----                 | 38                       |
| mru  | <i>Methanobrevibacter ruminantium</i>            | DSM1093  | 6.3-6.8           | -----                 | 33                       |

Cultures were grown in 120 mL pressurized serum bottles with a liquid phase of 50 mL (unless otherwise stated) under strictly anaerobic conditions based on the principles established by Hungate and improved by Bach and Wolf (Hungate 1950, Hungate and Macy 1973, Balch and Wolfe 1976)

*Methanothermobacter thermautotrophicus* and *Methanothermobacter marburgensis* were incubated at 65 °C with and without shaking (70 rpm) as specified. *Methanocaldococcus jannaschii* was grown at 85°C with 100rpm shaking and *Methanococcus maripaludis* were grown at 85 °C, 120 rpm and 37 °C, 100 rpm respectively.

### 2.3 Medium composition and cultivation

*Methanothermobacter thermautotrophicus*, *Methanothermobacter marburgensis*, *Methanobrevibacter smithii* and *Methanobrevibacter ruminantium*, were grown in 50 mL of bicarbonate buffered mineral salts medium containing the following per litre: 0.408g KH<sub>2</sub>PO<sub>4</sub>, 0.534g Na<sub>2</sub>HPO<sub>4</sub>·2H<sub>2</sub>O, 0.3g NH<sub>4</sub>Cl, 0.3g NaCl, 0.1g MgCl<sub>2</sub>·6H<sub>2</sub>O, 0.11g CaCl<sub>2</sub>·2H<sub>2</sub>O, 4g NaHCO<sub>3</sub>, 0.24g

Na<sub>2</sub>S.9 H<sub>2</sub>O and 0.5g of yeast extract, 0.0005g of resazurin, Trace elements H<sup>+</sup> trace elements OH<sup>-</sup> and vitamins. The pH of finished media was around 7. The headspace was composed either of H<sub>2</sub>/CO<sub>2</sub> (80:20) or N<sub>2</sub>/CO<sub>2</sub> (80:20) and increasing amounts of CO as specified.

Medium for *Methanocaldococcus jannaschii* was composed of: 0.14g K<sub>2</sub>HPO<sub>4</sub>, 0.534g Na<sub>2</sub>HPO<sub>4</sub>.2H<sub>2</sub>O, 0.25g NH<sub>4</sub>Cl, 30g NaCl, 4.1g MgCl<sub>2</sub>.6H<sub>2</sub>O, 0.14g CaCl<sub>2</sub>.2H<sub>2</sub>O, 1g NaHCO<sub>3</sub>, 0.24g Na<sub>2</sub>S.9 H<sub>2</sub>O and 0.5g of Yeast Extract, 0.0005g of Resazurin, 1ml of trace elements H<sup>+</sup>, 1ml trace elements OH<sup>-</sup> and vitamins. The pH of finished media was around 7. The headspace was composed either of H<sub>2</sub>/CO<sub>2</sub> (80:20) or N<sub>2</sub>/CO<sub>2</sub> (80:20) and increasing amounts of CO as specified.

*Methanococcus maripaludis* was inoculated in medium with the following components per litre: 0.34g KCl, 0.14g K<sub>2</sub>HPO<sub>4</sub>, 0.25g NH<sub>4</sub>Cl, 18g NaCl, 4g MgCl<sub>2</sub>.6H<sub>2</sub>O, 3.45g MgSO<sub>4</sub>.7H<sub>2</sub>O, 2g Fe(NH<sub>4</sub>)<sub>2</sub>(SO<sub>4</sub>)<sub>2</sub>.6H<sub>2</sub>O, 1g NaCH<sub>3</sub>CO<sub>2</sub>, 0.11g CaCl<sub>2</sub>.2H<sub>2</sub>O, 5g NaHCO<sub>3</sub>, 0.50g Na<sub>2</sub>S.9 H<sub>2</sub>O and 0.5g of yeast extract, 0.0005g of resazurin, Trace elements H<sup>+</sup> trace elements OH<sup>-</sup> and vitamins. The pH of finished media was around 7. The headspace was composed either of H<sub>2</sub>/CO<sub>2</sub> (80:20) or N<sub>2</sub>/CO<sub>2</sub> (80:20) and increasing amounts of CO as specified at a total pressure of 1.7 bar.

*Methanopyrus kandleri* medium has the following components per litre: 0.07g K<sub>2</sub>HPO<sub>4</sub>, 0.534g Na<sub>2</sub>HPO<sub>4</sub>.2H<sub>2</sub>O, 0.25g NH<sub>4</sub>Cl, 11.8g NaCl, 4.5g MgCl<sub>2</sub>.6H<sub>2</sub>O, 0.78g CaCl<sub>2</sub>.2H<sub>2</sub>O, 1g NaHCO<sub>3</sub>, 1g Na<sub>2</sub>S.9 H<sub>2</sub>O and 0.0005g of Resazurin, 1ml of trace elements H<sup>+</sup>, 1ml trace elements OH<sup>-</sup> and vitamins. The pH of finished media was around 6.5. The headspace was composed either of H<sub>2</sub>/CO<sub>2</sub> (80:20) or N<sub>2</sub>/CO<sub>2</sub> (80:20) and increasing amounts of CO as specified.

The acid trace elements solution used for all three media contained 1.8g HCl, 61.8 mg H<sub>3</sub>BO<sub>3</sub>, 61.25 mg MnCl<sub>2</sub>, 943.5 mg FeCl<sub>2</sub>, 64.5 mg CoCl<sub>2</sub>, 12.86 mg NiCl<sub>2</sub>, 67.7 mg ZnCl<sub>2</sub> per litre. Alkaline trace elements solution was composed of 400 mg NaOH, 17.3 mg Na<sub>2</sub>SeO<sub>3</sub>, 29.4 mg Na<sub>2</sub>WO<sub>4</sub>, 20.5 mg Na<sub>2</sub>MoO<sub>4</sub> per litre. Vitamins used were 20 mg Biotin, 200 mg Nicotinamid, 100 mg p-Aminobenzoic acid, 200 mg Thiamin (Vit B1), 100 mg Panthotenic acid, 500 mg Pyridoxamine, 100 mg Cyanocobalamine (Vit B12) and 100 mg Riboflavine.

**Table 3 – Operational conditions**

| Code       | Shaking<br>(rpm) | pH  | T (°C) |
|------------|------------------|-----|--------|
| <b>mru</b> | 100              | 7.0 | 37     |
| <b>msi</b> | 100              | 7.0 | 37     |
| <b>mja</b> | 120              | 6.0 | 85     |
| <b>mka</b> | --               | 6.5 | 98     |
| <b>mmg</b> | 70               | 7.0 | 65     |
| <b>mth</b> | 70               | 7.0 | 65     |
| <b>mmp</b> | 100              | 7.0 | 37     |

## 2.4 Adaptation studies

Adaptation studies were performed in 120 ml pressurized serum bottles with increasing amounts of CO in the headspace according to schematic in Figure 12 and aforementioned growth conditions. Cultures were routinely transferred (2% v/v of inoculum/media ratio) whenever all available electron donors were depleted or when CO was no longer being removed from the headspace for a considerable amount of time. Whenever robust growth and/or consumption of CO were detected in a syngas mixture, culture was also transferred into bottles with higher percentages of CO and bottles without H<sub>2</sub> in the headspace. If growth was successful in these conditions, subsequent transfers maintained the gas ratio.

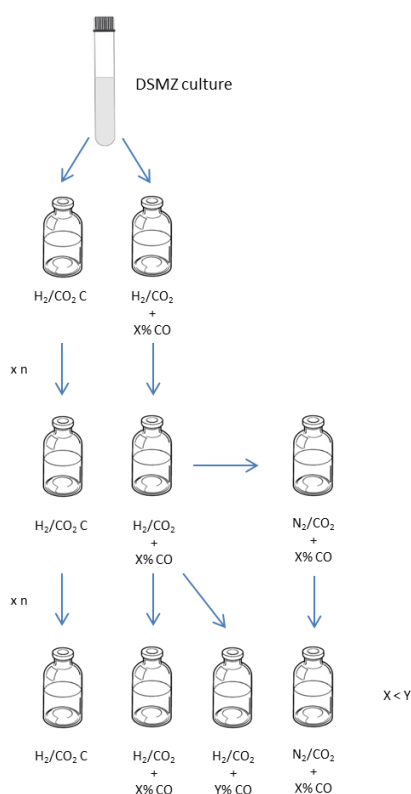


Figure 12 – Schematic of adaptation protocol

## 2.5 Microscopy

Cultures were regularly observed by phase contrast microscopy using a Leica DM 2000 microscope equipped with 100X magnification objective and a Leica DMC 2900 camera.

For fluorescence microscopy, a Leica DMR microscope equipped with a Leica DFC340FX camera was used. Fluorescence was observed utilizing a LEJ EBQ 100 Isolated Z Ballast Illuminator Mercury lamp for UV excitation.

## 2.6 Analytical techniques

### 2.6.1 GC measurements

Variations on the concentration of gaseous compounds (H<sub>2</sub>, CH<sub>4</sub>, CO and CO<sub>2</sub>) in the cultures' headspace were followed by gas chromatography using a GC-2014 from Shimadzu equipped with a thermal conductivity detector and possessing two separate measuring columns. H<sub>2</sub>, CH<sub>4</sub> and CO were measured in a Molsieve 13X column with dimensions of 2m in length and 3mm of inner diameter. Argon and helium were used as carrier gases at a flow rate of 50 ml/min and the injector, column and detector were set to 80, 60 and 130°C, respectively. CO<sub>2</sub> was assayed separately in a CP Paraplot column of 25 m x 0.53 mm, with a stationary phase film thickness of 20 µm, employing helium as carrier gas at a flow rate of 15 ml/min. For this column, the temperatures used were of 60 °C for the injector, 34°C for the column and 130°C for the detector.

Variations of gaseous compounds (H<sub>2</sub>, CH<sub>4</sub>, CO and CO<sub>2</sub>) in culture headspace were followed by means of gas chromatography using a GC-2014 from Shimadzu equipped with a thermal conductivity detector and possessing two separate measuring columns. H<sub>2</sub>, CH<sub>4</sub> and CO were measured in a Molsieve 13X column with dimensions of 2m in length and 3mm of inner diameter. Argon and helium were used as carrier gases at a flow rate of 50 ml/min and the injector, column and detector were set to 80, 60 and 130°C, respectively. CO<sub>2</sub> was assayed separately in a CP Paraplot column of 25 m x 0.53 mm, with a stationary phase film thickness of 20 µm, employing helium as carrier gas at a flow rate of 15 ml/min. For this column, the temperatures used were of 60 °C for the injector, 34°C for the column and 130°C for the detector.

### 2.6.2 HPLC measurements

Soluble compounds were determined using LKB high-performance liquid chromatograph (HPLC) with a Varian Metacarb 67H 300mm column. Mobile phase used was 0.01N of sulfuric acid at a flow rate of 0.8 ml/min and column temperature was set to 60 °C.

## 2.7 Protein Extraction for LC-MS/MS analysis

For protein extration cells were cultured in 1 litre anaerobic bottles and harvested at late exponential phase. Cultures were centrifuged and pellet was resuspended in TE buffer (10 mM Tris-Cl, pH 7.5; 1 mM EDTA). Protein extraction was then attempted by two methods:

- Centrifugation and resuspension of pellet in SDT lysis buffer (100mM Tris -Cl pH 7.5; 4% sodium dodecyl sulphate ; 0.1M dithiotreitol) followed by sonication cycles on 30s with 30 second intervals;

- Resuspending centrifuged pellet with TE buffer with phenylmethanesulfonyl fluoride, and passing cell suspensions through a French pressure cell operated at 138 megapascals.

Proteins were stabilized by addition of 8M of urea in a proportion of 1:1 and samples were concentrated using a 3.5 kDa MWCO filter.

Final protein concentration in samples obtained for LC-MS/MS analysis was assessed using several methods including Qubit® Protein Assay Kit in a Qubit® 2.0 Fluorometer (Life technologies), 2D-Quant kit (Amersham Biosciences) and BCA protein assay kit (Pierce).

## 2.8 LC-MS/MS analysis

Samples for LC-MS/MS analysis were sent to be analysed by the Proteomics centre in Radboud University of Nijmegen.

Experiments were performed on a 7-tesla Finnigan LTQ-FT mass spectrometer (Thermo Electron) equipped with a nanoelectrospray ion source (Proxeon Biosystems, Odense, Denmark). The LC part of the analytical system consisted of an Agilent Series 1100 nanoflow LC system (Waldbronn, Germany) comprising a solvent degasser, a nanoflow pump, and a thermostated microautosampler. Chromatographic separation of the peptides was performed in a 15-cm fused silica emitter (100- $\mu$ m inner diameter; New Objective) packed in-house with methanol slurry of reverse-phase ReproSil-Pur C18-AQ 3- $\mu$ m resin (Dr. Maisch GmbH, Ammerbuch-Entringen, Germany) at a constant pressure (20 bars) of helium. Then 5  $\mu$ l of the tryptic peptide mixtures were autosampled onto the packed emitter with a flow of 600 nl/min for 20 min and then eluted with a 5-min gradient from 3 to 10% followed by a 25-min gradient from 10 to 30% acetonitrile in 0.5% acetic acid at a constant flow of 300 nl/min. The mass spectrometer was operated in the data-dependent mode to automatically switch between MS and MS/MS acquisition. Survey MS spectra (from m/z 350 to 2,000) were acquired in the FTICR with  $r = 50,000$  at m/z 400 (after accumulation to a target value of 1,000,000). The three most intense ions were sequentially isolated for fragmentation in the linear ion trap using collisionally induced dissociation with normalized collision energy of 29% and a target value of 1,000. Former target ions selected for MS/MS were dynamically excluded for 30 s. Total cycle time was  $\sim 3$  s.

Proteins were identified via automated database searching (Matrix Science, London, UK) of all tandem mass spectra against both NCBI nr and an in-house curated *M. thermotrophicus* database. Carbamidomethylcysteine was set as fixed modification, and oxidized methionine and protein N-acetylation were searched as variable modifications. Initial mass tolerances for protein identification on MS and MS/MS peaks were 10 ppm and 0.5 Da, respectively. The instrument setting for the MASCOT search was specified as "ESI-Trap."

### 3 Results and Discussion

The main objective of this work was to get insight on methane metabolism of carboxidotrophic archaea, combining physiological studies with genomic and proteomic approaches. The work consisted of 3 main stages:

- Genomic screen of methanogens for CO-dehydrogenases (CODH) genes - selection of methanogens containing these genes for further physiological tests
- CO conversion tests and adaptation studies - incubation of the selected methanogens with CO and CO/H<sub>2</sub>
- Cultivation and protein extraction methods for (improved) LC-LC MS/MS-based proteomics of CO-converting methanogens.

Note: Proteomics analysis is not performed at our lab; proteins were sent for analysis to an external company but, due to time restrictions, it was not possible to have the results on time to include on this thesis.

## 3.1 Selection of methanogenic candidates

### 3.1.1 Genomic comparison of methanogens for potential carboxidotrophic abilities

As previously mentioned, the number of methanogens known to be capable of growth using carbon monoxide as sole carbon and energy source is relatively low, consisting of only 4 so far - *Methanosarcina barkeri*, *Methanosarcina acetivorans*, *Methanothermobacter thermautotrophicus* strain  $\Delta H$ , and *Methanobrevibacter arboriphilicus*. *M. barkeri* and *M. acetivorans* have recently been the subject of several studies, including very detailed proteomic analysis of the mechanisms behind carboxidotrophy for the latter (Lessner *et al.* 2006, Maeder *et al.* 2006, Rother *et al.* 2007). From the other two methanogens, only *M. thermautotrophicus* strain  $\Delta H$  has a fully annotated genome publically available at present. Even though *M. thermautotrophicus* was the first methanogen identified as capable of growth on CO, a thorough proteomic analysis related to the use of this substrate has yet to be performed for this species. Nevertheless, in the context of biological biomethanation of syngas with high CO percentages, this is a promising focus group for the further understanding of carboxidotrophy (Daniels *et al.* 1977, Alves 2013, Markowitz *et al.* 2014)-.

To eventually perform an adequate proteomic analysis for carboxidotrophy, an annotated genome sequence is advantageous. Therefore, the first step of this work was to canvas the JGI database for methanogens that possess a finished version of their genome. This selection resulted in a total of 51 archaeal candidates.

While the full requirements for carboxidotrophy remain unknown, the presence of carbon monoxide dehydrogenase (CODH) is naturally thought of as a key factor due to its known ability to convert CO into CO<sub>2</sub>, the initial substrate in hydrogenotrophic methanogenesis. Hence, an initial assessment of the presence of this protein complex was performed. For this purpose, the alpha subunit was chosen since it contains within its structure the catalytic site for this enzyme. Such analysis further reduced the previous list to 37 potential candidates.

To further select for methanogenic candidates for hydrogenotrophic carboxidotrophy, the physiological and genomic data available for *M. thermautotrophicus* was used as a basis for comparison with other hydrogenotrophic methanogens. This archaeon possesses one copy of CODH in its genome (vide Figure 13). For homologue comparison of the putative carboxidotrophs, the alpha subunit of the CODH protein complex was selected. This choice was due to the localization of the catalytic centre within the structure of this subunit. The full results from this alignment can be found on Table 8 in Annex I. A selection is presented in Figure 13 in the form of a phylogenetic tree.



Looking at the sequence alignment results, *M. marburgensis* rises above the rest as the methanogen that possesses a CODH/ACS alpha subunit with the closest similarity to the one from *M. thermautotrophicus* with an identity value of 93.7% (well above the second closest hit for *Methanobacterium* sp. SWAN-1 with 73.5%). Furthermore, the genome of this archaea seems to code for an additional set of catalytic subunits for CODH. This makes it a prime candidate for testing for carboxydrotrophy in this study.

This comparison is being performed with a CODH/ACS alpha subunit type enzyme since is the one present in *M. thermautotrophicus*. However there are other types of catalytic CODH subunits that can be present as discussed below.

### 3.1.2 Further selection by literature search

While the full scale analysis of the relatedness of the genome/CODH genes between the known carboxydrotroph (*M. thermautotrophicus*) provides crucial data for the selection, further refinement of the list was needed. With that purpose, an extensive literature search for promising physiological observations was conducted.

For *M. marburgensis*, the species on the top of the previously mentioned list, some studies regarding the metabolism of CO had been conducted but with growth on this substrate alone being unsuccessful. However it was recently noted that methyl-coenzyme M reductase (MCR) synthesis was induced by the presence of CO. MCR is the enzyme involved in the last step of methanogenesis (*vide* Figure 15) and thus one would expect it to be induced in conditions where this pathway could be performed. This observation further supports *M. marburgensis* status as a prime testing candidate (Zhou *et al.* 2013).

Due to its status as the first fully sequenced archaeon, *M. jannaschii* has been the target of several comparative genomic studies, including an in-depth side by side analysis with *M. thermautotrophicus*. This study detailed the key similarities and differences between the methanogenic metabolisms of the two. Looking at the genome of this species, it not only codes for the CODH/ACS alpha subunit that was previously mentioned, but also for a CooS type CODH catalytic subunit which could be favourable towards its carboxidrotrophic potential. Furthermore, proteomic analysis of methanogenesis (using H<sub>2</sub> as electron donor) has been conducted (Bult *et al.* 1996, Tersteegen and Hedderich 1999, Zhu *et al.* 2004, Kaster *et al.* 2011).

*Methanococcus maripaludis* S2 also possesses a relatively high sequence similarity with *M. thermautotrophicus* alpha subunit CODH. A recent study tested for growth with CO and formate but there is no indication of what would happen with only CO as an electron donor. Considering the already identified use of CO as a carbon source and the ability to perform the methanogenesis by an H<sub>2</sub>-independent pathway, the potential for growth on this substrate alone is considerable (Costa *et al.* 2013).

Out of all methanogens whose carboxidrotrophic ability has yet to be proven, *M. kandleri* AV19 seems to be one with the highest number of diverse CODH coding regions in its genome. The

conducted analysis showed already two dissimilar copies of CO dehydrogenase/acetyl-CoA synthase alpha subunit inside the same operon but another type of CODH can also be found: a *cooS* type CODH. This totals 3 CODH coding regions which make this hyperthermophile second only to *M. acetivorans*, the carboxidotrophic methanogen that presents the fastest growth on CO with 5 different CODH coding regions (Rother and Metcalf 2004, Techtmann *et al.* 2012).

Finally, in the same study that first described *M. thermotrophicus* ability to grown on CO as sole carbon and energy source, several other organisms were briefly mentioned as removing CO from the headspace (in the presence of H<sub>2</sub>). Amongst them were *Methanobrevibacter smithii* and *Methanobrevibacter ruminantium*. Considering their absence from the above mentioned list, this might seem surprising. Their genome does not seem to code for a CODH/ACS enzyme and therefore, considering the premise used that CODH is a necessary requirement for the conversion of CO, such results seem contradictory. Therefore, these two organisms were added to the already selected candidates as a counterpoint to this assumption (Daniels *et al.* 1977).

### 3.1.3 Final candidate list for physiological tests

In conclusion, this analysis yielded the candidate list presented in Table 4. As can be easily perceived through that list, there is a wide variety of optimum growth temperatures and the set includes three mesophiles, two thermophiles and two hyperthermophiles.

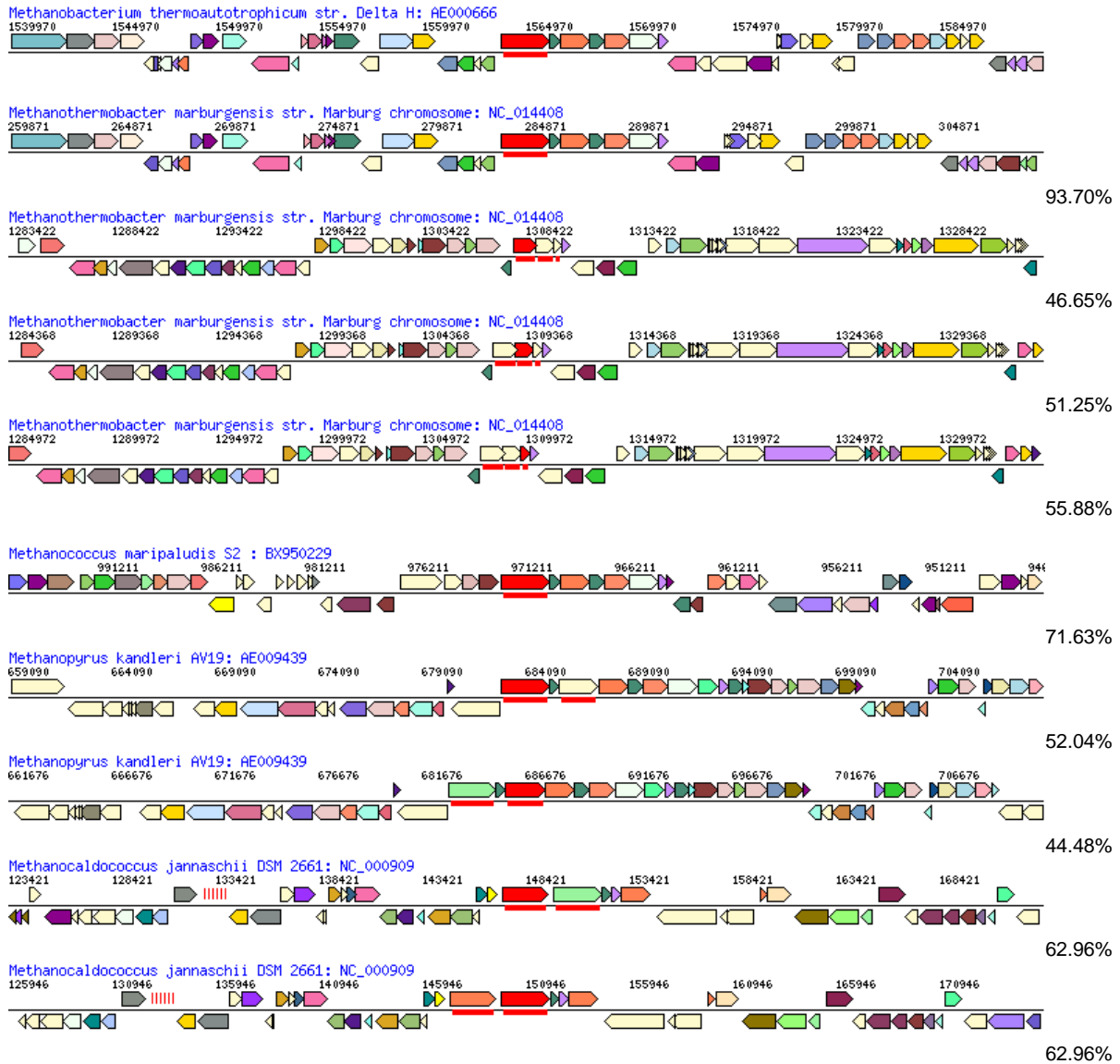
**Table 4 – Selected candidates for testing and their physiological characteristics**

| Code | Name  | DSM Id                   | pH <sub>min</sub> | pH <sub>opt</sub> | pH <sub>max</sub> | t <sub>d</sub> (h) | T <sub>min</sub> (°C) | T <sub>opt</sub> (°C) | T <sub>max</sub> (°C) |
|------|---|--------------------------|-------------------|-------------------|-------------------|--------------------|-----------------------|-----------------------|-----------------------|
| mru  | <i>Methanobrevibacter ruminantium</i> M1      | <a href="#">DSM1093</a>  | ----              | 6.3-6.8           | ----              | ----               | ----                  | 33                    | ----                  |
| msi  | <i>Methanobrevibacter smithii</i> PS          | <a href="#">DSM861</a>   | ----              | 6.9-7.4           | ----              | ----               | ----                  | 37-39                 | ----                  |
| mja  | <i>Methanocaldococcus jannaschii</i>          | <a href="#">DSM2661</a>  | 5.2               | 6.0               | 7.0               | 0.433              | 50                    | 85                    | 85                    |
| mka  | <i>Methanopyrus kandleri</i> AV19             | <a href="#">DSM6324</a>  | 5.5               | 6.5               | 7                 | 0.83               | 84                    | 98                    | 110                   |
| mmg  | <i>Methanothermobacter marburgensis</i>       | <a href="#">DSM2133</a>  | 5                 | 6.8-7.4           | 8                 | ----               | 45                    | 65                    | 70                    |
| mth  | <i>Methanothermobacter thermotrophicus</i> ΔH | <a href="#">DSM1053</a>  | 6                 | 7.2-7.6           | 8.8               | 1.486              | 40                    | 65                    | 70                    |
| mmp  | <i>Methanococcus maripaludis</i>              | <a href="#">DSM14266</a> | 6                 |                   | 8                 | 0.667              | 37                    | 37                    | 37                    |

As for their CODH coding regions, the basis for the selection study, they are present below in Figure 14.

***Cdh* type CODH**

Sequence  
similarity



***CooS* type CODH**

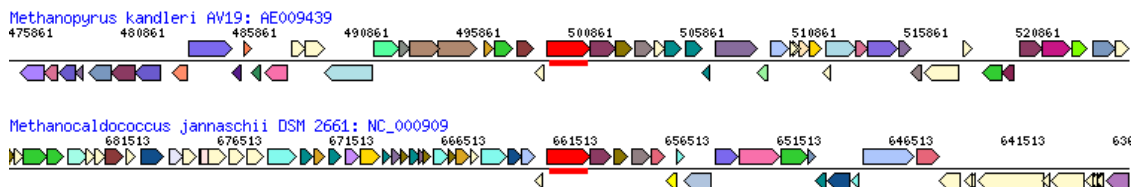


Figure 14 – Gene topology of CODH/ACS alpha subunit neighbourhood for selected strains. Aligned CODH catalytic subunit coding genes are marked in red.

While the selection of candidates was focused on the CODH enzymes due to its primary role in carboxydutrophy, it should be expected that some of the different enzymes involved in the methanogenesis pathway might play a substantial role as well. In particular, reducing steps in this pathway are of primary concern due to their requirement for electrons that need to be provided, directly or indirectly, by CO-oxidation. Figure 15 summarizes the main enzymes (and their respective coding genes) involved during the subsequent steps of methanogenesis:

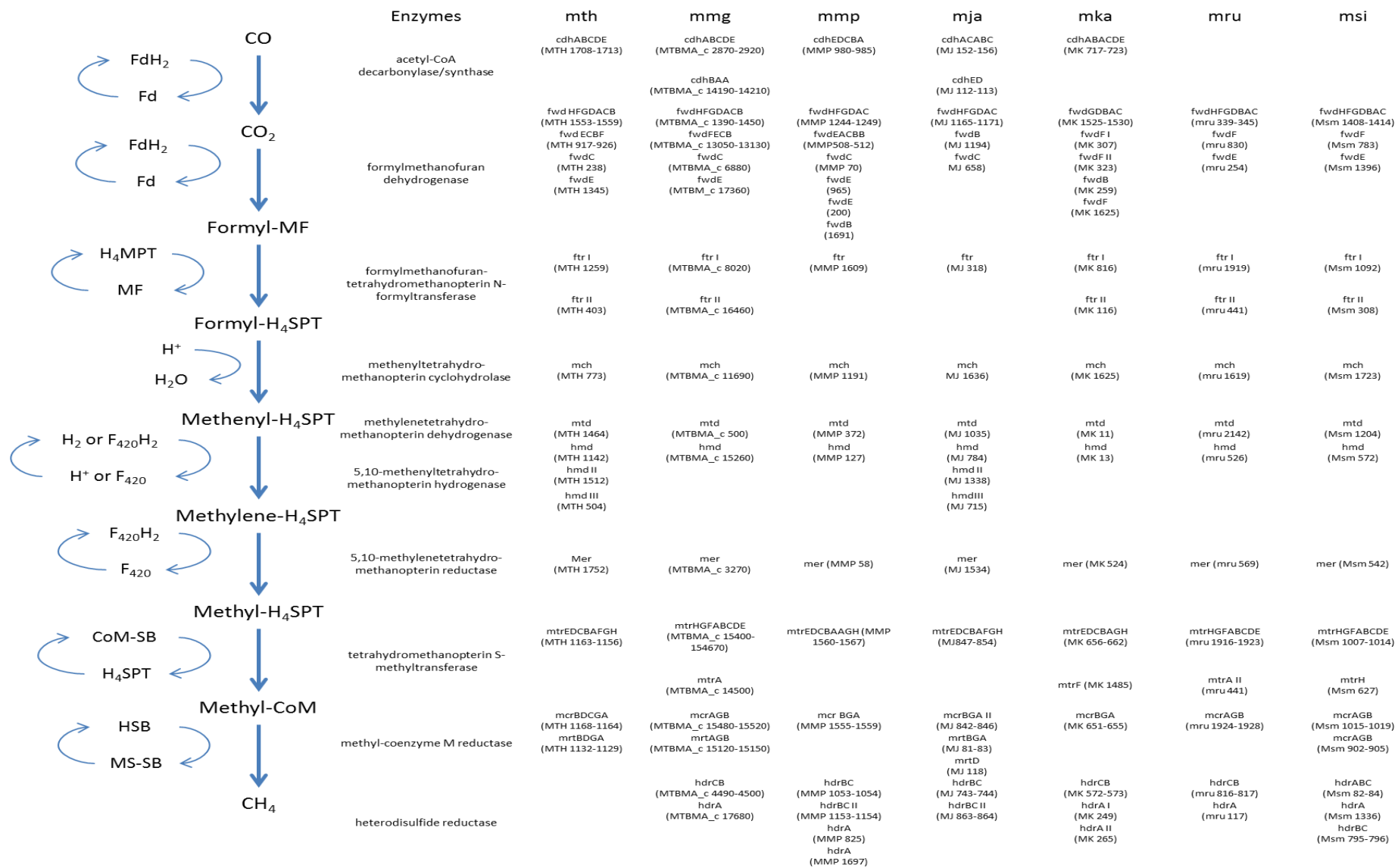


Figure 15 – Overview of the presence of possible genes involved in the putative pathway for carboxidotrophic methanogenesis in selective strains

### 3.2 Growth characteristics of selected methanogens in the presence of CO

All cultures were grown as described previously in the material and methods chapter, in the presence of different concentrations of CO or CO/H<sub>2</sub>. Table 5 summarizes the results of the adaptation studies for *Methanothermobacter thermautotrophicus*, *Methanothermobacter marburgensis*, *Methanothermococcus jannaschii* and *Methanococcus maripaludis* – which are the methanogenic species that were shown to use CO/H<sub>2</sub> from the headspace. Furthermore, *Methanothermobacter* strains could also grow on CO as sole carbon and energy source.

Contrastingly, under the experimental conditions available, *M. smithii*, *M. ruminantium* and *M. kandleri* cultures had difficulty growing. Growth of *M. smithii* and *M. ruminantium*, was sluggish even with the addition of growth supplements such as rumen fluid. Due to the short timeframe nature of the work and for the purpose of having a more comparable group in terms of growth requirements, research on these two organisms was discontinued. Regarding *M. kandleri* cultures, grown cultures revealed themselves to be sensitive to the experimental setup defined. Particularly, the cooling down and heating up cycles necessary for batch sampling of the serum bottles by gas chromatography seemed to be a problem. While the first transfers under H<sub>2</sub>/CO<sub>2</sub> grew successfully, growth with CO in the headspace was unsuccessful even at low concentrations 5% (0.15 bar of partial pressure). Additionally, further transfers of the control had their growth severely compromised and eventually no discernible growth could be detected either by gas chromatography or by microscopic visualization within a reasonable timeframe (10 times of what it took for the initial inoculation for the control).

Based on growth experiments on CO/H<sub>2</sub>, subsequent work was performed with the following strains: *M. thermautotrophicus*, *M. marburgensis*, *M. maripaludis* and *M. jannaschii*.

**Table 5 – Overview of growth success with CO in the headspace for the cultures tested**

| Species                      | Code | Growth with CO in headspace |              | Growth with CO as sole carbon and energy source |              |
|------------------------------|------|-----------------------------|--------------|---|--------------|
|                              |      | Result                      | Range tested | Result  | Range tested |
| <i>M. ruminantium</i>        | mru  | -                           | 0-15%        | -   | -            |
| <i>M. smithii</i>            | msi  | -                           | 0-15%        | -   | -            |
| <i>M. jannaschii</i>         | mja  | +                           | 0-40%        | -   | -            |
| <i>M. kandleri</i>           | mka  | -                           | 0-40%        | -   | -            |
| <i>M. marburgensis</i>       | mmg  | +                           | 0-60%        | +   | 10-50%       |
| <i>M. thermautotrophicus</i> | mth  | +                           | 0-40%        | +   | 10-30%       |
| <i>M. maripaludis</i>        | mmp  | +                           | 0-90%        | -   | -            |

### 3.3 Physiological observations/effects of CO

#### 3.3.1 Inhibition by carbon monoxide

For the purpose of testing the inhibition imparted by the presence of CO in the organisms tested, cultures grown in H<sub>2</sub>/CO<sub>2</sub> (80/20%, v/v) were transferred to bottles with increasing CO concentrations. If growth was observed, subsequent transfers to higher concentrations were attempted. Table 6 offers an overview of the inhibition observed.

**Table 6 - Inhibition by carbon monoxide on the production of methane for tested strains**

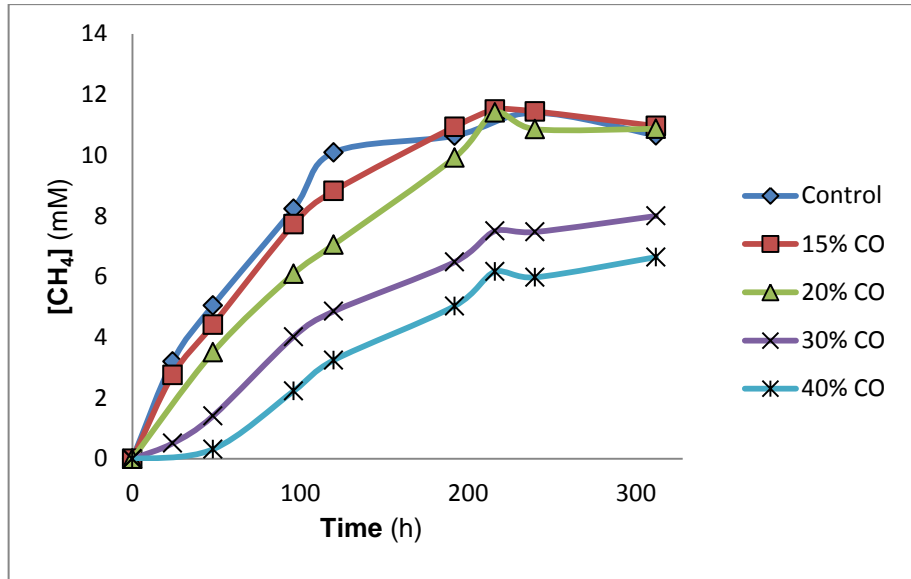
| Code       | Number of transfers | [CO] tested | CH <sub>4</sub> production rates (mM/h) |
|------------|---------------------|-------------|---|
| <b>mth</b> | 6                   | 15-40%      | 0.06-0.02                               |
| <b>mmg</b> | 12                  | 5-60%       | 0.32-0.06                               |
| <b>mja</b> | 4                   | 5-40%       | 0.93-0.16                               |
| <b>mmp</b> | 7                   | 5-90%       | 0.38-0.0004                             |

All archaea tested demonstrated inhibition by CO in some form. From the studies conducted in this work, it can be observed that inhibition was systematically increased with higher partial pressures of CO (Figure 16).

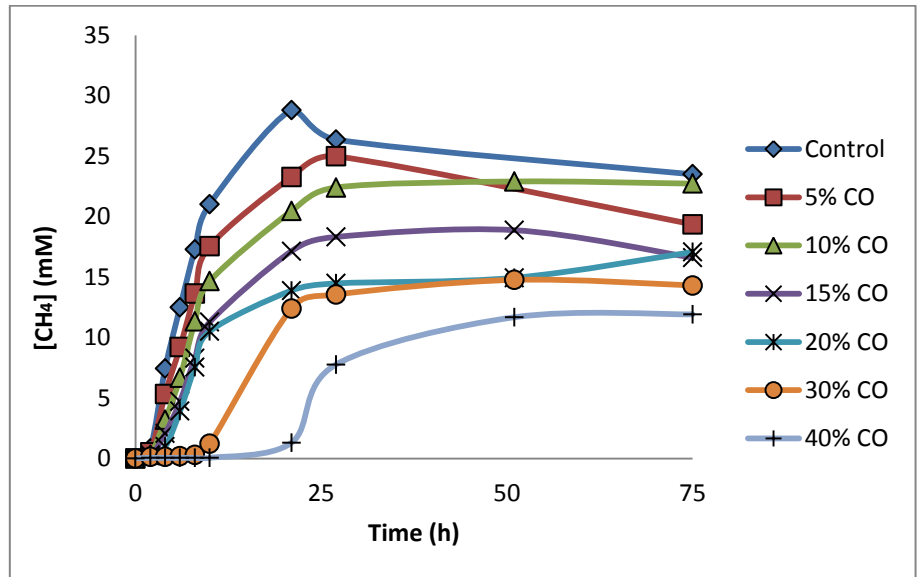
Comparing the methane production profiles of successive transfers for the same concentrations of CO, there was however no significant changes, indicating that these transfers were not strongly effective in attenuating the inhibition observed (Figure 17). The differences observed can be mostly attributed to modifications in the experimental setup factors such as changes in shaking speed and yeast extract concentration (both of which are discussed in more detail in sections 3.4.1.2 and 3.4.1.4 respectively).

It is known that one of the major obstacles for utilisation of carbon monoxide by microorganisms is the inherent toxicity of this gas to their metabolism mostly in the form of the high affinity of this compound to the metal centres of the organometallic enzymes. Of particular importance, in this case, are the hydrogenases which have been known to be inhibited by the presence of CO in other studies. It is therefore feasible to think that some differences in the hydrogenase system could justify differences in adaptability of different strains. Another possibility would be a response that would lower the internal levels of CO inside the cells. Ragsdale has suggested the presence of a gas channel inside the CODH/ACS complex with such purpose (Figure 19). By binding the CO molecules to the protein complex, it reduces its toxicity to other important enzymes such as the hydrogenases. As was assessed in section 3.1.1 during the genomic comparison of the CODHs of these methanogens, all strains tested possess CODH/ACS complexes which can convert CO to other, less toxic metabolites (CO<sub>2</sub> and acetyl-coA).

*M. thermautotrophicus*  
(2<sup>nd</sup> transfer)



*M. jannaschii*  
(2<sup>nd</sup> transfer)



*M. maripaludis*  
(2<sup>nd</sup> transfer)

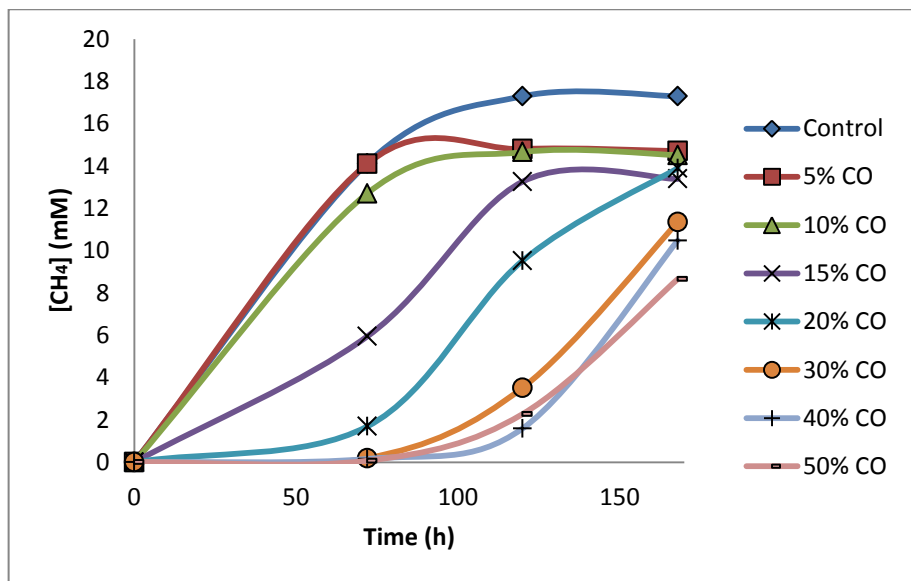


Figure 16 - Effects of inhibition in the production of methane with increasing concentrations of CO for different tested strains.

*M. marburgensis*

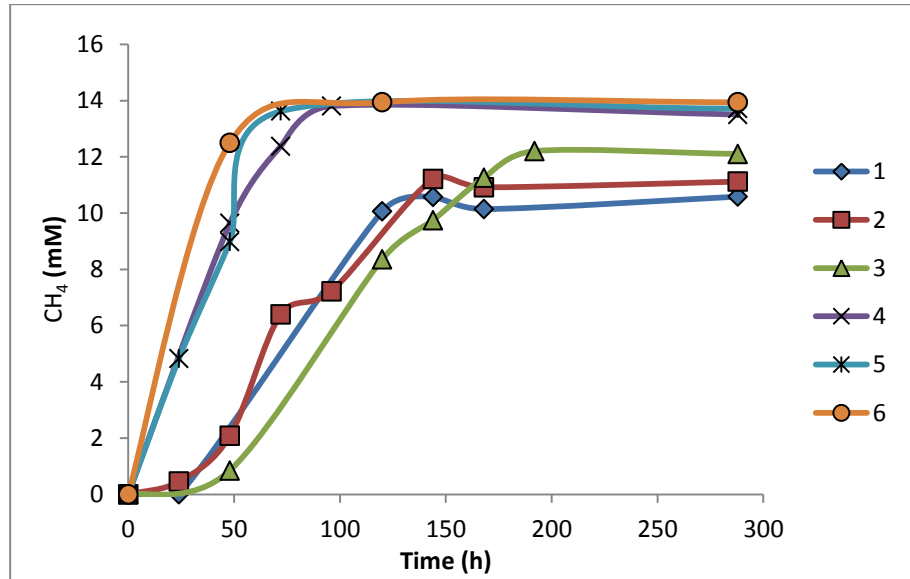


Figure 17 - Effects of inhibition in the production of methane with a fixed concentrations of CO (15%) for *M. marburgensis*

### 3.3.2 Cellular CO release in methanogenic carboxidotrophic strains growing on H<sub>2</sub>/CO<sub>2</sub>

Whilst the focused reaction is the consumption of carbon monoxide in order to generate carbon dioxide and the electrons necessary for the methanogenic pathway, in some conditions, the reverse reaction was observed at an early stage (high concentrations of H<sub>2</sub> and CO<sub>2</sub>). Indeed, this phenomenon was observed for all strains shown capable of removal of CO from the headspace.

This CO production was always detected alongside vigorous consumption of H<sub>2</sub> and CO<sub>2</sub> (Figure 18), suggesting a dependency on these substrates. Since all of these compounds are being simultaneously utilized for other reactions, a stoichiometry for this reaction cannot be confirmed but it seems to follow:



For *M. jannaschii*, this production was more substantial. A direct comparison with the other tested strains cannot be performed since this was likely partly due to the overall higher pressure in the system (3 bar versus the 1.7 bar in the other cultures). Since the reaction results in an overall decrease of moles of gas (thus reducing the pressure of the system), it would be encouraged by higher pressures.

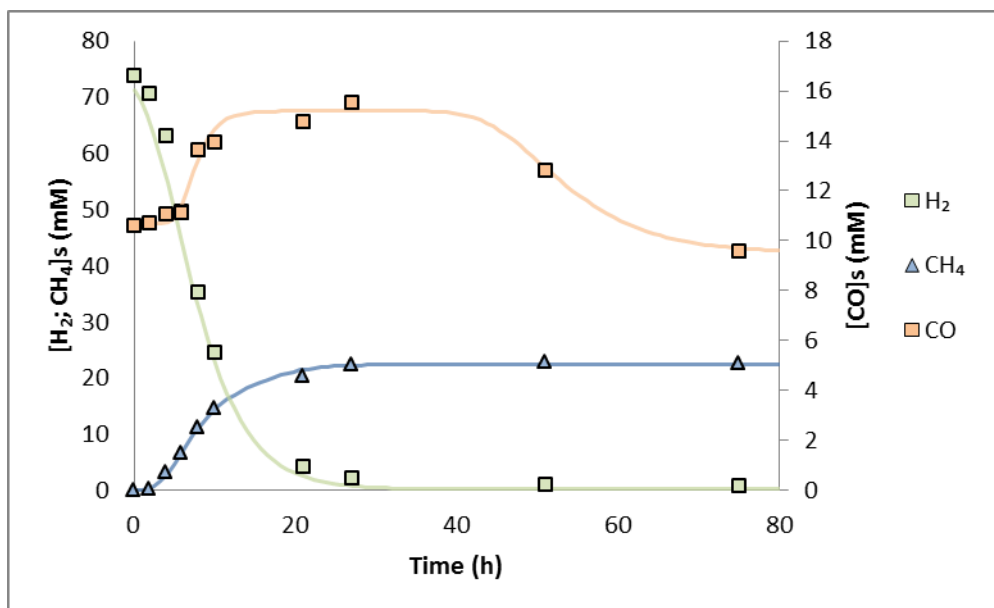


Figure 18 – Carbon monoxide formation from CO<sub>2</sub> and H<sub>2</sub> in *M. jannaschii* at 10% of CO (0.3 bar)

Similar observations have been made previously. Particularly, Thauer and associates have performed extensive studies with *M. marburgensis* to try to determine the origin of CO production (Conrad and Thauer 1983, Stupperich *et al.* 1983, Eikmanns *et al.* 1985, Bott and Thauer 1987).

In their work, it was concluded that CO observed came from the exchange of free with bound CO in the CODH/ACS complex. While often this CO acting as intermediary between CO<sub>2</sub> and acetyl-CoA is kept inside the gas channel, it was demonstrated by use of labelled compounds that such exchange was occurring for that strain and was responsible for the production of CO (Ragsdale 2004). The dependency on H<sub>2</sub> is therefore hypothesized as being mainly in the form of electron equivalent needed for conversion of CO<sub>2</sub> to CO. The methanogenesis pathway generates proton motive force that in turn provides energy that can be used on the formation of CO from CO<sub>2</sub>.

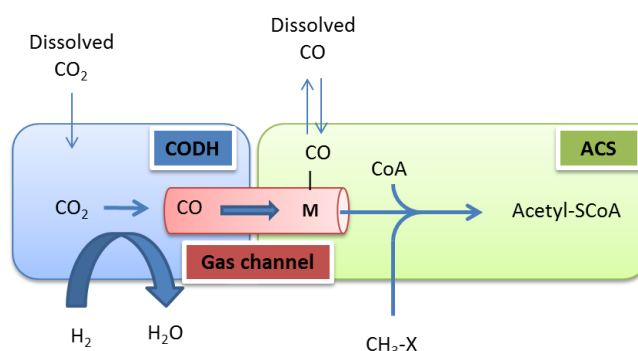
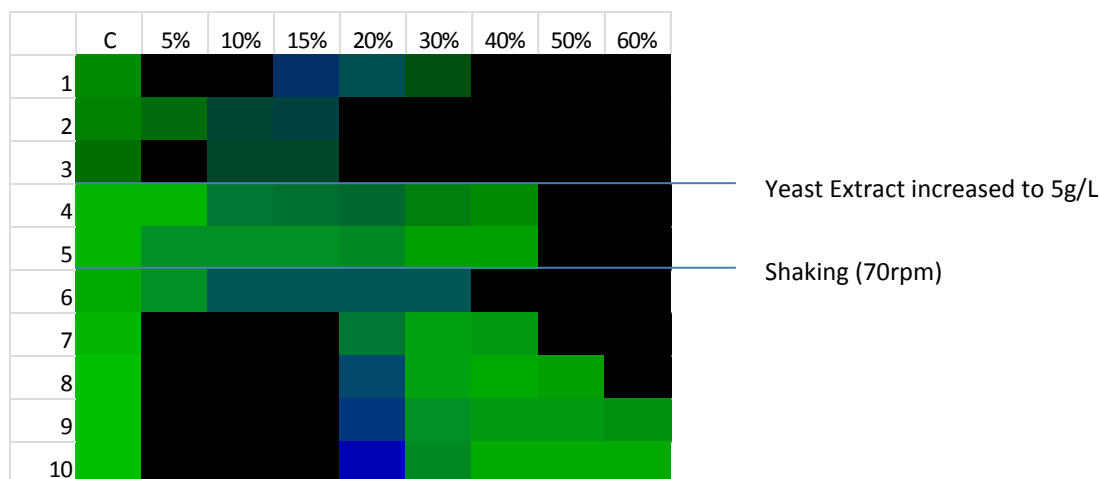


Figure 19 – Representation of equilibrium between bound and dissolved CO in the CODH/ACS complex.

### 3.4 Adaptation studies to CO

As previously mentioned, out of all tested strains, only *M. thermoautotrophicus* and *M. marburgensis* were observed as capable of carboxidotrophic growth in this study. To have a better qualitative overview of the data collected from the GC monitoring of the successive transfers for *M. marburgensis*, the main observations in terms of rate of consumption and amount of CO consumed have been summarized in a heat map.



**Figure 20 - Heat map of consumption. Black symbolizes untested parameters, green colour intensity corresponds to rate of H<sub>2</sub> consumption (increasing rates from light green to dark green) and blue tone to % of CO consumed (increasing rates from light to dark blue).**

By analysis of Figure 20, it is apparent that an optimal range of adaptation seems to be located between 10-20% of CO in headspace (equivalent to partial pressures of 0.17 to 0.34 bar). It was in this range that fastest consumption of CO was detected (in relation to the primary catabolism using H<sub>2</sub> as an energy source). Concordantly, the condition with 15% of CO (0.26 bar of partial pressure) was the first where carboxidotrophic growth was detected as discussed more thoroughly below in section 3.5.

An interesting observation that can be taken from the adaptation study is the decrease in relative CO consumption rates following the 1<sup>st</sup> and 6<sup>th</sup> transfer. Contrary to what was being attempted, there seems to be a loss of adaptation/preference to the use of CO as a substrate. Additionally the surge of CO consumption happened with increased shaking but not with the addition of yeast extract. Furthermore, the initial surge in CO consumption following the introduction of shaking, although substantial, seemed to regress almost completely in the subsequent transfer.

Both these instances mark a point immediately following a period of inferior availability of primary substrates. Transfer 1 follows prolonged cell inactivity (shipped inoculum from DSMZ) and transfer 6 corresponds to a surge in dissolution rates of electron donors (H<sub>2</sub> and CO). Thus, both times correspond to substantial relief of less favourable energetic conditions for the cells albeit due to different reasons. Situations of chronic energy stress might provide an incentive for the cells to utilize all possible sources of electrons (including CO). The momentary spike in the use of CO following

transfer 6 would therefore be due to faster replenishing of CO levels in the immediate vicinity of the cells. Once the cells readjust to the added energy availability they would reverse to using H<sub>2</sub> a more thermodynamically advantageous energy donor as a primary source of electrons foregoing CO consumption.

Contrastingly, from the 7<sup>th</sup> transfer onward, CO consumption rates increase in a sustainable way, even with frequent transfers. CO availability remains constant in these transfers.

The juxtaposition of these two phenomena indicates that some other process is influencing the CO use apart from its availability to the cell and/or the development of resistance mechanisms to inhibition.

### 3.4.1 Consumption of CO by methanogenic strains

One of the first observations that can be made is that H<sub>2</sub> is consumed at a faster rate than CO and, in the cases where CO levels are depleted, it occurs after H<sub>2</sub> partial pressures have been lowered significantly. This would seem to indicate that H<sub>2</sub> is the preferred electron donor for methanogenesis as would be expected. The reaction that describes the conversion of CO<sub>2</sub> with H<sub>2</sub> for methane production is thermodynamically more favourable than the one using only CO. Therefore, based on this criterion, as long as H<sub>2</sub> is present in non-limiting concentrations, this pathway should take precedence. Nevertheless, it should be noted that the simultaneous formation of carbon monoxide discussed in section 3.3.2, could be, at least partly, masking an early decrease of CO concentrations in the headspace.

Beside longer incubation times, successive transfers of cultures, maintaining the same CO concentrations, were effective reducing the lag time of CO consumption. This indicates a progressive adaptation of the cultures to CO levels.

Exactly what is behind this adaptation mechanism is unclear. Similar observations have been made for other CO utilizing organisms (Rother and Metcalf 2004, Sipma *et al.* 2006). In some cases, CO is metabolized to lower levels, thus diminishing its presence to levels below toxicity with growth occurring afterwards. However, results obtained in this study do not indicate such process since CO levels in the headspace only significantly decrease after H<sub>2</sub> is consumed and cultures are substantially grown.

Apart from the consumption of CO towards the production of methane, as indicated by the schematic in 1.4.4, CO can be converted into acetyl-CoA by the CODH/ACS complex. This reaction requires a methyl group that can be acquired through methyltetrahydro-methanopterin, an intermediary product of methanogenesis (Eikmanns *et al.* 1985).

### 3.4.1.1 Effect of CO partial pressure on the growth of methanogens

The most direct way of increasing the amount of CO dissolved in the media is to increase the partial pressure of the gas in the headspace. CO solubility drops considerably at high temperatures which can be a hindrance to the use of this substrate for thermophilic and hyperthermophilic species (Figure 21). It's therefore critical to regulate the partial pressures in a way that would circumvent this lower solubility but, at the same time, that would not be so high as to pose an overwhelming toxicity for cell growth. Analysis of Figure 20 indicated that such range is located within the 10-20% CO concentrations. Presumably, 5% would be too low for CO to reach the cells and be replenished in significant way to sustain growth and higher concentrations are toxic needed further attempts for adaptation.

$$k_H = k_H^\theta \times e^{\left[\frac{-\Delta_{\text{solution}}H}{R} \left(\frac{1}{T} - \frac{1}{T^\theta}\right)\right]}$$

Equation 8 - Henry's law equation

Table 7 - Henry's law constants dependency on temperature

| Constant                                   | H <sub>2</sub> | CO      |
|--|----------------|---------|
| $k_H^\theta \left[\frac{M}{atm}\right]$    | 0,00078        | 0,00099 |
| $\frac{-\Delta_{\text{solution}}H}{R} [K]$ | 2200           | 1300    |

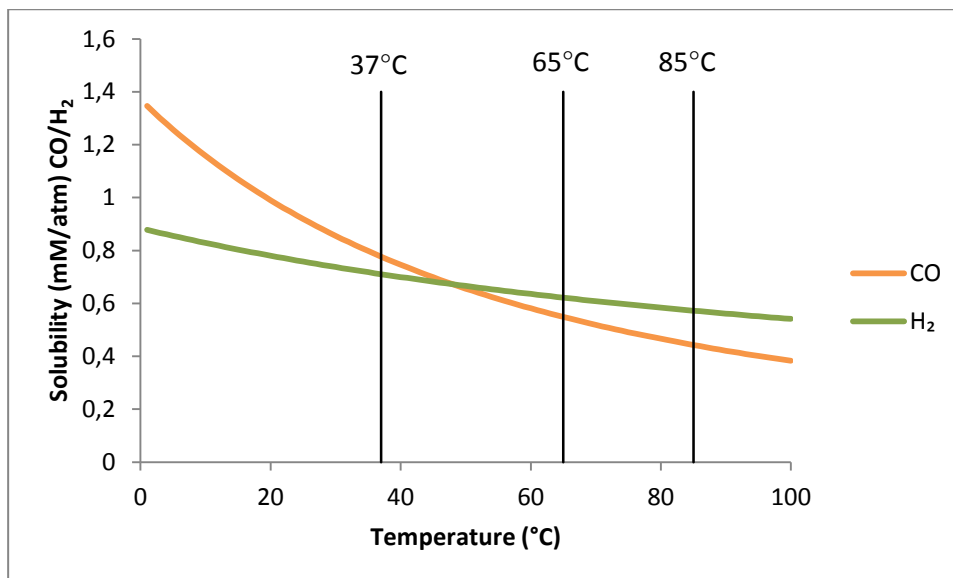


Figure 21 – Dependency of solubility of H<sub>2</sub> and CO on temperature.

#### **3.4.1.2 Effect of shaking speed on CO utilization rates**

For *M. marburgensis*, a clear shift in CO consumption was detected when cultures were subjected to a shaking speed of 70 rpm. Further increase to 120 rpm had also significant effect on CO consumption rates.

Shaking speed affects the mass transfer rate between the headspace and the media itself thus reducing the time required for the dynamic equilibrium to be achieved. At a microscopic level, this means that dissolved gas concentrations in the immediate vicinity of the cells are more quickly restored upon their consumption. Since H<sub>2</sub> and CO are both gases, they are both being affected by this change although not necessarily in the same way.

The increase in H<sub>2</sub> availability should result in an overall increase in growth rates. Indeed this can be observed for all concentrations of CO tested. Curiously, the initial transfers of the controls do not seem to share this effect at first with growth speed only increasing substantially after the 8<sup>th</sup> transfer.

The effect of increased dissolution of CO on growth is not as straightforward due to the triple effect of this gas as detailed in section 3.3. The faster dissolution of gases in the media would have opposite results depending on whether production or consumption of CO is dominant. On the other hand, the dual nature as inhibitory substance and catabolic substrate are in direct opposition to each other and would either hinder or aid the methanogenesis. The inhibitory effect of CO for key enzymes such as hydrogenases should be compounded further with higher concentrations of CO. However the additional availability of a second carbon and energy source could result in extra yields of methane and aid cell carbon material by means of acetyl-CoA synthesis by ACS.

#### **3.4.1.3 Effect of buffer used in the media**

While *M. thermotrophicus* grew slightly slower in the phosphate buffer, depletion of CO after considerable incubation periods was more successful than with bicarbonate buffer within the limited testing performed (Figure 22).

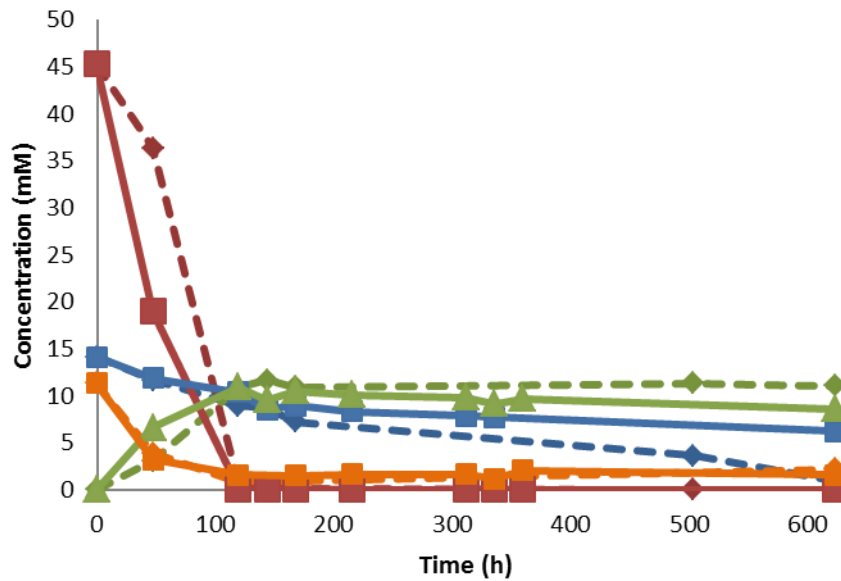


**Figure 22 – Difference in growth observed with phosphate buffer vs bicarbonate buffer at CO concentrations of 20%**

The impetus behind this difference is likely attributed to lower levels of overall dissolved CO<sub>2</sub> in the media that would drive the equilibrium presented in equation 9 towards the CO<sub>2</sub> + H<sub>2</sub> formation and thus contribute to a higher availability of methanogenesis substrates.

#### **3.4.1.4 Effect of supplementing methanogenic cultures with yeast extract**

From the first 3 transfers, it could be observed that growth rates were steadily diminishing for all incubation, including the controls without CO. With the assumption that this might be due to lower levels of growth supplements, following the 3<sup>rd</sup> transfer, yeast extract was increased from 2.5 g/L to 5 g/L. This resulted in an overall increase of the growth rate of the cultures in the 4<sup>th</sup> transfer series (Figure 20 and Figure 17). Furthermore, growth rates stabilized in the control for subsequent cultures.

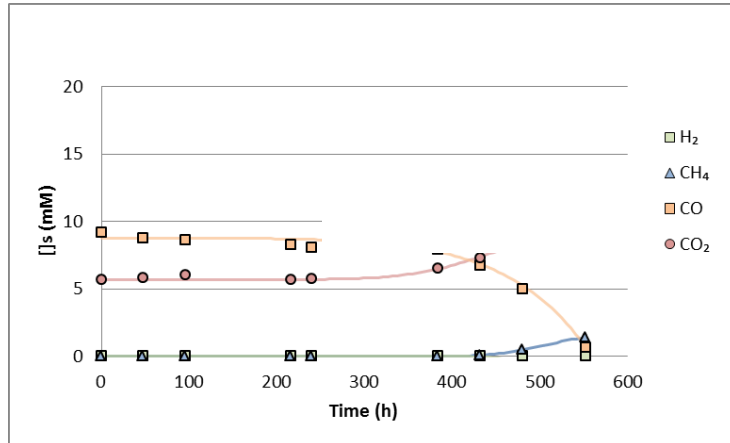
Regarding CO consumption rates, no significant difference could be detected. Yeast extract is composed of a mixture of nutrients. While it increases the availability of nutrients needed for growth, these results indicate that it does not significantly affect the ability of the cells to resist/consume CO.

### 3.5 Carboxidotrophic growth

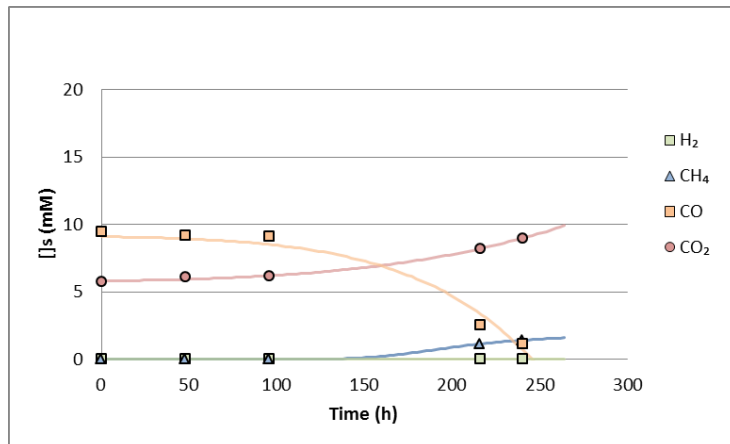
As previously mentioned, autotrophic growth on CO as a sole carbon and energy source (carboxydotrophy) was only successful for two of the tested microorganisms: *M. thermautotrophicus* and *M. marburgensis*.

While *M. thermautotrophicus* ability to grow on this substrate alone was previously reported (Daniels *et al.* 1977), *M. marburgensis* was not part of the group of known carboxidotrophic methanogens with this work being the first description of such capability.

*M. marburgensis*  
Growth with 10% CO  
(6<sup>th</sup> transfer)



*M. marburgensis*  
Growth with 15% CO  
(6<sup>th</sup> transfer)



*M. marburgensis*  
Growth with 20% CO  
(6<sup>th</sup> transfer)

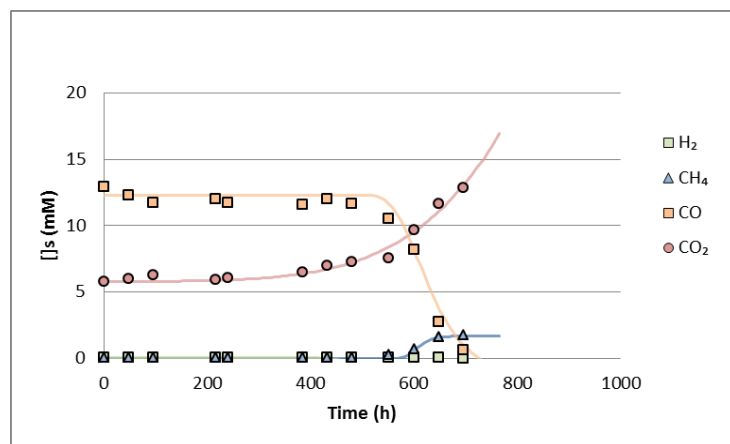
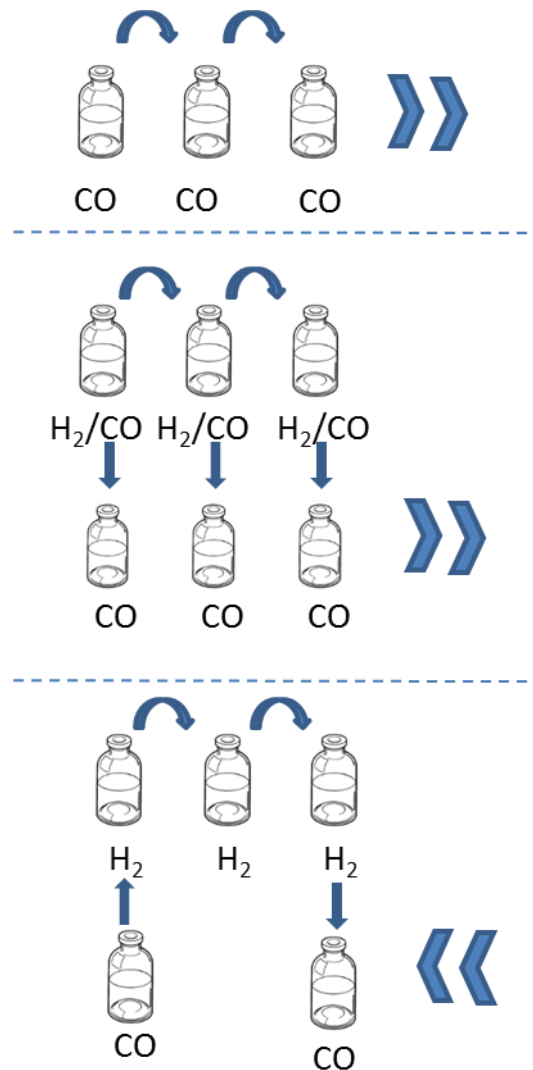


Figure 23 – Concentrations of gases in headspace for cultures growing on CO in the first transfer serie where carboxidotrophic growth was observed.



**Figure 24 – Adaptation of cultures to CO in the transfer series.**

Growth on CO for *M. marburgensis* was first achieved with inoculum from the 5th transfer series after long periods of incubation. Whilst medium turbidity was visualized in advance, methane production was not detectable until an incubation period longer than 150 h for cultures growing at 15% of CO (partial pressures of 0.26 bar). As for concentration of 10 and 20%, it took 450 and 600 h for methane to be detected in the headspace.

From the 6<sup>th</sup> transfer series onwards, new inoculations from bottles with H<sub>2</sub>/CO into bottles with only CO always resulted in carboxidotrophic growth in the range of 10-20% of CO in the headspace. Furthermore, the initial lag period diminished in bottles inoculated with cultures further along in the H<sub>2</sub>/CO transfer series. Additionally, both the adaptation period and growth rate were faster in new CO bottles inoculated from cultures already growing on CO. Furthermore, transfer of culture growing on CO back to control bottles without CO in the headspace, resulted in a loss of carboxidotrophic ability which indicated a reversal of the adaptation mechanism for this archaea. These observations are summarized in Figure 24.

### 3.5.1 Presence of hydrogen in headspace

In the cultures growing with CO as the only electron source, basal levels of H<sub>2</sub> were detected in the headspace (Figure 25).

The minute levels of hydrogen present in time 0 could be explained either by the transfer of dissolved hydrogen in the media from the previous inoculum or due to trace levels of hydrogen in the tubing of the gas exchanger.

Nevertheless, low level accumulation of H<sub>2</sub> (< 0.1mM) is clearly visible in the bottles with CO as only electron source. This build-up is sustained until production of CH<sub>4</sub> starts. At this point, the rate of consumption of CO quickly increases and the hydrogen levels drop below the detection limit.

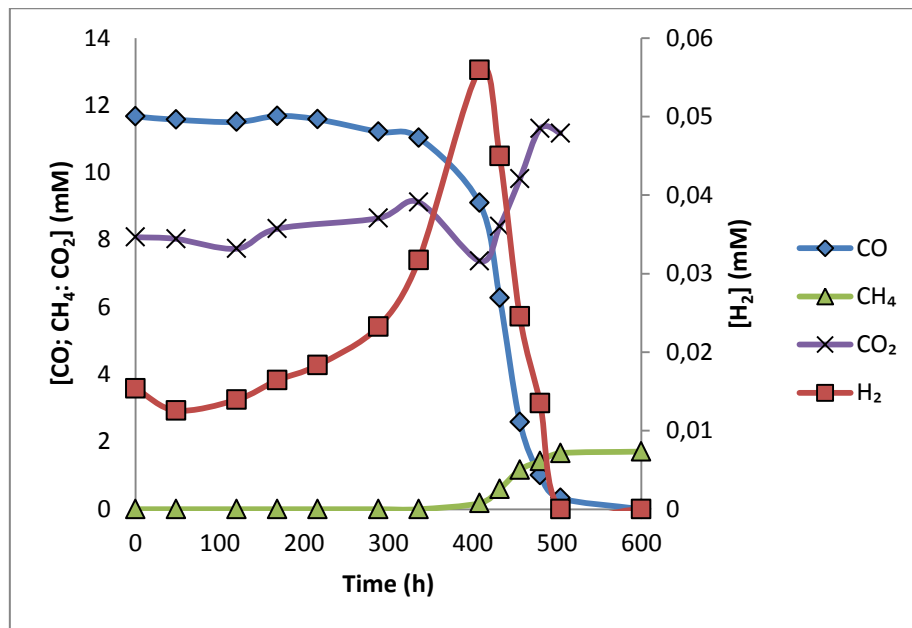


Figure 25 – Production of H<sub>2</sub> in cultures growing carboxidotrophically

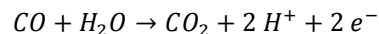
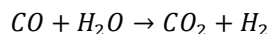
Concordantly, CO<sub>2</sub> levels seem to slowly rise at an early stage with a marked increase accompanying the quick consumption of CO and CH<sub>4</sub> production. It should be noted, however, that CO<sub>2</sub> in the headspace is at equilibrium with the bicarbonate in the media, making its assessment for stoichiometric purposes problematic.

Presumably, H<sub>2</sub> production is a consequence of CODH slowly oxidizing CO according to the biological water gas shift reaction (equation 9). Subsequently, that H<sub>2</sub> can be converted in the presence of CO<sub>2</sub> through the well-defined reaction for hydrogenotrophic methanogenesis (Equation 11) explaining the depletion measured.

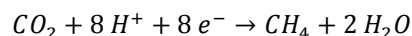
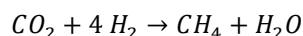
Another possible route for CO conversion into methanogenesis is detailed by equations equation 9 - Equation 13. In this pathway, the electrons formed by CO oxidation are directed towards the required steps of methanogenesis independently of H<sub>2</sub> formation.

Both of these processes result in the overall stoichiometry represented by Equation 13.

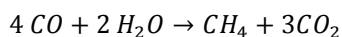
Equation 9  
Equation 10



Equation 11  
Equation 12



Equation 13



This would explain the accumulation of CO<sub>2</sub> despite production of methane. While CO<sub>2</sub> is an intermediary product in the conversion of CO to CH<sub>4</sub>, to provide enough electrons for the methanogenesis, a surplus of CO<sub>2</sub> must be produced beyond the carbon needs of the pathways in order to provide reducing power for steps 4 and 5 of methanogenesis. It should be noted that, unlike what happens during growth with H<sub>2</sub>/CO<sub>2</sub>, the overall stoichiometry indicated by Equation 13 does not result in a variation in total moles of gas. Consequently, closed system serum bottles with cultures growing according to this reaction should maintain a constant pressure in the headspace. That was indeed what was observed experimentally.

There is, however, insufficient information to fully determine if hydrogen formation is a necessary intermediate in carboxydrotrophy of *M. marburgensis*. The trend observed could suggest that H<sub>2</sub> is potentially produced as an electron carrier but is being immediately consumed at a superior rate dropping its levels in the headspace sharply. Hydrogen measured would therefore be excess molecules that are being leaked into the media and subsequently the headspace.

However the hypothesis that an excess of electrons is being generated and partly converted by hydrogenases into molecular hydrogen simply as an unnecessary side product cannot be discarded. Ultimately, the need for production of molecular hydrogen would depend on the mechanism being utilized in the reducing steps of methanogenesis. Mechanisms for H<sub>2</sub> independent methanogenesis in hydrogenotrophy are known to occur using electron carriers such as ferredoxins (Costa *et al.* 2013).

### 3.5.2 Visual observations

Cultures growing on CO have a notable different outward appearance. Cells acquire lighter shading compared to ones grown on the other tested gas mixtures. Microscopic observation show that cell size decreases with increase the amount of CO in the media/decrease of H<sub>2</sub>. Furthermore, there is a very noticeable visual difference between pellets obtained from the different conditions.

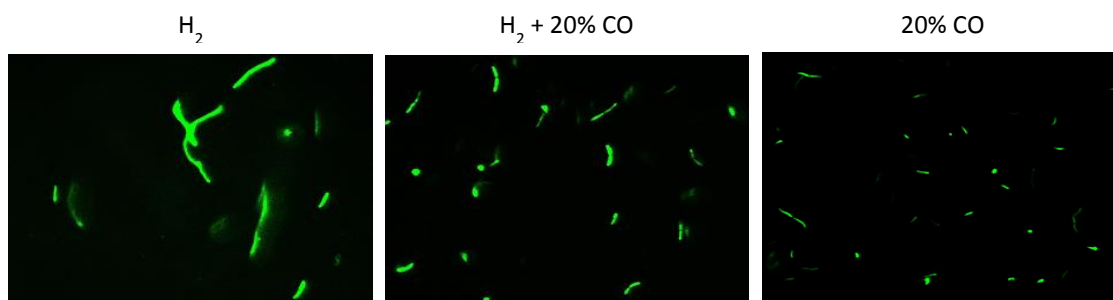


Figure 26 – Microscopic observation of *M. marburgensis* cultures using different combinations of electron donors.

While merely a circumstantial observation, during attempts of cell lysis of cultures grown in atmosphere with and without CO, it was noted that cells grown in CO alone were noticeably harder to lyse (*vide* chapter 3.6.1). This could also be attributed to the changes in the cell wall that make it more resilient.

Adaptations of the cell wall of *M. thermotrophicus* in response to environmental conditions in syntrophy have been reported previously (Nakamura *et al.* 2006). While the observation was made amidst comparison of pure culture with a co-culture, the author postulated that this archaea increases the thickness of its wall as a response to the low partial pressures of H<sub>2</sub> it is being subjected to.

If indeed that is the case, considering the experimental conditions tested, it seems likely that a similar process would be emerging. Such phenomena could, at least partly, explain the differences detected. Observations conducted in this work would seem to indicate the reported changes extend to *M. marburgensis*.

Whether this is only due to H<sub>2</sub> as hypothesised by Nakamura or if another feature, such as CO presence, also plays a role remains uncertain. Substantial differences between the control and 20% CO would seem to suggest that the presence of CO might also be a factor considering that the decrease in H<sub>2</sub> partial pressures is not substantial. Following the same logic as previously, if the cell wall can change due to low H<sub>2</sub> partial pressure, then it could change as a defence to CO. Being a polar molecule, the same mechanisms that prevent redundant proton exchange through the membrane would help keep CO from entering the cell which in turn would help with CO toxicity. There is, however, not enough data to conclude a direct correlation of this nature.

Differences in archaeal cell walls have been linked to adaptations to chronic energy stress conditions. By having a more tight structure to their walls, archaea can prevent redundant proton exchange, making them more energy efficient (Valentine 2007).

In conditions with low levels of H<sub>2</sub>, this is certainly an advantage. It could be postulated that this is a further refinement of this phenomena. When the preferential electron donor, H<sub>2</sub>, is removed from the headspace, we induce a state of chronic energy stress in the cells.

## 3.6 Proteomic studies of carboxidotrophic cultures

### 3.6.1 Optimization of protein extraction and quantification protocols

Initially, cell lysis was performed by the standard method used in the Microbiology Laboratory of Wageningen University which is based on sonication aided by the presence of surfactants (SDS). While previously tested successfully for bacterial strains and control samples of *M. marburgensis*, this lysis protocol proved ineffective for samples with H<sub>2</sub>/CO and CO.

In order to bypass this resistance, increasing the number of sonication cycles was attempted. While the number of cells detected under the microscope diminished with increasing cycles, lysis yield was not substantial until over 30 cycles for cells grown with CO (Figure 27). Furthermore, there was a noticeable difference between lysis for the different conditions. Cells grown on CO were the most resilient (Figure 28). Unfortunately this high number of cycles can also have a detrimental effect towards protein yields.

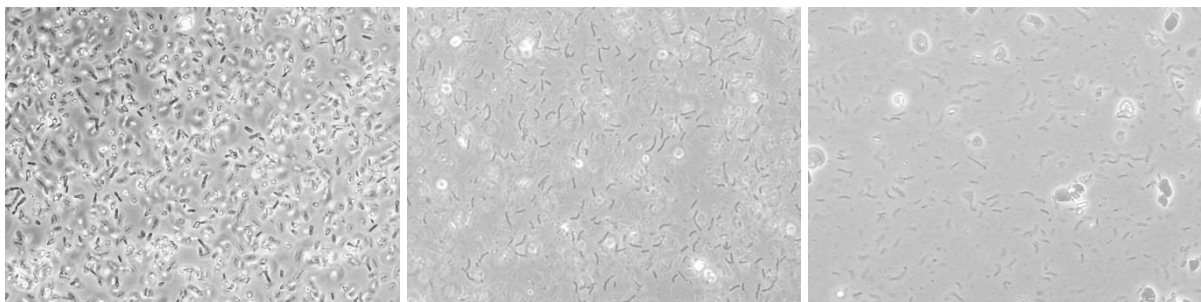


**Figure 27– Microscopic observations of cells grown with CO during lysis with sonication. From left to right: before sonication, 18 cycles and 30 cycles.**

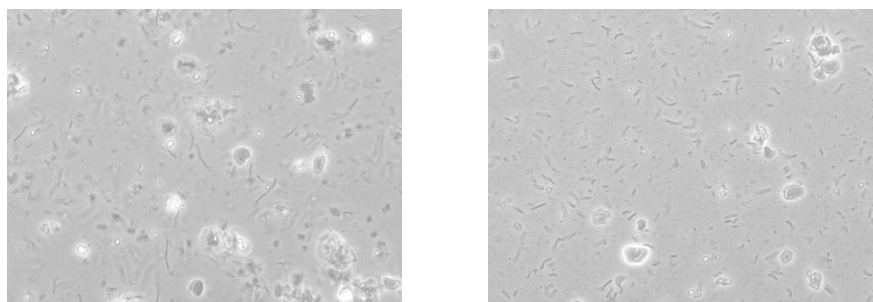


**Figure 28 - Microscopic observations of cells subjected to 30 cycles of sonication. From left to right: cells grown on H<sub>2</sub>+CO before sonication; cells grown on CO.**

Considering the poor results obtained, an alternative method of cell lysis for was needed. There are several methods for cell lysis, all of them with their own set of advantages and drawbacks.

Several other methods were assessed for cell lysis. Ultimately, taking in account previous results in other similar research and the equipment and reagents readily available in the laboratory, a French press method was chosen. This method proved to be highly effective but required a relatively

big volume of sample (> 3-5 ml) therefore producing a very dilute sample for the operational conditions tested.

While the primary purpose for optimization of the lysis protocol was intended for protein extraction towards proteomic analysis, lysis for other purposes might be impossible with this method. More specifically, for enzyme activity assays, anaerobic conditions (or as close to it as possible) need to be maintained. Consequently, the French press method can not be utilized for this purpose.

### 3.6.2 Proteomic analysis

As was previously mentioned, results from samples sent for proteomic analysis in an external laboratory weren't returned in time for their inclusion in this written dissertation. Consequently, in their place, this chapter will list the proteins identified in previous proteomics analysis of *M. thermotrophicus* growing in H<sub>2</sub>/CO<sub>2</sub> and discuss the expected modifications in the expression profiles of proteins in the other conditions sent for analysis.

A comprehensive list of proteins identified under high and low availabilities of H<sub>2</sub> in a previous study (Farhoud 2011) can be found in Annex II (kindly provided by Hans JCT Wessels from Radboud University).

Figure 29 details the pathways for methanogenesis (using either CO or H<sub>2</sub> as electron donors) in *M. thermotrophicus* and *M. marburgensis*. For the cells utilizing CO, the oxidation of this gas into CO<sub>2</sub> occurs at CODH/ACS protein complex. As such these should be the main enzymes whose expression is induced in the presence of CO.

Contrastingly, in cultures growing with CO as electron donor, H<sub>2</sub>-dependent pathways should be downregulated. This would potentially affect the reducing steps of methanogenesis. In particular, Hmd dependent pathway might not occur under H<sub>2</sub> limiting conditions. It's possible that CO oxidation might directly catalyse all the reductions of the ferredoxins needed for the methanogenesis enzymes, without the aid of H<sub>2</sub>. In that case, Eha (energy converting [Ni,Fe]-hydrogenase), Frh (F<sub>420</sub>-reducing [Ni,Fe]-hydrogenase), Mvh (F<sub>420</sub>-non reducing [Ni,Fe]-hydrogenase) and Hdr (heterodisulfide reductase) enzymes would play a limited role. However, it should be noted that H<sub>2</sub> production in cells growing on CO was detected. If H<sub>2</sub> is being produced as a necessary intermediary towards one or more of the reducing steps in the methanogenesis pathway, then the corresponding enzymes should still be present in the proteomic analysis.

Transcriptomic analysis of *M. marburgensis* already revealed that Mcr (methyl-coenzyme M reductase isoenzyme I), the protein involved in the last, rate-limiting step of methanogenesis, is induced by the presence of CO (Zhou *et al.* 2013).

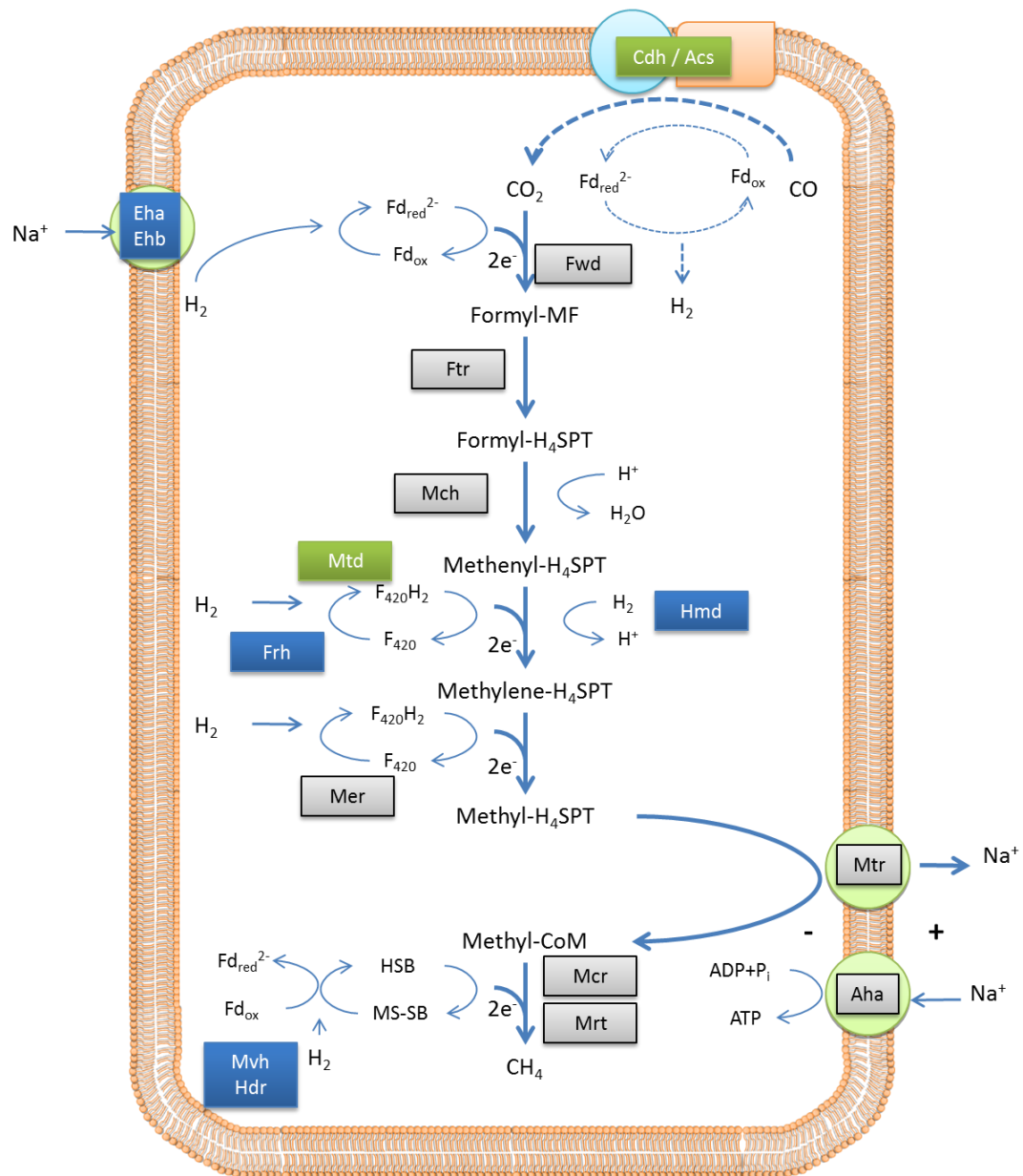


Figure 29 – Expected pathway for *M. thermautotrophicus* and *M. marburgensis*. Proteins whose expression is expected to increase in the presence of  $\text{CO}$  are marked in green. Those whose expression is expected to decrease are marked in blue.

## 4 Conclusions and Future Work

It is likely that the number of carboxidotrophic organisms documented in literature is grossly underestimated. Potential to grow on this substrate can easily be overlooked since it is not commonly tested in characterization studies and CO inhibition can induce false negatives. Surpassing this inhibition often requires time consuming and/or labour intensive adaptations through long term incubations or multiple transfers with gradual increase of CO percentages. Consequently, while a physiological approach to this problem is a necessary starting point, a readjustment of the testing parameters with the added knowledge gained from each newly determined carboxidotroph could be extremely beneficial. As such, detailed comparative genomic and proteomic analysis of the strains known to possess the desired ability to grown on CO alone in different experimental conditions are essential to provide further insight into the mechanisms behind carboxidotrophy and expand the knowledge on this field of study.

In this study, several different hydrogenotrophic methanogens were selected through genomic comparison to a known methanogenic carboxidotroph, *M. thermautotrophicus*, and tested for their capability to utilize CO for production of CH<sub>4</sub>. Out of the tested species, only *M. thermautotrophicus* and *M. marburgensis* were observed as capable of utilizing CO as a sole energy source. For the latter, this work marks the first report of carboxidotrophic growth.

Growth on CO is a complex process that is not fully understood. Observations in this work for *M. marburgensis* seem to confirm the presence of several parameters that affect such ability. In particular, mass transfer rates (affected by shaking) and specific ranges of CO partial pressures were crucial to the success of carboxidotrophy. Moreover, while *M. thermautotrophicus* ability to adapt to grow on CO alone is extensively reported, within the parameters tested, it was harder to achieve and growth rates were considerably lower than the ones observed for *M. marburgensis*.

It should be noted that, while adaptations for carboxidotrophic growth in other strains were unsuccessful, this does not mean necessarily that they are incapable of such. Merely that, in the conditions tested and within the limited timeframe of this study, such growth could not be observed. It is feasible that extra transfers and longer incubation times might be fruitful were this study was not. Likewise, several operational parameters could be further readjusted such as media composition, shaking speed, partial pressures of headspace components, etc. The combination of these factors provides a myriad of potential combinations to test.

For the confirmed carboxidotrophic strains, *M. thermautotrophicus* and *M. marburgensis*, a comparative proteomic was begun. However, the results of that analysis still need to be thoroughly examined and could not be included in this thesis because of time limitations. Carboxidotrophs are slow growers and cell yields were extremely low. This resulted in very long experiments and the need to grow high volumes of cell culture for protein isolation. Another drawback was the need to optimize cell disruption for protein extraction. First trials with sonication did not result for efficiently breaking the archaeal cell membranes. Further tests with the French press were necessary for successful protein extraction from the methanogenic cultures.

With adaptation of *M. marburgensis* to use of CO as sole energy source, it is now possible to further characterize its growth. While methane production was measured closely, to determine growth rates accurately, a more direct measurement of cells still needs to be performed. Also interesting to study is the full range of CO partial pressures for which adaptation can be successful. Concurrently, optimum operational conditions maximizing CO conversion can be perceived with the fully adapted cultures at different CO partial pressures.

Morphological changes observed for *Methanothermobacter* cultures in H<sub>2</sub>/CO and CO also offer an interesting avenue for further research. Additional analysis of cell wall can be done either through more refined microscopic methods or through direct study of cell wall components. Transmission electron microscopy (TEM) and membrane specific metabolome analysis, respectively, would be the preferred methods for such study.

Hydrogen formation observed can also be a possible avenue of study. From this work it is still unclear whether molecular hydrogen is a necessary intermediary for carboxidotrophic methanogenesis pathway of *M. marburgensis*. Enzyme activity assays targeting the hydrogenases thorough the build-up and depletion phase would provide us with further insight into this question. Additionally, deletion mutants blocking this H<sub>2</sub> formation from CO, if grown successfully, would give a definitive answer to whether the methanogenesis can occur in a H<sub>2</sub>-independent way or not. Moreover, these deletion mutants could potentially be used to selectively remove CO from the syngas mixture.

## 5 References

- Abubackar, H. N., M. C. Veiga and C. Kennes (2011). "Biological conversion of carbon monoxide: rich syngas or waste gases to bioethanol." Biofuels Bioproducts & Biorefining-Biofpr **5**(1): 93-114.
- Alves, J. I. (2013). Microbiology of thermophilic anaerobic syngas conversion. PhD, University of Minho.
- Balch, W. E. and R. S. Wolfe (1976). "New approach to the cultivation of methanogenic bacteria: 2-mercaptoethanesulfonic acid (HS-CoM)-dependent growth of *Methanobacterium ruminantium* in a pressurized atmosphere." Appl Environ Microbiol **32**(6): 781-791.
- Beijerinck, M. and A. van Delden (1903). "On a colorless bacterium, whose carbon-food comes from the atmosphere." Proceedings of the Koninklijke Nederlandse Akademie van Wetenschappen(5): 25.
- Beijerinck, M. W. and A. van Delden (1914). "Über das Nitratferment und über fiber physiologische Artbildung." Fol. Microbiol(3): 23.
- Bott, M., B. Eikmanns and R. K. Thauer (1986). "Coupling of carbon monoxide oxidation to CO<sub>2</sub> and H<sub>2</sub> with the phosphorylation of ADP in acetate-grown *Methanosarcina barkeri*." Eur J Biochem **159**(2): 393-398.
- Bott, M. and R. K. Thauer (1987). "Proton-motive-force-driven formation of CO from CO<sub>2</sub> and H<sub>2</sub> in methanogenic bacteria." Eur J Biochem **168**(2): 407-412.
- Bult, C. J., O. White, G. J. Olsen, L. Zhou, R. D. Fleischmann, G. G. Sutton, J. A. Blake, L. M. FitzGerald, R. A. Clayton, J. D. Gocayne, A. R. Kerlavage, B. A. Dougherty, J. F. Tomb, M. D. Adams, C. I. Reich, R. Overbeek, E. F. Kirkness, K. G. Weinstock, J. M. Merrick, A. Glodek, J. L. Scott, N. S. Geoghagen and J. C. Venter (1996). "Complete genome sequence of the methanogenic archaeon, *Methanococcus jannaschii*." Science **273**(5278): 1058-1073.
- Carere, C. R., R. Sparling, N. Cicek and D. B. Levin (2008). "Third generation biofuels via direct cellulose fermentation." Int J Mol Sci **9**(7): 1342-1360.
- Colby, J., E. Williams and A. P. F. Turner (1985). "Applications of Co-Utilizing Microorganisms." Trends Biotechnol **3**(1): 12-17.
- Conrad, R. and R. K. Thauer (1983). "Carbon monoxide production by *Methanobacterium thermoautotrophicum*." FEMS Microbiol Lett **20**(2): 229-232.
- Costa, K. C., T. J. Lie, M. A. Jacobs and J. A. Leigh (2013). "H<sub>2</sub>-independent growth of the hydrogenotrophic methanogen *Methanococcus maripaludis*." MBio **4**(2).

- Daniel, S. L., T. Hsu, S. I. Dean and H. L. Drake (1990). "Characterization of the H<sub>2</sub>- and CO-dependent chemolithotrophic potentials of the acetogens *Clostridium thermoaceticum* and *Acetogenium kivui*." J Bacteriol **172**(8): 4464-4471.
- Daniels, L., G. Fuchs, R. K. Thauer and J. G. Zeikus (1977). "Carbon monoxide oxidation by methanogenic bacteria." J Bacteriol **132**(1): 118-126.
- Dashekvicz, M. P. and R. L. Uffen (1979). "Identification of a Carbon Monoxide Metabolizing Bacterium as a Strain of *Rhodospseudomonas-Gelatinosa* (Molisch) Vanniel." International Journal of Systematic Bacteriology **29**(2): 145-148.
- de Poorter, L. M., W. J. Geerts and J. T. Keltjens (2007). "Coupling of Methanothermobacter thermoautotrophicus methane formation and growth in fed-batch and continuous cultures under different H<sub>2</sub> gassing regimens." Appl Environ Microbiol **73**(3): 740-749.
- Diekert, G. B. and R. K. Thauer (1978). "Carbon monoxide oxidation by *Clostridium thermoaceticum* and *Clostridium formicoaceticum*." J Bacteriol **136**(2): 597-606.
- Dioum, E. M., J. Rutter, J. R. Tuckerman, G. Gonzalez, M. A. Gilles-Gonzalez and S. L. McKnight (2002). "NPAS2: a gas-responsive transcription factor." Science **298**(5602): 2385-2387.
- Eikmanns, B., G. Fuchs and R. K. Thauer (1985). "Formation of carbon monoxide from CO<sub>2</sub> and H<sub>2</sub> by *Methanobacterium thermoautotrophicum*." Eur J Biochem **146**(1): 149-154.
- Ensign, S. A. and P. W. Ludden (1991). "Characterization of the CO oxidation/H<sub>2</sub> evolution system of *Rhodospirillum rubrum*. Role of a 22-kDa iron-sulfur protein in mediating electron transfer between carbon monoxide dehydrogenase and hydrogenase." J Biol Chem **266**(27): 18395-18403.
- Farhoud, M. (2011). Disease Biology of Mitochondrial Complex-I: proteomics insights. PhD, Radboud University Nijmegen.
- Ferry, J. G. (2010). "CO in methanogenesis." Annals of Microbiology **60**(1): 1-12.
- Ferry, J. G. and D. J. Lessner (2008). "Methanogenesis in marine sediments." Ann N Y Acad Sci **1125**: 147-157.
- Fischer, F., L. R. and W. K. (1931). "Biologische gasreaktionen. I. Mitteilung: die umsetzung des kohlenoxyds." Biochemische Zeitschrift(236): 21.
- Fischer, F., L. R. and W. K. (1932). "Uber die bildung von essigsäure bei der biologischen umsetzung von kohlenoxyd und kohlenäure mit wasserstoff zu methan." Biochemische Zeitschrift(245): 11.
- Gonzalez, J. M. and F. T. Robb (2000). "Genetic analysis of *Carboxythermus hydrogenoformans* carbon monoxide dehydrogenase genes *cooF* and *cooS*." FEMS Microbiol Lett **191**(2): 243-247.

Henstra, A. M., J. Sipma, A. Rinzema and A. J. Stams (2007). "Microbiology of synthesis gas fermentation for biofuel production." Curr Opin Biotechnol **18**(3): 200-206.

Henstra, A. M. and A. J. Stams (2004). "Novel physiological features of Carboxydothemus hydrogenoformans and Thermoterrabacterium ferrireducens." Appl Environ Microbiol **70**(12): 7236-7240.

Hirsch, P. (1968). "Photosynthetic bacterium growing under carbon monoxide." Nature **217**(5128): 555-556.

Hungate, R. E. (1950). "The anaerobic mesophilic cellulolytic bacteria." Bacteriol Rev **14**(1): 1-49.

Hungate, R. E. and J. Macy (1973). "The Roll-Tube Method for Cultivation of Strict Anaerobes." Bulletins from the Ecological Research Committee(17): 123-126.

Hussain, A., S. R. Guiot, P. Mehta, V. Raghavan and B. Tartakovsky (2011). "Electricity generation from carbon monoxide and syngas in a microbial fuel cell." Appl Microbiol Biotechnol **90**(3): 827-836.

Jansen, K., R. K. Thauer, F. Widdel and G. Fuchs (1984). "Carbon Assimilation Pathways in Sulfate Reducing Bacteria - Formate, Carbon-Dioxide, Carbon-Monoxide, and Acetate Assimilation by Desulfovibrio-Baarsii." Arch Microbiol **138**(3): 257-262.

Jensen, A. and K. Finster (2005). "Isolation and characterization of Sulfurospirillum carboxydovorans sp. nov., a new microaerophilic carbon monoxide oxidizing epsilon Proteobacterium." Antonie Van Leeuwenhoek **87**(4): 339-353.

Jung, G. Y., H. O. Jung, J. R. Kim, Y. Ahn and S. Park (1999). "Isolation and characterization of Rhodospseudomonas palustris P4 which utilizes CO with the production of H<sub>2</sub>." Biotechnology Letters **21**(6): 525-529.

Kaster, A. K., M. Goenrich, H. Seedorf, H. Liesegang, A. Wollherr, G. Gottschalk and R. K. Thauer (2011). "More than 200 genes required for methane formation from H<sub>2</sub> and CO<sub>2</sub> and energy conservation are present in Methanothermobacter marburgensis and Methanothermobacter thermoautotrophicus." Archaea **2011**: 973848.

Kerby, R., W. Niemczura and J. G. Zeikus (1983). "Single-carbon catabolism in acetogens: analysis of carbon flow in Acetobacterium woodii and Butyrivibrio methylotrophicum by fermentation and <sup>13</sup>C nuclear magnetic resonance measurement." J Bacteriol **155**(3): 1208-1218.

Kim, D. and I. S. Chang (2009). "Electricity generation from synthesis gas by microbial processes: CO fermentation and microbial fuel cell technology." Bioresour Technol **100**(19): 4527-4530.

Klemp, R., H. Cypionka, F. Widdel and N. Pfennig (1985). "Growth with hydrogen, and further physiological characteristics of Desulfotomaculum species." Arch Microbiol **143**(2): 203-208.

Kluyver, A. J. and C. G. Schnellen (1947). "On the fermentation of carbon monoxide by pure cultures of methane bacteria." Arch Biochem **14**(1-2): 57-70.

Lantusch, K. (1922). "Actinomyces oligocarophilus, sein Formwechsel und seine Physiologie." Zentralblatt für Bakteriologie(57): 11.

Lessner, D. J., L. Li, Q. Li, T. Rejtar, V. P. Andreev, M. Reichlen, K. Hill, J. J. Moran, B. L. Karger and J. G. Ferry (2006). "An unconventional pathway for reduction of CO<sub>2</sub> to methane in CO-grown *Methanosarcina acetivorans* revealed by proteomics." Proc Natl Acad Sci U S A **103**(47): 17921-17926.

Liou, J. S., D. L. Balkwill, G. R. Drake and R. S. Tanner (2005). "Clostridium carboxidivorans sp. nov., a solvent-producing clostridium isolated from an agricultural settling lagoon, and reclassification of the acetogen Clostridium scatologenes strain SL1 as Clostridium drakei sp. nov." Int J Syst Evol Microbiol **55**(Pt 5): 2085-2091.

Ljungdahl, L. G. (1986). "The autotrophic pathway of acetate synthesis in acetogenic bacteria." Annu Rev Microbiol **40**: 415-450.

Lorowitz, W. H. and M. P. Bryant (1984). "Peptostreptococcus-Productus Strain That Grows Rapidly with Co as the Energy-Source." Appl Environ Microbiol **47**(5): 961-964.

Lupton, F. S., R. Conrad and J. G. Zeikus (1984). "Co Metabolism of Desulfovibrio-Vulgaris Strain Madison - Physiological-Function in the Absence or Presence of Exogeneous Substrates." FEMS Microbiol Lett **23**(2-3): 263-268.

Maeder, D. L., I. Anderson, T. S. Brettin, D. C. Bruce, P. Gilna, C. S. Han, A. Lapidus, W. W. Metcalf, E. Saunders, R. Tapia and K. R. Sowers (2006). "The *Methanosarcina barkeri* genome: comparative analysis with *Methanosarcina acetivorans* and *Methanosarcina mazei* reveals extensive rearrangement within methanosarcinal genomes." J Bacteriol **188**(22): 7922-7931.

Markowitz, V. M., I.-M. A. Chen, K. Palaniappan, E. S. Ken Chu, Y. Grechkin, A. Ratner, B. Jacob, J. Huang, P. Williams, M. Huntemann, I. Anderson, K. Mavromatis, N. N. Ivanova and N. C. Kyrpides (2014). IMG: the integrated microbial genomes database and comparative analysis system

Maron, P. A., L. Ranjard, C. Mougél and P. Lemanceau (2007). "Metaproteomics: a new approach for studying functional microbial ecology." Microbial Ecology **53**(3): 486-493.

Matschiavelli, N., E. Oelgeschlager, B. Cocchiarraro, J. Finke and M. Rother (2012). "Function and regulation of isoforms of carbon monoxide dehydrogenase/acetyl coenzyme A synthase in *Methanosarcina acetivorans*." J Bacteriol **194**(19): 5377-5387.

- Mehta, P., A. Hussain, B. Tartakovsky, V. Neburchilov, V. Raghavan, H. Wang and S. R. Guiot (2010). "Electricity generation from carbon monoxide in a single chamber microbial fuel cell." Enzyme and Microbial Technology **46**(6): 450-455.
- Meyer, O. and K. Fiebig (1985). Enzymes Oxidizing Carbon Monoxide. Gas Enzymology. H. Degn, R. P. Cox and H. Toftlund, Springer Netherlands: 147-168.
- Meyer, O. and H. G. Schlegel (1983). "Biology of aerobic carbon monoxide-oxidizing bacteria." Annu Rev Microbiol **37**: 277-310.
- Mohammadi, M., G. D. Najafpour, H. Younesi, P. Lahijani, M. H. Uzir and A. R. Mohamed (2011). "Bioconversion of synthesis gas to second generation biofuels: A review." Renewable & Sustainable Energy Reviews **15**(9): 4255-4273.
- Mörsdorf, G., K. Frunzke, D. Gadkari and O. Meyer (1992). "Microbial growth on carbon monoxide." Biodegradation **3**(1): 61-82.
- Nakamura, K., T. Terada, Y. Sekiguchi, N. Shinzato, X. Y. Meng, M. Enoki and Y. Kamagata (2006). "Application of pseudomurein endoisopeptidase to fluorescence in situ hybridization of methanogens within the family Methanobacteriaceae." Appl Environ Microbiol **72**(11): 6907-6913.
- O'Brien, J. M., R. H. Wolkin, T. T. Moench, J. B. Morgan and J. G. Zeikus (1984). "Association of hydrogen metabolism with unitrophic or mixotrophic growth of *Methanosarcina barkeri* on carbon monoxide." J Bacteriol **158**(1): 373-375.
- O'Farrell, P. H. (1975). "High resolution two-dimensional electrophoresis of proteins." J Biol Chem **250**(10): 4007-4021.
- Oelgeschlager, E. and M. Rother (2008). "Carbon monoxide-dependent energy metabolism in anaerobic bacteria and archaea." Arch Microbiol **190**(3): 257-269.
- Parshina, S. N., S. Kijlstra, A. M. Henstra, J. Sipma, C. M. Plugge and A. J. Stams (2005). "Carbon monoxide conversion by thermophilic sulfate-reducing bacteria in pure culture and in co-culture with *Carboxydotherrmus hydrogenoformans*." Appl Microbiol Biotechnol **68**(3): 390-396.
- Parshina, S. N., J. Sipma, Y. Nakashimada, A. M. Henstra, H. Smidt, A. M. Lysenko, P. N. Lens, G. Lettinga and A. J. Stams (2005). "*Desulfotomaculum carboxydivorans* sp. nov., a novel sulfate-reducing bacterium capable of growth at 100% CO." Int J Syst Evol Microbiol **55**(Pt 5): 2159-2165.
- Ragsdale, S. W. (2004). "Life with carbon monoxide." Crit Rev Biochem Mol Biol **39**(3): 165-195.
- Ragsdale, S. W., J. E. Clark, L. G. Ljungdahl, L. L. Lundie and H. L. Drake (1983). "Properties of purified carbon monoxide dehydrogenase from *Clostridium thermoaceticum*, a nickel, iron-sulfur protein." J Biol Chem **258**(4): 2364-2369.

Rother, M. and W. W. Metcalf (2004). "Anaerobic growth of Methanosarcina acetivorans C2A on carbon monoxide: an unusual way of life for a methanogenic archaeon." Proc Natl Acad Sci U S A **101**(48): 16929-16934.

Rother, M., E. Oelgeschlager and W. M. Metcalf (2007). "Genetic and proteomic analyses of CO utilization by Methanosarcina acetivorans." Arch Microbiol **188**(5): 463-472.

Santiago, B., U. Schubel, C. Egelseer and O. Meyer (1999). "Sequence analysis, characterization and CO-specific transcription of the cox gene cluster on the megaplasmid pHCG3 of Oligotropha carboxidovorans." Gene **236**(1): 115-124.

Schauder, R., A. Preuss, M. Jetten and G. Fuchs (1989). "Oxidative and Reductive Acetyl Coa Carbon Monoxide Dehydrogenase Pathway in Desulfobacterium-Autotrophicum .2. Demonstration of the Enzymes of the Pathway and Comparison of Co Dehydrogenase." Arch Microbiol **151**(1): 84-89.

Sipma, J., A. M. Henstra, S. M. Parshina, P. N. Lens, G. Lettinga and A. J. Stams (2006). "Microbial CO conversions with applications in synthesis gas purification and bio-desulfurization." Crit Rev Biotechnol **26**(1): 41-65.

Sowers, K. R., S. F. Baron and J. G. Ferry (1984). "Methanosarcina acetivorans sp. nov., an Acetotrophic Methane-Producing Bacterium Isolated from Marine Sediments." Appl Environ Microbiol **47**(5): 971-978.

Stephenson, M. and L. H. Stickland (1933). "Hydrogenase: The bacterial formation of methane by the reduction of one-carbon compounds by molecular hydrogen." Biochem J **27**(5): 1517-1527.

Stupperich, E., K. E. Hammel, G. Fuchs and R. K. Thauer (1983). "Carbon monoxide fixation into the carboxyl group of acetyl coenzyme A during autotrophic growth of Methanobacterium." FEBS Lett **152**(1): 21-23.

Svetlichny, V. A., T. G. Sokolova, M. Gerhardt, N. A. Kostrikina and G. A. Zavarzin (1991). "Anaerobic extremely thermophilic carboxydophilic bacteria in hydrotherms of Kuril Islands." Microbial Ecology **21**(1): 1-10.

Svetlitchnyi, V., C. Peschel, G. Acker and O. Meyer (2001). "Two membrane-associated NiFeS-carbon monoxide dehydrogenases from the anaerobic carbon-monoxide-utilizing eubacterium Carboxydothemus hydrogenofmans." J Bacteriol **183**(17): 5134-5144.

Techtmann, S. M., A. S. Colman and F. T. Robb (2009). "'That which does not kill us only makes us stronger': the role of carbon monoxide in thermophilic microbial consortia." Environ Microbiol **11**(5): 1027-1037.

Techtmann, S. M., A. V. Lebedinsky, A. S. Colman, T. G. Sokolova, T. Woyke, L. Goodwin and F. T. Robb (2012). "Evidence for horizontal gene transfer of anaerobic carbon monoxide dehydrogenases." Front Microbiol **3**: 132.

Tersteegen, A. and R. Hedderich (1999). "Methanobacterium thermoautotrophicum encodes two multisubunit membrane-bound [NiFe] hydrogenases. Transcription of the operons and sequence analysis of the deduced proteins." Eur J Biochem **264**(3): 930-943.

Thauer, R. K., K. Jungermann and K. Decker (1977). "Energy conservation in chemotrophic anaerobic bacteria." Bacteriol Rev **41**(1): 100-180.

Tiquia-Arashiro, S. (2014). Biotechnological Applications of Thermophilic Carboxydrotrophs. Thermophilic Carboxydrotrophs and their Applications in Biotechnology, Springer International Publishing: 29-101.

Uffen, R. L. (1976). "Anaerobic Growth of a Rhodospseudomonas Species in Dark with Carbon-Monoxide as Sole Carbon and Energy Substrate." Proc Natl Acad Sci U S A **73**(9): 3298-3302.

Uffen, R. L. (1981). "Metabolism of Carbon-Monoxide." Enzyme and Microbial Technology **3**(3): 197-206.

Valentine, D. L. (2007). "Adaptations to energy stress dictate the ecology and evolution of the Archaea." Nat Rev Microbiol **5**(4): 316-323.

Verma, A., D. Hirsch, C. Glatt, G. Ronnett and S. Snyder (1993). "Carbon monoxide: a putative neural messenger." Science **259**(5093): 381-384.

Wang, V. C., S. W. Ragsdale and F. A. Armstrong (2013). "Investigations of two bidirectional carbon monoxide dehydrogenases from Carboxydotherrmus hydrogenoformans by protein film electrochemistry." Chembiochem **14**(14): 1845-1851.

Wood, H. G. (1991). "Life with CO or CO<sub>2</sub> and H<sub>2</sub> as a source of carbon and energy." FASEB J **5**(2): 156-163.

Yagi, T. (1958). "Enzymic Oxidation of Carbon Monoxide." Biochim Biophys Acta **30**(1): 194-195.

Yagi, T. (1959). "Enzymic Oxidation of Carbon Monoxide .2." Journal of Biochemistry **46**(7): 949-955.

Yagi, T. and N. Tamiya (1962). "Enzymic Oxidation of Carbon Monoxide .3. Reversibility." Biochim Biophys Acta **65**(3): 508-&.

Yang, H. C. and H. L. Drake (1990). "Differential-Effects of Sodium on Hydrogen-Dependent and Glucose-Dependent Growth of the Acetogenic Bacterium Acetogenium-Kivui." Appl Environ Microbiol **56**(1): 81-86.

Zhao, Y., R. Cimpoaia, Z. Liu and S. R. Guiot (2011). "Kinetics of CO conversion into H<sub>2</sub> by *Carboxydothermus hydrogenoformans*." *Appl Microbiol Biotechnol* **91**(6): 1677-1684.

Zhou, Y., A. E. Dorchak and S. W. Ragsdale (2013). "In vivo activation of methyl-coenzyme M reductase by carbon monoxide." *Front Microbiol* **4**: 69.

Zhu, W., C. I. Reich, G. J. Olsen, C. S. Giometti and J. R. Yates, 3rd (2004). "Shotgun proteomics of *Methanococcus jannaschii* and insights into methanogenesis." *J Proteome Res* **3**(3): 538-548.

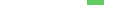


## Annex I

**Table 8 - Sequence alignment results for putative CODH gene coding results in reference to the CODH of *M. methanothermobacter thermoautotrophicus*.**

| Homolog           | Product Name  | Percent Identity | Alignment On Query Gene   | Alignment On Subject Gene   | Length | E-value | Bit Score | Genome  | Scaffold ID | Scaffold GC |
|-------------------|---|------------------|---|---|--------|---------|-----------|---|-------------|-------------|
| <b>640792748</b>  | acetyl-CoA decarbonylase/synthase, subunit alpha            | 93.70%           |    |    | 777aa  | 0.0e+00 | 1503      | Methanothermobacter marburgensis Marburg DSM 2133 | NC_014408   | 0.49        |
| <b>650872298</b>  | acetyl-CoA decarbonylase/synthase complex subunit alpha     | 73.50%           |    |    | 783aa  | 0.0e+00 | 1219      | Methanobacterium sp. SWAN-1                       | NC_015574   | 0.36        |
| <b>650750581</b>  | acetyl-CoA decarbonylase/synthase complex subunit alpha     | 73.10%           |    |    | 781aa  | 0.0e+00 | 1209      | Methanobacterium sp. AL-21                        | NC_015216   | 0.36        |
| <b>2563556927</b> | CO dehydrogenase/acyl-CoA synthase complex subunit alpha    | 71.30%           |  |  | 778aa  | 0.0e+00 | 1178      | Methanococcus maripaludis S2                      | BX950229    | 0.33        |
| <b>640166306</b>  | CO dehydrogenase/acyl-CoA synthase complex, epsilon subunit | 71.20%           |  |  | 778aa  | 0.0e+00 | 1178      | Methanococcus maripaludis C5                      | NC_009135   | 0.33        |
| <b>649738126</b>  | acetyl-CoA decarbonylase/synthase alpha subunit             | 70.80%           |  |  | 774aa  | 0.0e+00 | 1143      | Methanothermobacter fervidus V24S, DSM 2088       | NC_014658   | 0.32        |

|                   |  |        |   |   |       |          |      |  |           |      |
|-------------------|--|--------|---|---|-------|----------|------|--|-----------|------|
| <b>641284174</b>  | CO<br>dehydrogenase/acet<br>yl-CoA synthase<br>complex, epsilon<br>subunit | 70.40% |    |    | 778aa | 0.0e+00  | 1165 | Methanococcu<br>s maripaludis<br>C6                  | NC_009975 | 0.33 |
| <b>640785975</b>  | CO<br>dehydrogenase/acet<br>yl-CoA synthase<br>complex, epsilon<br>subunit | 70.30% |    |    | 779aa | 0.0e+00  | 1151 | Methanococcu<br>s vannielii SB                       | NC_009634 | 0.31 |
| <b>2511671884</b> | acetyl-CoA<br>decarbonylase/synth<br>ase complex subunit<br>alpha          | 70.30% |    |    | 779aa | 0.0e+00  | 1152 | Methanococcu<br>s maripaludis<br>X1                  | NC_015847 | 0.33 |
| <b>640792748</b>  | CO<br>dehydrogenase/acet<br>yl-CoA synthase<br>complex, epsilon<br>subunit | 70.20% |    |    | 778aa | 0.0e+00  | 1164 | Methanococcu<br>s maripaludis<br>C7                  | NC_009637 | 0.33 |
| <b>650857088</b>  | acetyl-CoA<br>decarbonylase/synth<br>ase complex subunit<br>alpha          | 62.60% |    |    | 782aa | 2.8e-293 | 1013 | Methanotorris<br>igneus Kol5,<br>DSM 5666            | NC_015562 | 0.32 |
| <b>638201440</b>  | acetyl-CoA<br>decarbonylase/synth<br>ase, subunit alpha<br>(cdhA)          | 62.30% |    |    | 774aa | 3.6e-288 | 996  | Methanocaldo<br>coccus<br>jannaschii<br>DSM 2661     | NC_000909 | 0.31 |
| <b>646622637</b>  | CO<br>dehydrogenase/acet<br>yl-CoA synthase<br>complex, epsilon<br>subunit | 61.80% |    |    | 773aa | 4.8e-285 | 986  | Methanocaldo<br>coccus sp.<br>FS406-22               | NC_013887 | 0.32 |
| <b>644969638</b>  | CO<br>dehydrogenase/acet<br>yl-CoA synthase<br>complex, epsilon<br>subunit | 61.70% |  |  | 774aa | 6.6e-288 | 995  | Methanocaldo<br>coccus fervens<br>AG86               | NC_013156 | 0.32 |
| <b>646367701</b>  | CO<br>dehydrogenase/acet<br>yl-CoA synthase<br>complex, epsilon<br>subunit | 61.00% |  |  | 774aa | 3.5e-281 | 973  | Methanocaldo<br>coccus<br>vulcanius M7,<br>DSM 12094 | NC_013407 | 0.31 |
| <b>650917575</b>  | acetyl-CoA<br>decarbonylase/synth<br>ase complex subunit<br>alpha          | 58.90% |  |  | 774aa | 5.9e-275 | 952  | Methanotherm<br>ococcus<br>okinawensis<br>IH1        | NC_015636 | 0.29 |

|                   |  |        |   |   |       |          |     |  |                                    |      |
|-------------------|--|--------|---|---|-------|----------|-----|--|------------------------------------|------|
| <b>637896327</b>  | CO<br>dehydrogenase/acet<br>yl-CoA synthase<br>complex, epsilon<br>subunit | 57.00% |    |    | 787aa | 1.9e-255 | 887 | Methanospirillum<br>hungatei JF-<br>1  | NC_007796                          | 0.45 |
| <b>640788579</b>  | CO<br>dehydrogenase/acet<br>yl-CoA synthase<br>complex, epsilon<br>subunit | 57.00% |    |    | 786aa | 1.4e-268 | 931 | Methanococcus<br>aeolicus<br>Nankai-3  | NC_009635                          | 0.30 |
| <b>646777846</b>  | CO<br>dehydrogenase/acet<br>yl-CoA synthase<br>complex, epsilon<br>subunit | 56.60% |    |    | 758aa | 1.9e-257 | 894 | Methanocaldococcus<br>infernus ME  | NC_014122                          | 0.34 |
| <b>2509038682</b> | CO<br>dehydrogenase/acet<br>yl-CoA synthase<br>complex, epsilon<br>subunit | 56.40% |    |    | 783aa | 1.7e-256 | 891 | Methanoregula<br>formicica<br>SMSP, DSM<br>22288                               | Metfor_Contig<br>51.1              | 0.55 |
| <b>648151855</b>  | acetyl-CoA<br>decarbonylase/synth<br>ase complex, alpha<br>subunit         | 55.90% |    |    | 139aa | 2.7e-38  | 166 | Methanothermobacter<br>marburgensis<br>Marburg DSM<br>2133                     | NC_014408                          | 0.49 |
| <b>640868606</b>  | CO<br>dehydrogenase/acet<br>yl-CoA synthase<br>complex, epsilon<br>subunit | 55.90% |    |    | 786aa | 8.9e-253 | 879 | Methanoregula<br>boonei 6A8  | NC_009712                          | 0.55 |
| <b>2505970200</b> | CO<br>dehydrogenase/acet<br>yl-CoA synthase<br>alpha subunit               | 55.40% |   |   | 770aa | 4.7e-254 | 883 | Methanocella<br>arvoryzae<br>MRE50<br>(reannotation)                           | LRC50LV__64<br>0427159stand<br>ard | 0.55 |
| <b>2504145711</b> | Acetyl-CoA<br>decarbonylase/synth<br>ase complex subunit<br>alpha          | 53.80% |  |  | 797aa | 1.8e-239 | 834 | Archaeoglobus<br>veneficus<br>SNP6, DSM<br>11195                               | Aven11195_un<br>known1             | 0.47 |
| <b>2522261782</b> | acetyl-CoA<br>decarbonylase/synth<br>ase alpha subunit<br>(EC 1.2.99.2)    | 53.10% |  |  | 800aa | 3.4e-236 | 823 | Archaeoglobus<br>sulfatocaldus<br>PM70-1, DSM<br>19444<br>(Asulf_version<br>1) | Asulf_Archaeo<br>globus.1          | 0.43 |
| <b>641592958</b>  | CO<br>dehydrogenase/acet<br>yl-CoA synthase<br>complex, epsilon            | 52.40% |  |  | 766aa | 3.8e-235 | 820 | Candidatus<br>Desulfurudis<br>audaxviator<br>MP104C                            | NC_010424                          | 0.61 |

| subunit           |   |        |  |  |       |          |     |   |                    |      |
|-------------------|---|--------|--|--|-------|----------|-----|---|--------------------|------|
| <b>2588655581</b> | acetyl-CoA decarboxylase/synthase alpha subunit (EC 1.2.99.2) | 52.10% |  |  | 798aa | 1.3e-232 | 812 | Archaeoglobus fulgidus DSM 8774                   | CP006577           | 0.48 |
| <b>2509662624</b> | CO dehydrogenase/acetyl-CoA synthase complex, epsilon subunit | 52.10% |  |  | 804aa | 1.9e-234 | 818 | Methanomethylovorans hollandica DSM 15978         | Metho_Contig 141.1 | 0.43 |
| <b>640787866</b>  | CO dehydrogenase/acetyl-CoA synthase complex, epsilon subunit | 52.10% |  |  | 768aa | 7.1e-242 | 842 | Methanococcus aeolicus Nankai-3                   | NC_009635          | 0.30 |
| <b>638158998</b>  | acetyl-CoA decarboxylase/synthase, subunit alpha (cdhA-2)     | 52.00% |  |  | 798aa | 9.0e-229 | 799 | Archaeoglobus fulgidus VC-16, DSM 4304            | AE000782           | 0.49 |
| <b>638168739</b>  | CO dehydrogenase/acetyl-CoA synthase alpha subunit            | 52.00% |  |  | 760aa | 6.7e-232 | 809 | Methanopyrus kandleri AV19                        | AE009439           | 0.61 |
| <b>648151854</b>  | acetyl-CoA decarboxylase/synthase complex, alpha subunit      | 51.30% |  |  | 311aa | 9.7e-74  | 284 | Methanothermobacter marburgensis Marburg DSM 2133 | NC_014408          | 0.49 |
| <b>646611862</b>  | CO dehydrogenase/acetyl-CoA synthase complex, epsilon subunit | 51.30% |  |  | 804aa | 2.1e-224 | 784 | Ferroglobus placidus AEDII12DO, DSM 10642         | NC_013849          | 0.44 |
| <b>638157644</b>  | acetyl-CoA decarboxylase/synthase, subunit alpha (cdhA-1)     | 51.20% |  |  | 802aa | 6.6e-226 | 789 | Archaeoglobus fulgidus VC-16, DSM 4304            | AE000782           | 0.49 |
| <b>648055108</b>  | CO dehydrogenase/acetyl-CoA synthase complex subunit epsilon  | 51.20% |  |  | 801aa | 8.4e-235 | 819 | Methanohalobium evestigatum Z-7303, DSM 3721      | NC_014253          | 0.37 |
| <b>2588654165</b> | acetyl-CoA decarboxylase/synthase alpha subunit (EC 1.2.99.2) | 51.00% |  |  | 802aa | 9.3e-226 | 789 | Archaeoglobus fulgidus DSM 8774                   | CP006577           | 0.48 |

|                   |  |        |   |   |       |          |     |  |              |      |
|-------------------|--|--------|---|---|-------|----------|-----|--|--------------|------|
| <b>2519474196</b> | CO<br>dehydrogenase/acet<br>yl-CoA synthase<br>complex subunit<br>epsilon  | 51.00% |    |    | 802aa | 6.6e-234 | 816 | Methanobolus<br>psychrophilus<br>R15             | CP003083     | 0.45 |
| <b>646707218</b>  | acetyl-CoA<br>decarbonylase/synth<br>ase alpha subunit                     | 50.60% |    |    | 801aa | 1.8e-232 | 811 | Methanohalop<br>hilus mahii<br>SLP, DSM<br>5219  | NC_014002    | 0.43 |
| <b>2502871140</b> | CO<br>dehydrogenase/acet<br>yl-CoA synthase<br>complex, epsilon<br>subunit | 49.50% |    |    | 803aa | 5.8e-230 | 803 | Methanosalsu<br>m zhilinae<br>WeN5, DSM<br>4017  | Sent_unknown | 0.39 |
| <b>637958643</b>  | CO<br>dehydrogenase/acet<br>yl-CoA synthase<br>complex, epsilon<br>subunit | 49.20% |    |    | 802aa | 3.1e-223 | 780 | Methanococci<br>des burtonii<br>DSM 6242         | NC_007955    | 0.41 |
| <b>638178729</b>  | carbon-monoxide<br>dehydrogenase,<br>subunit alpha                         | 48.20% |    |    | 805aa | 2.1e-216 | 758 | Methanosarcin<br>a acetivorans<br>C2A            | AE010299     | 0.43 |
| <b>639699298</b>  | CO<br>dehydrogenase/acet<br>yl-CoA synthase<br>complex, epsilon<br>subunit | 48.00% |    |    | 805aa | 2.9e-221 | 774 | Methanosaeta<br>thermophila<br>PT                | NC_008553    | 0.54 |
| <b>638166633</b>  | CO<br>dehydrogenase/acet<br>yl-CoA synthase<br>alpha subunit               | 47.90% |    |    | 806aa | 6.7e-216 | 756 | Methanosarcin<br>a mazei Go1,<br>DSM 3647        | AE008384     | 0.41 |
| <b>650797560</b>  | CO<br>dehydrogenase/acet<br>yl-CoA synthase<br>complex subunit<br>alpha    | 47.80% |  |  | 793aa | 2.2e-214 | 751 | Methanosaeta<br>concilii GP-6                    | NC_015416    | 0.51 |
| <b>638179299</b>  | carbon-monoxide<br>dehydrogenase,<br>subunit alpha                         | 47.80% |  |  | 805aa | 1.8e-216 | 758 | Methanosarcin<br>a acetivorans<br>C2A            | AE010299     | 0.43 |
| <b>637699328</b>  | acetyl-CoA<br>decarbonylase/synth<br>ase complex subunit<br>alpha          | 47.50% |  |  | 806aa | 7.6e-214 | 749 | Methanosarcin<br>a barkeri<br>Fusaro, DSM<br>804 | NC_007355    | 0.39 |
| <b>2540562562</b> | acetyl-CoA<br>decarbonylase/synth<br>ase complex subunit<br>alpha          | 47.30% |  |  | 807aa | 2.9e-213 | 747 | Methanosarcin<br>a mazei Tuc01                   | CP004144     | 0.42 |

|                   |  |        |   |   |       |          |     |  |           |      |
|-------------------|--|--------|---|---|-------|----------|-----|--|-----------|------|
| <b>638165176</b>  | CO<br>dehydrogenase/acet<br>yl-CoA synthase<br>alpha subunit       | 47.30% |  |  | 807aa | 1.8e-213 | 748 | Methanosarcin<br>a mazei Go1,<br>DSM 3647                      | AE008384  | 0.41 |
| <b>638175771</b>  | carbon-monoxide<br>dehydrogenase,<br>subunit alpha                 | 47.20% |  |  | 806aa | 4.0e-215 | 753 | Methanosarcin<br>a acetivorans<br>C2A                          | AE010299  | 0.43 |
| <b>637699095</b>  | acetyl-CoA<br>decarbonylase/synth<br>ase complex subunit<br>alpha  | 47.00% |  |  | 806aa | 1.1e-213 | 749 | Methanosarcin<br>a barkeri<br>Fusaro, DSM<br>804               | NC_007355 | 0.39 |
| <b>2512009248</b> | Acetyl-CoA<br>decarbonylase/synth<br>ase alpha subunit             | 46.80% |  |  | 809aa | 4.6e-217 | 760 | Methanosaeta<br>harundinacea<br>6Ac                            | CP003117  | 0.61 |
| <b>648151853</b>  | acetyl-CoA<br>decarbonylase/synth<br>ase complex, alpha<br>subunit | 46.60% |  |  | 395aa | 1.8e-96  | 359 | Methanotherm<br>obacter<br>marburgensis<br>Marburg DSM<br>2133 | NC_014408 | 0.49 |
| <b>2512010787</b> | Acetyl-CoA<br>decarbonylase/synth<br>ase complex subunit<br>alpha  | 46.50% |  |  | 811aa | 2.6e-214 | 751 | Methanosaeta<br>harundinacea<br>6Ac                            | CP003117  | 0.61 |

## Annex II

**Table 9 – Protein detected by LC-MS/MS for *Methanothermobacter thermautotrophicus* for high and low availability of H<sub>2</sub> as electron donor (data from (Farhoud 2011)). Proteins known to be involved in H<sub>2</sub> activation are marked in aqua, proteins involved in the methanogenesis pathway from CO<sub>2</sub> are marked in green and genes involved in CO oxidation into CO<sub>2</sub> are marked in red**

| General information |          |  | Proteomics                       |                                   |                          |                           |
|---------------------|----------|--|----------------------------------|-----------------------------------|--------------------------|---------------------------|
| locus tag           | Gi       | Product name   | LC-MS/MS H <sub>2</sub> membrana | LC-MS/MS H <sub>2</sub> cytonlaem | LC-MS/MS Low H. membrana | LC-MS/MS Low H. cytonlaem |
| MTH1                | 15678032 | conserved protein; predicted RNA-binding protein   |                                  | 1                                 |                          | 1                         |
| MTH2                | 15678033 | 50S ribosomal protein L3 (E.coli L3P)  | 1                                | 1                                 | 1                        | 1                         |
| MTH3                | 15678034 | 50S ribosomal protein L4 (E.coli L4) (L1E)   | 1                                | 1                                 | 1                        | 1                         |
| MTH4                | 15678035 | 50S ribosomal protein L23a (E.coli L23P)   |                                  |                                   |                          | 1                         |
| MTH5                | 15678036 | 50S ribosomal protein L8 (E.coli L2P)  | 1                                | 1                                 | 1                        |                           |
| MTH6                | 15678037 | 30S ribosomal protein S15 (E.coli S19P)  |                                  | 1                                 | 1                        |                           |
| MTH7                | 15678038 | 50S ribosomal protein L17 (E.coli L22P)  |                                  | 1                                 | 1                        | 1                         |
| MTH8                | 15678039 | 30S ribosomal protein S3 (E.coli S3P)  | 1                                | 1                                 | 1                        | 1                         |
| MTH12               | 15678043 | 30S ribosomal protein S11 (E.coli S17P)  | 1                                | 1                                 | 1                        | 1                         |
| MTH13               | 15678044 | 50S ribosomal protein L23 (E.coli L14P)  |                                  | 1                                 |                          | 1                         |
| MTH14               | 15678045 | 50S ribosomal protein L26 (E.coli L24P)  | 1                                | 1                                 |                          | 1                         |
| MTH15               | 15678046 | 30S ribosomal protein S4e  | 1                                | 1                                 | 1                        | 1                         |
| MTH16               | 15678047 | 50S ribosomal protein L11 (E.coli L5P)   | 1                                | 1                                 | 1                        | 1                         |
| MTH18               | 15678049 | 30S ribosomal protein S15a (E.coli S8P)  |                                  | 1                                 |                          | 1                         |
| MTH19               | 15678050 | 50S ribosomal protein L9 (E.coli L6P)  | 1                                | 1                                 | 1                        | 1                         |
| MTH20               | 15678051 | 50S ribosomal protein L32E   |                                  |                                   |                          | 1                         |
| MTH21               | 15678052 | 50S ribosomal protein L19E   |                                  |                                   | 1                        |                           |
| MTH22               | 15678053 | 50S ribosomal protein L5 (L18P)  | 1                                | 1                                 | 1                        | 1                         |
| MTH23               | 15678054 | 30S ribosomal protein S2 (E.coli S5P)  | 1                                | 1                                 | 1                        | 1                         |
| MTH24               | 15678055 | 50S ribosomal protein L7 (E.coli L30P)   |                                  | 1                                 |                          | 1                         |
| MTH25               | 15678056 | 50S ribosomal protein L27a (E.coli L15P)   | 1                                | 1                                 | 1                        |                           |
| MTH26               | 15678057 | preprotein translocase subunit secY; protein transport protein SEC61 subunit alpha homolog       |                                  | 1                                 |                          | 1                         |
| MTH27               | 15678058 | adenylate kinase   | 1                                | 1                                 | 1                        |                           |
| MTH28               | 15678059 | conserved archaea-specific membrane-spanning protein MTH28 (COG1422, DUF107)                     |                                  | 1                                 |                          |                           |
| MTH30               | 15678061 | cytidylate kinase  |                                  | 1                                 |                          | 1                         |
| MTH31               | 15678062 | 50S ribosomal protein L14E   |                                  |                                   |                          | 1                         |
| MTH34               | 15678064 | 30S ribosomal protein S18P (E.coli S13P)   | 1                                | 1                                 | 1                        |                           |
| MTH35               | 15678065 | 30S ribosomal protein S9 (E.coli S4P)  |                                  | 1                                 | 1                        |                           |
| MTH36               | 15678066 | 30S ribosomal protein S14 (E.coli S11P)  |                                  | 1                                 |                          | 1                         |
| MTH37               | 15678067 | DNA-dependent RNA polymerase, subunit D (RpoD)   |                                  | 1                                 |                          | 1                         |
| MTH38               | 15678068 | 50S ribosomal protein L18E (E.coli L17)  |                                  | 1                                 |                          | 1                         |
| MTH39               | 15678069 | 30S ribosomal protein S16 (E.coli S9); fused L13/S9 ribosomal protein                            | 1                                | 1                                 | 1                        | 1                         |
| MTH43               | 15678072 | enolase (eno)  | 1                                | 1                                 | 1                        | 1                         |
| MTH44               | 15678073 | 30S ribosomal protein Sa (E.coli S2P)  | 1                                | 1                                 | 1                        | 1                         |
| MTH45               | 15678074 | conserved protein (UPF0103); DNA-repair protein MutT related                                     |                                  | 1                                 |                          | 1                         |
| MTH46               | 15678075 | mevalonate kinase  |                                  | 1                                 |                          |                           |
| MTH47               | 15678076 | mevalonate-5-phosphate kinase, phosphomevalonate kinase (PMVK)                                   |                                  | 1                                 |                          | 1                         |
| MTH48               | 15678077 | isopentenyl-diphosphate delta-isomerase (EC 5.3.3.2) (IPP isomerase)                             |                                  | 1                                 |                          | 1                         |
| MTH49               | 15678078 | predicted mevalonatediphosphate decarboxylase, diphosphomevalonate decarboxylase                 | 1                                | 1                                 | 1                        | 1                         |
| MTH50               | 15678079 | bifunctional short chain isoprenyl diphosphate synthase (IdsA)                                   | 1                                | 1                                 | 1                        |                           |
| MTH51               | 15678080 | glutamyl-tRNA synthetase   | 1                                | 1                                 | 1                        |                           |
| MTH52               | 15678081 | LL-diaminopimelate aminotransferase  | 1                                | 1                                 | 1                        | 1                         |
| MTH54               | 15678083 | conserved methanogen-specific membrane protein MTH54 containing metal chelatase domain (COG5643) | 1                                | 1                                 |                          |                           |
| MTH55               | 15678084 | conserved methanogen-specific protein MTH55 containing cell surface anchor domain (COG5643)      | 1                                | 1                                 |                          |                           |

|               |          |   |   |   |   |
|---------------|----------|---|---|---|---|
| <b>MTH56</b>  | 15678085 | conserved methanogen-specific protein MTH56 (COG5643)   | 1 |   |   |
| <b>MTH59</b>  | 15678088 | conserved membrane-bound protein MTH59 associated with fimbrin MTH60  | 1 |   | 1 |
| <b>MTH60</b>  | 15678089 | fimbrin (fimbriae protein) (verified)   | 1 |   | 1 |
| <b>MTH63</b>  | 15678092 | conserved protein (gamma-carboxymuconolactone decarboxylase homolog; alkylhydroperoxidase AhpD core)  | 1 |   |   |
| <b>MTH72</b>  | 15678100 | O-linked GlcNAc transferase containing TPR-domain (11x)   | 1 |   | 1 |
| <b>MTH75</b>  | 15678103 | membrane-associated cell wall-binding surface protease (double gly) related protein (pkd repeat; pseudomurein binding repeat, PF09373)                                | 1 |   |   |
| <b>MTH87</b>  | 15678115 | cell wall-binding surface (double gly) protease related protein (pkd repeat; pseudomurein binding repeat, PF09373)  | 1 |   |   |
| <b>MTH101</b> | 15678129 | conserved methanogen-specific protein MTH101 (COG4883)  | 1 | 1 | 1 |
| <b>MTH102</b> | 15678130 | conserved methanogen-specific small zinc-finger protein (COG4855)   | 1 |   |   |
| <b>MTH105</b> | 15678133 | glutamate synthase (NADPH), alpha subunit   | 1 | 1 | 1 |
| <b>MTH106</b> | 15678134 | tungsten formylmethanofuran dehydrogenase, subunit C homolog; glutamate synthase subunit (COG0070)  | 1 |   |   |
| <b>MTH115</b> | 15678143 | conserved protein MTH115 (SOUL heme-binding protein; pfam04832)   | 1 |   | 1 |
| <b>MTH117</b> | 15678145 | membrane-associated cell surface protein containing pseudomurein binding repeat (PF09373)   | 1 |   | 1 |
| <b>MTH119</b> | 15678147 | ATP phosphoribosyltransferase related protein   | 1 | 1 | 1 |
| <b>MTH120</b> | 15678148 | conserved protein (NADP oxidoreductase/nitroreductase; FMN binding) (COG0778)   | 1 |   |   |
| <b>MTH121</b> | 15678149 | conserved (Methanospaera) small zinc-finger protein   | 1 | 1 | 1 |
| <b>MTH126</b> | 15678154 | inosine-5'-monophosphate dehydrogenase related protein VII (contains 2xCBS-domain; HcrA-ArsR regulat. domain)   | 1 |   | 1 |
| <b>MTH129</b> | 15678157 | orotidine 5' monophosphate decarboxylase (PyrF)   | 1 |   |   |
| <b>MTH133</b> | 15678161 | cobalt transport ATP-binding protein O (CbiO)   | 1 |   | 1 |
| <b>MTH134</b> | 15678162 | riboflavin synthase (EC 2.5.1.9)  | 1 |   |   |
| <b>MTH135</b> | 15678163 | NADP-dependent FMN oxidoreductase, multimeric flavodoxin (WrbA family)  | 1 |   | 1 |
| <b>MTH138</b> | 15678166 | glycosyl transferase (GT4 family); GlcNAc-phosphatidylinositol related biosynthetic protein   | 1 |   |   |
| <b>MTH140</b> | 15678168 | conserved protein (4Fe-4S domain) (COG1139, DUF162), predicted fumarate reductase subunit   | 1 |   | 1 |
| <b>MTH141</b> | 15678169 | conserved protein (COG1891, UPF0264, DUF556); methanopterin/methanofuran biosynthesis protein   | 1 |   | 1 |
| <b>MTH142</b> | 15678170 | inosine-5'-monophosphate dehydrogenase (guaB)   | 1 | 1 | 1 |
| <b>MTH143</b> | 15678171 | molybdopterin-guanine dinucleotide biosynthesis MobA related protein  | 1 |   |   |
| <b>MTH145</b> | 15678173 | conserved membrane-bound protein MTH145   | 1 | 1 | 1 |
| <b>MTH146</b> | 15678174 | precorrin-8W decarboxylase (CbiT), precorrin methyltransferase  | 1 |   |   |
| <b>MTH147</b> | 15678175 | aromatic acid decarboxylase (EC 4.1.1.-); 3-octaprenyl-4-hydroxybenzoate carboxy-lyase  | 1 | 1 | 1 |
| <b>MTH149</b> | 15678177 | molybdenum cofactor biosynthesis protein MoaE   | 1 |   |   |
| <b>MTH150</b> | 15678178 | nicotinamide mononucleotide adenylyltransferase (NadM)  | 1 |   |   |
| <b>MTH151</b> | 15678179 | methyl coenzyme M reductase system, component A2 homolog; ATPase subunit of an ABC-type transport system with duplicated ATPase domain                                | 1 | 1 |   |
| <b>MTH153</b> | 15678181 | universal stress protein (UspA); ATP-dependent chaperone  | 1 |   | 1 |
| <b>MTH155</b> | 15678183 | rubredoxin  | 1 |   | 1 |
| <b>MTH157</b> | 15678185 | flavoprotein A homolog (III); F420H2 oxidase (III)  | 1 |   |   |
| <b>MTH158</b> | 15678186 | ferritin-like protein (RsgA)  | 1 | 1 | 1 |
| <b>MTH159</b> | 15678187 | alkyl hydroperoxide reductase, probable peroxiredoxin (PRX)   | 1 | 1 | 1 |
| <b>MTH160</b> | 15678188 | superoxide dismutase [Fe] (EC 1.15.1.1).  | 1 | 1 |   |
| <b>MTH161</b> | 15678189 | coenzyme F390 synthetase III (FtsAIII)  | 1 |   |   |
| <b>MTH162</b> | 15678190 | regulatory subunit (ACT domain family) linked with coenzyme F390 synthetase III   | 1 |   | 1 |
| <b>MTH163</b> | 15678191 | helix-turn-helix transcriptional regulator (type 11 domain; Crp/Fnr family)   | 1 |   | 1 |
| <b>MTH167</b> | 15678195 | S-adenosyl-L-methionine uroporphyrinogen methyltransferase (CysGB)  | 1 | 1 | 1 |
| <b>MTH168</b> | 15678196 | phosphoribosylformylglycinamide synthase I, PurQ subunit  | 1 |   | 1 |
| <b>MTH169</b> | 15678197 | phosphoribosylformylglycinamide synthase I, PurS subunit  | 1 |   | 1 |
| <b>MTH170</b> | 15678198 | phosphoribosylaminoimidazolesuccinocarboxamide synthase (SAICAR synthetase) (PurC)  | 1 |   | 1 |
| <b>MTH171</b> | 15678199 | glucosamine--fructose-6-phosphate aminotransferase [isomerizing] (EC 2.6.1.16); L-glutamine-D-fructose-6-phosphate amidotransferase/ glucosamine-6-phosphate synthase | 1 | 1 | 1 |
| <b>MTH173</b> | 15678201 | glycosyl transferase (GT4 family); LPS biosynthesis RfbU related protein  | 1 |   |   |
| <b>MTH174</b> | 15678202 | sensory transduction histidine kinase (PAS/PAC domain) MTH_proteome   | 1 |   |   |
| <b>MTH176</b> | 15678204 | 7-cyano-7-deazaguanine tRNA-ribosyltransferase (EC 2.4.2.-); Archaeal   | 1 |   | 1 |

|               |          |   |   |   |   |   |
|---------------|----------|---|---|---|---|---|
|               |          | tRNA-guanine transglycosylase   |   |   |   |   |
| <b>MTH177</b> | 15678205 | nascent polypeptide-associated complex (NAC) protein  | 1 | 1 | 1 | 1 |
| <b>MTH179</b> | 15678207 | conserved methanogen-specific protein MTH179 containing zinc finger (CCCH-type)   | 1 |   |   |   |
| <b>MTH180</b> | 15678208 | conserved methanogen-specific membrane-bound protein MTH180   | 1 |   |   | 1 |
| <b>MTH183</b> | 15678211 | acetylglutamate kinase (EC 2.7.2.8) (NAG kinase) (AGK); N- acetyl-L-glutamate 5-phosphotransferase                        | 1 | 1 |   |   |
| <b>MTH193</b> | 15678221 | coenzyme F420-reducing hydrogenase, beta subunit homolog; putative glutamate synthase, subunit 2                          | 1 |   |   |   |
| <b>MTH194</b> | 15678222 | glutamate synthase (F420 dependent), subunit 1  | 1 |   |   |   |
| <b>MTH198</b> | 15678226 | conserved zinc finger CDGSH-type domain protein MTH198 (COG3369, 2x)  | 1 |   |   |   |
| <b>MTH199</b> | 15678227 | conserved (Methanobrevibacter) membrane-spanning protein MTH199   | 1 | 1 |   |   |
| <b>MTH204</b> | 15678232 | conserved (N-terminal) membrane protein (COG1714) fused(C-terminal) with 5-formyl-H4folate cycloligase                    | 1 |   |   |   |
| <b>MTH205</b> | 15678233 | hydrogenase expression/formation protein HypE (HypE)  | 1 | 1 | 1 |   |
| <b>MTH207</b> | 15678235 | 30S ribosomal protein S8E   | 1 | 1 | 1 | 1 |
| <b>MTH209</b> | 15678237 | conserved protein (HAD-superfamily hydrolase/phosphatase, COG1011)  | 1 |   |   | 1 |
| <b>MTH210</b> | 15678238 | predicted AAA+ class ATPase with chaperone activity   | 1 | 1 | 1 | 1 |
| <b>MTH211</b> | 15678239 | uncharacterized membrane-bound protein MTH211   | 1 |   |   |   |
| <b>MTH212</b> | 15678240 | exodeoxyribonuclease III (xthA); DNA uridine endonuclease   | 1 |   |   | 1 |
| <b>MTH213</b> | 15678241 | ferrous iron transport protein B (FeoB)   | 1 |   |   | 1 |
| <b>MTH214</b> | 15678242 | iron dependent transcriptional regulator (Fe2+-binding) (FeoA)  | 1 |   |   |   |
| <b>MTH218</b> | 15678246 | thermosome alpha subunit, chaperonine (HSP60) I   | 1 | 1 | 1 | 1 |
| <b>MTH219</b> | 15678247 | uncharacterized protein MTH219 containing TonB-dependent receptor protein motif (PF00593)                                 | 1 | 1 | 1 | 1 |
| <b>MTH220</b> | 15678248 | flavoprotein A homolog (II); F420H2 oxidase II  | 1 | 1 |   | 1 |
| <b>MTH222</b> | 15678250 | conserved methanogen-specific hypothetical protein MTH222 (COG4740); predicted metalloprotease fused to aspartyl protease | 1 |   |   | 1 |
| <b>MTH223</b> | 15678251 | cyclic 2,3-diphosphoglycerate-synthetase  | 1 | 1 |   | 1 |
| <b>MTH226</b> | 15678254 | aspartyl-tRNA synthetase  | 1 | 1 | 1 |   |
| <b>MTH227</b> | 15678255 | precorrin isomerase; precorrin-8X methylmutase (CbiC; CobH)   | 1 |   |   | 1 |
| <b>MTH228</b> | 15678256 | glutamate-1-semialdehyde aminotransferase (HemL)  | 1 |   |   |   |
| <b>MTH230</b> | 15678258 | conserved Methanobacteriaceae-specific membrane-spanning protein MTH230 containing TPR repeat                             | 1 | 1 | 1 | 1 |
| <b>MTH231</b> | 15678259 | conserved methanogen-specific protein (COG4002) predicted phosphotransacetylase   | 1 |   |   |   |
| <b>MTH232</b> | 15678260 | undecaprenyl pyrophosphate synthetase (UPP synthetase) (Di-trans-poly-cis-decaprenylcistransferase)                       | 1 |   |   | 1 |
| <b>MTH235</b> | 15678263 | 2,5-diamino-6-hydroxy-4-(5-phosphoribosylamino)pyrimidine 1-reductase (RibD) (EC 1.1.1.193)                               | 1 |   |   |   |
| <b>MTH236</b> | 15678264 | conserved methanogen-specific protein MTH236 (COG1790, DUF483)  | 1 |   |   | 1 |
| <b>MTH237</b> | 15678265 | hydrogenocobyrinic acid a,c-diamide cobaltochelate (CobN)   | 1 | 1 |   |   |
| <b>MTH241</b> | 15678269 | replication factor C, small subunit   | 1 | 1 | 1 | 1 |
| <b>MTH242</b> | 15678270 | shikimate 5-dehydrogenase (chorismate synthesis) (AroE)   | 1 |   |   |   |
| <b>MTH243</b> | 15678271 | conserved DNA-binding protein containing PIN domain (COG1458, UPF0278 )   | 1 | 1 | 1 | 1 |
| <b>MTH244</b> | 15678272 | histidyl-tRNA synthetase (HisRS)  | 1 | 1 |   | 1 |
| <b>MTH246</b> | 15678274 | twitching mobility (PilT) related protein; bacterial type II secretion system ATPase                                      | 1 | 1 | 1 | 1 |
| <b>MTH247</b> | 15678275 | conserved protein (COG1082); predicted TIM barrel sugar phosphate isomerase/epimerase or endonuclease (endonuclease IV)   | 1 |   |   |   |
| <b>MTH248</b> | 15678276 | F420-dependent NADP reductase   | 1 | 1 | 1 | 1 |
| <b>MTH249</b> | 15678277 | hexulose-6-phosphate isomerase  | 1 |   |   | 1 |
| <b>MTH250</b> | 15678278 | tRNA-splicing endonuclease (EC 3.1.27.9); tRNA-intron endonuclease  | 1 |   |   | 1 |
| <b>MTH251</b> | 15678279 | tryptophanyl-tRNA synthetase (TrpRS)  | 1 | 1 | 1 | 1 |
| <b>MTH253</b> | 15678281 | threonine synthase (thrC)   | 1 | 1 | 1 | 1 |
| <b>MTH254</b> | 15678282 | histone HMTB  | 1 |   |   | 1 |
| <b>MTH255</b> | 15678283 | 50S ribosomal protein L7Ae; snoRNA-dependent rRNA methylase   | 1 |   |   | 1 |
| <b>MTH256</b> | 15678284 | 30S ribosomal protein S28E  | 1 |   |   | 1 |
| <b>MTH257</b> | 15678285 | 50S ribosomal protein L24E  | 1 |   |   |   |
| <b>MTH258</b> | 15678286 | nucleoside diphosphate kinase   | 1 | 1 | 1 |   |
| <b>MTH259</b> | 15678287 | translation initiation factor IF2 homolog   | 1 |   |   | 1 |
| <b>MTH260</b> | 15678288 | 30S ribosomal protein S6e   | 1 | 1 | 1 | 1 |
| <b>MTH261</b> | 15678289 | translation initiation factor eIF-2, gamma subunit  | 1 | 1 | 1 | 1 |
| <b>MTH263</b> | 15678291 | inorganic pyrophosphatase   | 1 | 1 | 1 | 1 |
| <b>MTH264</b> | 15678292 | DNA-dependent RNA polymerase, subunit E' (RpoE')  | 1 |   |   | 1 |
| <b>MTH265</b> | 15678293 | DNA-dependent RNA polymerase, subunit E'' (RpoE'')  | 1 |   |   | 1 |

|        |          |  |   |   |       |
|--------|----------|--|---|---|-------|
| MTH267 | 15678295 | 30S ribosomal protein S24E   |   | 1 | 1     |
| MTH269 | 15678297 | argininosuccinate lyase (ArgH)   |   | 1 |       |
| MTH272 | 15678300 | hexarepeat-containing acetyl transferase   |   | 1 |       |
| MTH273 | 15678301 | phosphatidylethanolamine-binding protein, PBP family (COG1881)   |   | 1 | 1     |
| MTH277 | 15678305 | digeranylgeranylgercerophospholipid reductase/ FAD-dependent geranylgeranyl reductase (FixC)   | 1 | 1 |       |
| MTH280 | 15678308 | coenzyme F420-dependent sulfite reductase (Fsr) (verified)   |   | 1 | 1     |
| MTH292 | 15678320 | sensory transduction histidine kinase  |   | 1 | 1     |
| MTH301 | 15678329 | cell wall-binding surface protease related protein (pseudomurein binding repeat, PF09373)  |   | 1 | 1     |
| MTH302 | 15678330 | uncharacterized protein MTH302, putative adhesin   |   | 1 |       |
| MTH309 | 15678337 | uncharacterized protein MTH309 (DUF587)  |   | 1 |       |
| MTH311 | 15678339 | signal transduction histidine kinase (COG0642)   |   | 1 |       |
| MTH326 | 15678354 | CRISPR-associated protein Csx11  |   | 1 |       |
| MTH333 | 15678361 | GDP-mannose 4,6-dehydratase  |   | 1 | 1     |
| MTH340 | 15678368 | polysaccharide-pyruvyl transferase (S-layer biosynthesis)  |   | 1 | 1     |
| MTH341 | 15678369 | coenzyme F420-reducing hydrogenase, beta subunit homolog   |   | 1 |       |
| MTH346 | 15678374 | formate acetyltransferase 2; pyruvate-formate lyase (COG1882)  |   | 1 |       |
| MTH351 | 15678379 | membrane-bound metal chelatase belonging to the CobN/BchH family   | 1 | 1 |       |
| MTH357 | 15678385 | cell wall-binding pseudomureine (pseudomurein binding repeat, PF09373) endopeptidase containing transglutaminase and GH18-type chitinase domains |   | 1 | 1 1   |
| MTH359 | 15678387 | cell wall-binding pseudomureine endopeptidase (pseudomurein binding repeat, PF09373, 2x)   |   |   | 1     |
| MTH360 | 15678388 | sensory transduction histidine kinase  |   | 1 | 1     |
| MTH361 | 15678389 | teichoic acid biosynthesis protein RodC related protein; CDP-glycerol:poly(glycerophosphate) glycerophosphotransferase                           |   | 1 |       |
| MTH362 | 15678390 | glycosyl transferase (GT4 family); capsular polysaccharide biosynthesis protein  |   | 1 |       |
| MTH365 | 15678393 | teichoic acid biosynthesis protein RodC related protein; CDP-glycerol:poly(glycerophosphate) glycerophosphotransferase                           |   | 1 |       |
| MTH368 | 15678396 | glycerol-3-phosphate dehydrogenase, NAD(P)   |   | 1 |       |
| MTH369 | 15678397 | UDP-N-acetylglucosamine pyrophosphorylase related protein  | 1 | 1 | 1     |
| MTH370 | 15678398 | glycosyl transferase (GT4 family); LPS biosynthesis RfbU related protein/ N-acetylglucosaminyl-phosphatidylinositol biosynthetic protein         |   | 1 |       |
| MTH373 | 15678401 | dTDP-glucose 4,6-dehydratase related protein   |   | 1 | 1 1   |
| MTH374 | 15678402 | membrane-bound dolichyl-phosphate beta-D-mannosyltransferase   |   | 1 | 1 1   |
| MTH375 | 15678403 | UDP-glucose 4-epimerase homolog  |   | 1 | 1 1 1 |
| MTH376 | 15678404 | conserved protein (predicted glycosyltransferase, COG0438)   |   | 1 | 1 1   |
| MTH389 | 15678417 | conserved membrane protein (EhaF)  |   | 1 | 1     |
| MTH397 | 15678425 | formate hydrogenlyase, subunit 7 (EhaN); small subunit NiFe H2ase  |   | 1 | 1     |
| MTH398 | 15678426 | formate hydrogenlyase, subunit 5 (EhaO); large (alpha) subunit NiFe H2ase  |   | 1 | 1     |
| MTH399 | 15678427 | polyferredoxin (EhaP)  |   | 1 | 1     |
| MTH400 | 15678428 | polyferredoxin (EhaQ)  |   | 1 |       |
| MTH401 | 15678429 | polyferredoxin (EhaQ)  |   | 1 | 1     |
| MTH403 | 15678431 | formylmethanofuran:tetrahydromethanopterin formyltransferase II (EhaS, ftr II)   |   | 1 | 1     |
| MTH405 | 15678433 | polyferredoxin   |   | 1 |       |
| MTH406 | 15678434 | conserved membrane-bound protein containing signal transduction CBS-domain (2x)  | 1 | 1 | 1 1   |
| MTH412 | 15678440 | cell wall-binding pseudomureine endopeptidase (pseudomurein binding repeat, PF09373)   |   | 1 |       |
| MTH413 | 15678441 | conserved protein, pyridoxamine 5'-phosphate oxidase-related (FMN-binding; COG3576)  |   | 1 | 1 1   |
| MTH414 | 15678442 | asparagine synthetase (glutamine-hydrolyzing) AsnB   |   | 1 |       |
| MTH415 | 15678443 | Gln/asn-dependent aspartyl-tRNA(Asn) amidotransferase subunit C (GatC)   |   | 1 |       |
| MTH416 | 15678444 | predicted allosteric regulator of homoserine dehydrogenase   | 1 | 1 | 1 1   |
| MTH417 | 15678445 | homoserine dehydrogenase (thrA2, metL2) homolog  |   | 1 | 1     |
| MTH419 | 15678447 | CTP synthase (pyrG)  |   | 1 | 1     |
| MTH421 | 15678449 | membrane-bound prepilin-cleaving (type IV) signal peptidase (EppA/TFPP-like signal peptidase)  |   | 1 | 1     |
| MTH423 | 15678451 | conserved archaeal membrane-spanning hypothetical protein MTH423 (COG4025)   |   | 1 | 1     |
| MTH426 | 15678454 | uncharacterized protein MTH426   |   | 1 | 1     |
| MTH427 | 15678455 | conserved membrane-spanning hypothetical protein MTH427  |   | 1 | 1     |
| MTH428 | 15678456 | uncharacterized membrane-bound protein MTH428  |   | 1 | 1     |
| MTH429 | 15678457 | conserved membrane-spanning protein MTH429   |   | 1 |       |

|               |          |  |   |   |   |   |
|---------------|----------|--|---|---|---|---|
| <b>MTH435</b> | 15678463 | conserved archaeal protein (COG1701); pantothenate synthase (PS; PanC) (verified)  | 1 |   |   |   |
| <b>MTH437</b> | 15678465 | tetrahydral aminopeptidase (TET); family M42 deblocking aminopeptidase/ glutamyl aminopeptidase  | 1 | 1 | 1 | 1 |
| <b>MTH439</b> | 15678467 | recombinase/ RecA superfamily ATPase   | 1 |   |   | 1 |
| <b>MTH440</b> | 15678468 | sensory transduction regulatory protein containing PAS/PAC domain  | 1 | 1 | 1 | 1 |
| <b>MTH442</b> | 15678470 | excinuclease ABC subunit B (UvrB)  | 1 |   |   |   |
| <b>MTH443</b> | 15678471 | excinuclease ABC subunit A (UvrA)  | 1 | 1 | 1 | 1 |
| <b>MTH444</b> | 15678472 | sensory transduction histidine kinase  |   |   |   | 1 |
| <b>MTH445</b> | 15678473 | sensory transduction regulatory protein  | 1 | 1 |   |   |
| <b>MTH446</b> | 15678474 | sensory transduction regulatory protein containing PAS/PAC domain  |   |   |   | 1 |
| <b>MTH447</b> | 15678475 | sensory transduction regulatory protein  | 1 |   |   |   |
| <b>MTH477</b> | 15678505 | tungstate transport ABC system ATP-binding (TupC)  | 1 |   |   | 1 |
| <b>MTH478</b> | 15678506 | tungstate transport ABC system permease protein (TupB)   | 1 |   |   |   |
| <b>MTH479</b> | 15678507 | tungstate transport ABC system TupA protein  | 1 | 1 | 1 | 1 |
| <b>MTH480</b> | 15678508 | conserved protein MTH480 containing ATP cone domain (PF03477)  |   |   |   | 1 |
| <b>MTH487</b> | 15678515 | superfamily I DNA and RNA helicase; Very Short Patch Repair (Vsr), endonuclease subunit  | 1 | 1 | 1 | 1 |
| <b>MTH488</b> | 15678516 | superfamily I DNA and RNA helicase; Very Short Patch Repair (Vsr), endonuclease subunit  |   |   |   | 1 |
| <b>MTH504</b> | 15678532 | H(2)-dependent N5,N10-methylenetetrahydromethanopterin dehydrogenase homolog (III)   | 1 |   |   |   |
| <b>MTH511</b> | 15678539 | ATP-dependent DNA helicase II (UvrD, PcrA)   | 1 |   |   |   |
| <b>MTH517</b> | 15678545 | predicted regulator of CRISPR system (COG2462 fused to ArsR-HTH5 (COG1517))  | 1 | 1 | 1 | 1 |
| <b>MTH519</b> | 15678547 | conserved Methanobacteriaceae-specific protein MTH519  | 1 | 1 |   | 1 |
| <b>MTH526</b> | 15678554 | conserved protein MTH526 (COG2043, DUF169)   | 1 | 1 | 1 | 1 |
| <b>MTH527</b> | 15678555 | uncharacterized protein MTH527   | 1 |   |   | 1 |
| <b>MTH528</b> | 15678556 | uncharacterized MobA-related protein (COG2068); UDP-N-acetylglucosamine pyrophosphorylase/ N-acetylglucosamine 1-phosphuridyltransferase | 1 |   |   | 1 |
| <b>MTH529</b> | 15678557 | conserved methanogen-specific protein MTH529   |   |   |   | 1 |
| <b>MTH530</b> | 15678558 | UDP-N-acetylmuramate-alanine ligase  | 1 | 1 | 1 | 1 |
| <b>MTH531</b> | 15678559 | UDP-N-acetylmuramoylalanine-D-glutamate ligase   | 1 |   | 1 |   |
| <b>MTH532</b> | 15678560 | UDP-N-acetylmuramoylalanine-D-glutamate ligase homolog   | 1 |   |   |   |
| <b>MTH540</b> | 15678568 | DNA double-strand break repair rad50 ATPase (Rad50)  | 1 |   |   | 1 |
| <b>MTH541</b> | 15678569 | Mla(2)- Mre11 fusion protein   | 1 |   |   |   |
| <b>MTH542</b> | 15678570 | DNA segregation ATPase Mla(1)/ FtsK (gene split)   | 1 |   |   |   |
| <b>MTH544</b> | 15678572 | conserved protein MTH544 (DUF74 UPF0145)   | 1 | 1 |   |   |
| <b>MTH552</b> | 15678580 | geranylgeranyl glyceryl phosphate synthase   | 1 |   |   | 1 |
| <b>MTH554</b> | 15678582 | conserved protein MTH554 (COG2042, DUF367, UPF0293)  | 1 | 1 |   |   |
| <b>MTH556</b> | 15678584 | protoporphyrin IX magnesium-chelatase subunit ChII   | 1 | 1 |   |   |
| <b>MTH562</b> | 15678590 | 3-hydroxy-3-methylglutaryl CoA reductase (HmgA)  | 1 | 1 |   | 1 |
| <b>MTH563</b> | 15678591 | succinyl-CoA synthetase, alpha subunit (sucC)  | 1 | 1 | 1 | 1 |
| <b>MTH566</b> | 15678594 | 3-dehydroquinate dehydratase, chorismate synthesis (AroD)  | 1 |   |   | 1 |
| <b>MTH567</b> | 15678595 | signal peptidase I   | 1 |   |   | 1 |
| <b>MTH569</b> | 15678597 | heat shock protein X; protease htpX homolog (EC 3.4.24.-)  | 1 |   |   | 1 |
| <b>MTH570</b> | 15678598 | conserved adhesin-like protein   | 1 |   |   | 1 |
| <b>MTH574</b> | 15678602 | conserved flavodoxin family protein (FMN binding, Ni binding) (COG1853)  | 1 | 1 |   |   |
| <b>MTH579</b> | 15678607 | fructose-1,6-bisphosphate aldolase/ 2-amino-3,7-dideoxy-D-threo-hept-6-ulosonate (ADTH) synthase (aroA')                                 | 1 | 1 | 1 | 1 |
| <b>MTH580</b> | 15678608 | 3-dehydroquinate synthase (AroB')  | 1 | 1 | 1 |   |
| <b>MTH582</b> | 15678610 | conserved protein related to HPr kinase (C-terminal part)  | 1 |   |   |   |
| <b>MTH583</b> | 15678611 | 2',5'-RNA ligase   | 1 | 1 |   | 1 |
| <b>MTH584</b> | 15678612 | CCA-adding enzyme/ tRNA CCA-pyrophosphorylase (tRNA adenyllyl-/cytidyllyl- transferase) (EC 2.7.7.25)                                    | 1 |   |   |   |
| <b>MTH587</b> | 15678615 | methionyl-tRNA synthetase (MetG)   | 1 | 1 | 1 |   |
| <b>MTH592</b> | 15678620 | RecA/ Rad55 superfamily ATPase involved in homologous recombination (COG0467)  | 1 |   |   | 1 |
| <b>MTH593</b> | 15678621 | RecA/ Rad55 superfamily ATPase involved in homologous recombination (COG0467)  | 1 |   |   |   |
| <b>MTH594</b> | 15678622 | RecA/ Rad55 superfamily ATPase/GTPase (COG0467; COG2229)   | 1 | 1 | 1 |   |
| <b>MTH595</b> | 15678623 | conserved protein (COG2018); regulatory roadblock-LC7 domain   | 1 |   |   |   |
| <b>MTH599</b> | 15678627 | uncharacterized protein MTH599   |   |   |   | 1 |
| <b>MTH604</b> | 15678632 | zinc (Mn) ABC transporter, periplasmic zinc-binding protein  | 1 |   |   |   |
| <b>MTH605</b> | 15678633 | zinc (Mn) ABC transporter, ATP-binding protein ABC transporter   | 1 |   |   |   |

|               |          |   |   |   |   |   |
|---------------|----------|---|---|---|---|---|
| <b>MTH611</b> | 15678639 | prolyl-tRNA synthetase (+cysteinyl-tRNA)  | 1 | 1 | 1 | 1 |
| <b>MTH612</b> | 15678640 | uncharacterized membrane-bound protein MTH612   |   | 1 |   |   |
| <b>MTH613</b> | 15678641 | conserved protein (COG1920, DUF121); GTP:lactate guanylyl transferase involved in F420 biosynthesis (CofC)            |   | 1 |   | 1 |
| <b>MTH614</b> | 15678642 | phosphomethylpyrimidine kinase (HMPP-kinase) (ThiD/ transcriptional regulator)  |   | 1 |   |   |
| <b>MTH615</b> | 15678643 | adenylosuccinate synthetase (EC 6.3.4.4) (IMP-aspartate ligase) (PurA)  |   | 1 |   | 1 |
| <b>MTH616</b> | 15678644 | predicted AAA+ class ATPase with chaperone activity   |   |   | 1 |   |
| <b>MTH619</b> | 15678647 | sensory transduction histidine kinase containing PAS/PAC domain   |   | 1 |   | 1 |
| <b>MTH622</b> | 15678650 | thiosulfate sulfurtransferase; 3-mercaptopyruvate sulfurtransferase (rhodanese-related sulfurtransferase)             |   | 1 |   | 1 |
| <b>MTH627</b> | 15678655 | partially conserved membrane-bound protein MTH627   |   | 1 |   |   |
| <b>MTH631</b> | 15678659 | UDP-glucose 4-epimerase   |   | 1 |   | 1 |
| <b>MTH632</b> | 15678660 | conserved protein MTH632; putative (sugar) kinase (COG0464)   |   | 1 |   |   |
| <b>MTH634</b> | 15678662 | UDP-glucose pyrophosphorylase, UTP-glucose-1-phosphate uridylyltransferase (GalU)                                     |   | 1 |   | 1 |
| <b>MTH635</b> | 15678663 | membrane-associated porin-like protein  |   | 1 |   | 1 |
| <b>MTH643</b> | 15678670 | nitrogenase NifH subunit; nitrogenase iron protein (EC 1.18.6.1) (nitrogenase component II) (NifH)                    |   | 1 |   | 1 |
| <b>MTH644</b> | 15678671 | inosine-5'-monophosphate dehydrogenase related protein with regulatory CBS domain                                     |   | 1 | 1 | 1 |
| <b>MTH646</b> | 15678673 | amidophosphoribosyltransferase (glutamine phosphoribosylpyrophosphate amidotransferase) (PurF)                        | 1 | 1 |   |   |
| <b>MTH647</b> | 15678674 | topoisomerase-primase (TOPRIM)-domain-containing protein, potential nuclease (gene split with MTH838, MTH839)         |   | 1 |   | 1 |
| <b>MTH648</b> | 15678675 | 50S ribosomal protein L37E  |   | 1 |   |   |
| <b>MTH649</b> | 15678676 | small nuclear ribonucleoprotein (snRNP/Sm protein)  |   | 1 |   | 1 |
| <b>MTH650</b> | 15678677 | RNA-binding translation factor (PUA domain)   |   | 1 |   | 1 |
| <b>MTH651</b> | 15678678 | 2-amino-5-formylamino-6-ribosylamino-4(3H)-pyrimidinone 5'-monophosphate formamide hydrolase                          |   | 1 |   | 1 |
| <b>MTH653</b> | 15678680 | putative membrane-bound dolichyl-phosphate-mannose-protein mannosyltransferase  |   | 1 |   | 1 |
| <b>MTH654</b> | 15678681 | conserved methanogen-specific membrane-spanning protein; adhesin-like protein   |   | 1 | 1 | 1 |
| <b>MTH657</b> | 15678684 | long-chain-fatty-acid-CoA ligase  | 1 | 1 | 1 | 1 |
| <b>MTH658</b> | 15678685 | acyl-CoA thioesterase   |   | 1 |   | 1 |
| <b>MTH659</b> | 15678686 | helix-turn-helix transcriptional regulator, XRE family (COG1396)  | 1 | 1 | 1 |   |
| <b>MTH664</b> | 15678691 | nitrogen regulatory protein P-II 2  |   | 1 |   | 1 |
| <b>MTH666</b> | 15678693 | pyridoxal biosynthesis lyase pdxS (EC 4.-.-.); pyridoxal-5-phosphate biosynthesis protein (pdx2)                      | 1 | 1 | 1 |   |
| <b>MTH670</b> | 15678697 | conserved membrane-spanning protein MTH670  |   | 1 |   |   |
| <b>MTH671</b> | 15678698 | predicted B12 transporter (btuT)  | 1 | 1 | 1 | 1 |
| <b>MTH673</b> | 15678700 | B12 transporter (BtuS; CbiN-related)  | 1 | 1 |   |   |
| <b>MTH674</b> | 15678701 | conserved protein MTH674 containing a metal-binding domain as in formylmethanofuran dehydrogenase subunit E (COG5643) | 1 | 1 |   |   |
| <b>MTH675</b> | 15678702 | conserved protein (COG0500); SAM-dependent methyltransferase, putative nicotianamine synthase (plant iron chelator)   |   | 1 |   |   |
| <b>MTH678</b> | 15678705 | prefoldin beta subunit (GimC; Cpn beta subunit)   |   | 1 |   | 1 |
| <b>MTH680</b> | 15678707 | Brix domain-containing ribosomal biogenesis protein (IMP4/RPC10) (known structure)                                    |   | 1 |   |   |
| <b>MTH681</b> | 15678708 | 50S ribosomal protein L37Ae   |   | 1 |   |   |
| <b>MTH682</b> | 15678709 | exosome complex exonuclease 2 Rrp41 (EC 3.1.13.-)   | 1 | 1 | 1 |   |
| <b>MTH683</b> | 15678710 | exosome complex exonuclease 1 Rrp42 (EC 3.1.13.-)   | 1 | 1 | 1 |   |
| <b>MTH684</b> | 15678711 | exosome complex RNA-binding protein 1 Rrp4  | 1 | 1 | 1 | 1 |
| <b>MTH685</b> | 15678712 | conserved protein (COG1500)   | 1 | 1 | 1 |   |
| <b>MTH686</b> | 15678713 | proteasome, alpha subunit   | 1 | 1 | 1 | 1 |
| <b>MTH688</b> | 15678715 | ribonuclease P protein component 3 (EC 3.1.26.5) (RNase P component 3) exosome subunit Rpp30                          |   | 1 |   |   |
| <b>MTH691</b> | 15678718 | conserved protein (COG599); gamma-carboxymuconolactone decarboxylase homolog/ alkylhydroperoxidase AhpD core          |   | 1 |   | 1 |
| <b>MTH692</b> | 15678719 | p-stomatatin (stomatatin band 7 homolog) (COG0330)  |   | 1 |   | 1 |
| <b>MTH693</b> | 15678720 | conserved membrane-bound stomatatin operon partner protein (STOPP) (COG1585, DUF107), regulatory protease             |   | 1 |   |   |
| <b>MTH694</b> | 15678721 | uncharacterized protein MTH694 (contains HTH-3 domain) (COG1476)  | 1 | 1 |   |   |
| <b>MTH695</b> | 15678722 | conserved protein (COG0577; PF02687); ABC transporter, permease protein   |   | 1 |   |   |
| <b>MTH696</b> | 15678723 | ABC-type transport system, ATPase component   |   | 1 |   |   |
| <b>MTH697</b> | 15678724 | conserved Archaeoflavoprotein AfpA (COG1036), dihydromethanopterin reductase  | 1 | 1 |   | 1 |

|               |          |   |   |   |   |   |
|---------------|----------|---|---|---|---|---|
| <b>MTH698</b> | 15678725 | conserved Methanobacteriaceae-specific hypothetical protein MTH698  | 1 | 1 |   |   |
| <b>MTH699</b> | 15678726 | conserved protein (COG1839, DUF355)   | 1 |   |   |   |
| <b>MTH700</b> | 15678727 | transcriptional regulator, PbsX/ XRE family (COG1396)   | 1 |   |   | 1 |
| <b>MTH701</b> | 15678728 | acetyl-CoA synthetase 2 (N-terminal part) (COG0365)   | 1 | 1 | 1 |   |
| <b>MTH704</b> | 15678731 | 2-oxoisovalerate oxidoreductase, beta subunit   | 1 | 1 |   |   |
| <b>MTH705</b> | 15678732 | 2-oxoisovalerate oxidoreductase, alpha subunit  | 1 |   |   |   |
| <b>MTH706</b> | 15678733 | Asn/gln-dependent glutamyl-tRNA(Gln) amidotransferase subunit D (EC 6.3.5.-) (Glu-ADT subunit D)  | 1 |   |   | 1 |
| <b>MTH707</b> | 15678734 | Asn/gln-dependent glutamyl-tRNA(Gln) amidotransferase subunit E (EC 6.3.5.-) (Glu-ADT subunit E)  | 1 | 1 |   | 1 |
| <b>MTH708</b> | 15678735 | thioredoxin reductase   | 1 |   |   |   |
| <b>MTH709</b> | 15678736 | GMP synthase [glutamine-hydrolyzing] subunit A (EC 6.3.5.2) (Glutamine amidotransferase)  | 1 | 1 |   | 1 |
| <b>MTH710</b> | 15678737 | GMP synthase [glutamine-hydrolyzing] subunit B (EC 6.3.5.2)   | 1 |   |   | 1 |
| <b>MTH714</b> | 15678741 | membrane-bound metal chelatase (CobN/BchH family) containing cell adhesion related domain (CardB)   | 1 | 1 |   |   |
| <b>MTH715</b> | 15678742 | membrane-bound methanogen-specific cell surface protein   | 1 | 1 |   |   |
| <b>MTH716</b> | 15678743 | cell wall-binding glycoprotein (s-layer protein) (2x pkd repeat;CASH, NosD and CARBD domains; pseudomurein binding repeat, PF09373)         | 1 | 1 |   |   |
| <b>MTH717</b> | 15678744 | membrane-bound methanogen-specific cell surface protein (COG1572) containing cell adhesion related domain (CardB)                           | 1 |   |   |   |
| <b>MTH719</b> | 15678746 | membrane-bound cell wall-binding glycoprotein (s-layer protein) containing CASH and NosD domains; pseudomurein binding repe (PF09373)       | 1 |   |   | 1 |
| <b>MTH721</b> | 15678748 | conserved pyridoxal phosphate-dependent protein (COG0075, COG1167); putative amino-sugar biosynthesis prot.                                 | 1 |   |   |   |
| <b>MTH723</b> | 15678750 | R-citramalate (CimA)/ R-homocitrate synthase  | 1 |   |   |   |
| <b>MTH726</b> | 15678753 | conserved membrane-bound protein MTH726 containing DUF304 domain (COG3428, PF3703)  | 1 |   |   |   |
| <b>MTH728</b> | 15678755 | ATP-dependent 26S protease regulatory subunit 4, proteasome-activating nucleotidase   | 1 |   |   |   |
| <b>MTH729</b> | 15678756 | eukaryotic multiprotein bridging factor MBF1 homolog  | 1 |   |   |   |
| <b>MTH730</b> | 15678757 | conserved archaeal protein MTH730 (COG1844, DUF356)   | 1 |   |   |   |
| <b>MTH731</b> | 15678758 | conserved methanogen-specific membrane-spanning protein MTH731  | 1 |   |   | 1 |
| <b>MTH733</b> | 15678760 | conserved methanogen-specific membrane-spanning protein MTH733  | 1 |   |   | 1 |
| <b>MTH735</b> | 15678761 | phospho-N-acetylmuramoyl-pentapeptide-transferase; UDP-MurNAc-pentapeptide phosphotransferase   | 1 |   |   |   |
| <b>MTH739</b> | 15678765 | nickel responsive regulator 2 NikR (copG-HTH4)  | 1 | 1 | 1 | 1 |
| <b>MTH740</b> | 15678766 | conserved protein containing signal transduction CBS domain (2x)  |   |   |   | 1 |
| <b>MTH741</b> | 15678767 | conserved Methanobacteriaceae-specific protein MTH741   |   |   |   | 1 |
| <b>MTH742</b> | 15678768 | phenylalanyl-tRNA synthetase alpha chain (EC 6.1.1.20); phenylalanine--tRNA ligase alpha chain  | 1 |   |   | 1 |
| <b>MTH743</b> | 15678769 | ATP:dephospho-CoA triphosphoribosyl transferase (CitG; DPCK)  | 1 | 1 | 1 |   |
| <b>MTH744</b> | 15678770 | porphobilinogen synthase; delta-aminolevulinic acid dehydratase (EC 4.2.1.24) (HemB)  | 1 | 1 | 1 |   |
| <b>MTH747</b> | 15678773 | conserved protein (COG2013, DUF124)/ HTH DNA-binding protein  | 1 |   |   | 1 |
| <b>MTH748</b> | 15678774 | chorismate synthase, 5-enolpyruvylshikimate-3-phosphate phospholyase (AroC)   | 1 |   |   |   |
| <b>MTH752</b> | 15678777 | conserved methanogen-specific (not Methanosphaera) protein MTH752 (COG4079)   | 1 | 1 |   |   |
| <b>MTH753</b> | 15678778 | conserved protein (COG1331, DUF255), DsbD gamma family protein involved in electron transfer to thiol-disulfide isomerase (N-terminal part) | 1 |   |   | 1 |
| <b>MTH755</b> | 15678780 | copper (Cu2+) transporting CPX-type ATPase (CopB)   | 1 |   |   |   |
| <b>MTH756</b> | 15678781 | rubrerythrin  | 1 |   |   |   |
| <b>MTH757</b> | 15678782 | rubredoxin oxidoreductase; desulfoferredoxin homolog (Dfx)  | 1 |   |   |   |
| <b>MTH758</b> | 15678783 | S-D-lactoylglutathione methylglyoxal lyase  | 1 |   |   |   |
| <b>MTH759</b> | 15678784 | partially (C-terminal) conserved protein involved in exopolysaccharide biosynthesis   | 1 |   |   |   |
| <b>MTH763</b> | 15678788 | archaea-specific RecJ protein, ss-DNA specific exonuclease  | 1 | 1 | 1 | 1 |
| <b>MTH765</b> | 15678790 | small GTP-binding protein Rab-related protein; translation initiation factor 2  | 1 | 1 | 1 | 1 |
| <b>MTH766</b> | 15678791 | 5-enolpyruvylshikimate 3-phosphate synthase (3-phosphoshikimate 1-carboxyvinyltransferase (EC 2.5.1.19)(aroA)                               | 1 |   |   |   |
| <b>MTH767</b> | 15678792 | valyl-tRNA synthetase   | 1 | 1 | 1 | 1 |
| <b>MTH770</b> | 15678795 | phenylalanyl-tRNA synthetase beta chain (EC 6.1.1.20); phenylalanine-tRNA ligase beta chain   | 1 | 1 | 1 |   |
| <b>MTH771</b> | 15678796 | conserved protein (COG0432, UPF0047)  | 1 |   |   |   |
| <b>MTH773</b> | 15678798 | N5,N10-methenyl-tetrahydromethanopterin cyclohydrolase  | 1 | 1 | 1 | 1 |
| <b>MTH774</b> | 15678799 | thymidylate synthase (EC 2.1.1.45) (TS) (TSase).  | 1 |   |   |   |

|               |          |  |   |   |   |
|---------------|----------|--|---|---|---|
| <b>MTH775</b> | 15678800 | methylcobalamin:homocysteine methyltransferase (EC 2.1.1.-); cobalamin-independent methionine synthase                                   | 1 | 1 | 1 |
| <b>MTH777</b> | 15678802 | conserved methanogen-specific protein (COG4081)  | 1 |   | 1 |
| <b>MTH781</b> | 15678805 | conserved archaeal protein MTH781 (COG1817, DUF354)  | 1 |   |   |
| <b>MTH782</b> | 15678806 | hydrogenase expression/formation protein HypB  | 1 |   | 1 |
| <b>MTH784</b> | 15678808 | ribose-phosphate pyrophosphokinase (EC 2.7.6.1) (RPPK) (Phosphoribosyl pyrophosphate synthetase) (P-Rib-PP synthetase) (PRPP synthetase) | 1 |   | 1 |
| <b>MTH785</b> | 15678809 | ATP-dependent protease LA/ Lon protease  | 1 | 1 | 1 |
| <b>MTH786</b> | 15678810 | sensory transduction histidine kinase related protein conaining PAS/PAC domain   | 1 |   | 1 |
| <b>MTH792</b> | 15678814 | 3-hydroxy-3-methylglutaryl-CoA-synthase  | 1 | 1 | 1 |
| <b>MTH793</b> | 15678815 | lipid-transfer protein (sterol or nonspecific)   | 1 | 1 | 1 |
| <b>MTH794</b> | 15678816 | thermosome subunit 2, chaperonine (HSP60) I)   | 1 | 1 | 1 |
| <b>MTH797</b> | 15678819 | conserved hypothetical protein (COG1196), putative chromosome segregation ATPase   | 1 | 1 | 1 |
| <b>MTH799</b> | 15678821 | aspartate-semialdehyde dehydrogenase (asd)   | 1 |   | 1 |
| <b>MTH800</b> | 15678822 | dihydrodipicolinate reductase (DapB)   | 1 |   |   |
| <b>MTH801</b> | 15678823 | dihydrodipicolinate synthase (DapA)  | 1 | 1 | 1 |
| <b>MTH802</b> | 15678824 | aspartokinase II alpha subunit (thrA1, metL) containing regulatory ACT domain  | 1 | 1 | 1 |
| <b>MTH805</b> | 15678827 | shikimate kinase (GHMP kinase) (EC 2.7.1.71) (AroK)  | 1 | 1 |   |
| <b>MTH806</b> | 15678828 | type IV signal peptide peptidase (SPP)   | 1 | 1 | 1 |
| <b>MTH807</b> | 15678829 | thioredoxin (glutaredoxin-like protein).   | 1 |   | 1 |
| <b>MTH808</b> | 15678830 | cobalt-precorrin-6A synthase [deacetylating], anaerobic ring methylation   | 1 |   |   |
| <b>MTH809</b> | 15678831 | molybdenum cofactor biosynthesis protein MoaC  |   |   | 1 |
| <b>MTH810</b> | 15678832 | SF2- (ski2)-type DNA helicase (Hel308; EC 3.6.1.-)   | 1 |   | 1 |
| <b>MTH814</b> | 15678836 | conserved methanogen-specific protein MTH814 (COG4014)   | 1 |   | 1 |
| <b>MTH815</b> | 15678837 | conserved Methanobacteriaceae-specific protein (COG1873) implicated in RNA metabolism  | 1 |   | 1 |
| <b>MTH817</b> | 15678839 | histone acetyltransferase Elp3 homolog, component RNA polymerase II complex  | 1 |   |   |
| <b>MTH818</b> | 15678840 | 2-deoxyribose-5-phosphate aldolase (deoC)  | 1 |   |   |
| <b>MTH821</b> | 15678843 | histone HMTa1  | 1 |   | 1 |
| <b>MTH822</b> | 15678844 | rubrerythrin   | 1 |   | 1 |
| <b>MTH827</b> | 15678847 | protein L-isoaspartyl carboxyl methyltransferase (SAM-dependent methyltransferase)   | 1 | 1 | 1 |
| <b>MTH829</b> | 15678849 | 3-isopropylmalate dehydratase small subunit 1 (EC 4.2.1.33) (Isopropylmalate isomerase 1)  | 1 | 1 | 1 |
| <b>MTH831</b> | 15678851 | molybdenum cofactor biosynthesis-related protein, MoaA; radical SAM protein  | 1 | 1 | 1 |
| <b>MTH834</b> | 15678854 | conserved protein (COG1548); pantheonate/ sugar kinase-like protein  | 1 |   | 1 |
| <b>MTH836</b> | 15678856 | UDP-N-acetyl-D-mannosaminuronic/ talosaminuronic acid dehydrogenase  | 1 |   | 1 |
| <b>MTH840</b> | 15678860 | pseudouridylate synthase I, tRNA pseudouridine synthase A (EC 4.2.1.70)  | 1 |   |   |
| <b>MTH843</b> | 15678863 | phosphoribosylformimino-5-aminoimidazole carboxamide ribotide isomerase (HisA)   | 1 |   | 1 |
| <b>MTH845</b> | 15678865 | cell surface pseudomureine (transglutaminase) endopeptidase  | 1 |   |   |
| <b>MTH846</b> | 15678866 | N-acetyl-gamma-glutamyl-phosphate reductase (ArgC)   | 1 | 1 | 1 |
| <b>MTH847</b> | 15678867 | flavodoxin   | 1 | 1 | 1 |
| <b>MTH848</b> | 15678868 | protein-export membrane protein, SecF  | 1 | 1 | 1 |
| <b>MTH849</b> | 15678869 | protein-export membrane protein, SecD  | 1 |   | 1 |
| <b>MTH850</b> | 15678870 | aspartate carbamoyltransferase regulatory subunit (PyrI)   | 1 | 1 | 1 |
| <b>MTH851</b> | 15678871 | cell surface protein containing pseudomurein binding repeat (PF09373)  | 1 |   | 1 |
| <b>MTH852</b> | 15678872 | membrane-bound metal-dependent hydrolase of the aminoacylase-2/ carboxypeptidase Z family  | 1 |   |   |
| <b>MTH854</b> | 15678874 | ferredoxin   | 1 |   | 1 |
| <b>MTH855</b> | 15678875 | inosine-5'-monophosphate dehydrogenase related protein VIII containing (2x) signal transduction CBS-domain                               | 1 | 1 | 1 |
| <b>MTH857</b> | 15678877 | conserved AMMECR1 domain protein (COG2078, DUF51)  | 1 |   |   |
| <b>MTH858</b> | 15678878 | archaeal GTP-binding protein (TGS domain), GTP1/OBG family   | 1 |   |   |
| <b>MTH859</b> | 15678879 | heat shock protein, class I (HSP20)  | 1 | 1 | 1 |
| <b>MTH860</b> | 15678880 | glucosamine-fructose-6-phosphate aminotransferase (SIS domain)   | 1 |   |   |
| <b>MTH862</b> | 15678882 | conserved methanogen-specific protein MTH862 (COG4090)   | 1 |   |   |
| <b>MTH867</b> | 15678887 | lysine-oxoglutarate dehydrogenase/ saccharopine dehydrogenase bifunctional enzyme (LOR/SDH)  | 1 |   |   |
| <b>MTH869</b> | 15678889 | translation initiation factor 5A (eIF-5A), hypusine-containing protein   | 1 | 1 | 1 |
| <b>MTH871</b> | 15678891 | bifunctional inositol-1 monophosphatase/fructose-1,6-bisphosphatase  | 1 |   |   |
| <b>MTH872</b> | 15678892 | inorganic polyphosphate/ATP-NAD kinase (EC 2.7.1.23); poly(P)/ATP NAD  | 1 |   |   |

|               |          |   |   |   |   |   |
|---------------|----------|---|---|---|---|---|
|               |          | kinase)   |   |   |   |   |
| <b>MTH873</b> | 15678893 | UDP-N-acetylmuramyl tripeptide synthetase related protein   | 1 |   |   |   |
| <b>MTH875</b> | 15678895 | NAD-dependent 3"-UDP-N-acetyl-D-glucosamine dehydrogenase   | 1 |   | 1 |   |
| <b>MTH876</b> | 15678896 | orotate phosphoribosyltransferase homolog (PyrE-like protein)                                     | 1 | 1 | 1 | 1 |
| <b>MTH878</b> | 15678898 | peptide chain release factor eRF, subunit 1; translation termination factor aRF1                  | 1 | 1 | 1 | 1 |
| <b>MTH879</b> | 15678899 | uridine monophosphate kinase (pyrH)   | 1 |   |   | 1 |
| <b>MTH880</b> | 15678900 | conserved methanogen-specific small zinc-finger protein(COG4068)                                  | 1 |   |   |   |
| <b>MTH883</b> | 15678903 | conserved methanogen-specific membrane-spanning protein MTH883 (COG2985)                          | 1 |   |   |   |
| <b>MTH885</b> | 15678905 | transcription initiation factor TFIIB   | 1 | 1 |   | 1 |
| <b>MTH888</b> | 15678908 | conserved protein; 2-demethylmenaquinone methyltransferase (menG) (COG0684, PF03737)              | 1 |   |   | 1 |
| <b>MTH889</b> | 15678909 | conserved archaeal protein (COG1888, DUF211)  | 1 |   |   | 1 |
| <b>MTH891</b> | 15678911 | bacterial DNA primase (DnaG, Toprim domain)   | 1 | 1 | 1 | 1 |
| <b>MTH892</b> | 15678912 | ATP-dependent protease LA related protein   | 1 |   |   | 1 |
| <b>MTH897</b> | 15678917 | pyrroline-5-carboxylate reductase (ProC)  | 1 |   |   |   |
| <b>MTH898</b> | 15678918 | universal stress protein (UspA); chaperone (ATP-dependent)  | 1 | 1 |   | 1 |
| <b>MTH901</b> | 15678921 | sensory transduction regulatory protein   | 1 |   |   |   |
| <b>MTH905</b> | 15678925 | conserved protein (COG1268); biotine transport protein (BioY)                                     | 1 |   |   | 1 |
| <b>MTH909</b> | 15678929 | tRNA acetylating (4-acetylcytidine) enzyme  | 1 |   |   |   |
| <b>MTH911</b> | 15678931 | cell surface adhesin-like protein   | 1 | 1 |   |   |
| <b>MTH914</b> | 15678934 | conserved methanogen-specific membrane-bound protein MTH914                                       | 1 |   |   |   |
| <b>MTH916</b> | 15678936 | DNA-binding protein tfx (HTH3; Mo-uptake regulator)   | 1 | 1 | 1 | 1 |
| <b>MTH917</b> | 15678937 | molybdenum formylmethanofuran dehydrogenase, subunit E  | 1 | 1 | 1 | 1 |
| <b>MTH918</b> | 15678938 | molybdenum formylmethanofuran dehydrogenase, subunit C  | 1 | 1 | 1 | 1 |
| <b>MTH919</b> | 15678939 | molybdenum formylmethanofuran dehydrogenase, subunit B  | 1 | 1 | 1 | 1 |
| <b>MTH922</b> | 15678942 | molybdenum transport system permease protein (COG2014), modB (N-terminus) related                 | 1 | 1 |   | 1 |
| <b>MTH923</b> | 15678943 | molybdenum transport system permease protein, modB (C-terminus) related                           | 1 |   | 1 |   |
| <b>MTH924</b> | 15678944 | molybdate-binding periplasmic protein (modA)  | 1 | 1 |   | 1 |
| <b>MTH925</b> | 15678945 | conserved protein (COG2014, DUF364)   | 1 | 1 |   | 1 |
| <b>MTH926</b> | 15678946 | tungsten formylmethanofuran dehydrogenase subunit F homolog; polyferredoxin                       | 1 | 1 |   | 1 |
| <b>MTH927</b> | 15678947 | ferredoxin  | 1 |   |   |   |
| <b>MTH928</b> | 15678948 | membrane-bound metal chelatase belonging to the CobN/BchH family                                  | 1 | 1 |   |   |
| <b>MTH943</b> | 15678963 | phosphoenolpyruvate carboxylase (PpcA) (verified)   | 1 | 1 | 1 | 1 |
| <b>MTH944</b> | 15678964 | conserved membrane-spanning protein MTH944  | 1 | 1 |   |   |
| <b>MTH949</b> | 15678967 | conserved archaeal protein MTH949 (COG2083, DUF61, UPF0216)                                       | 1 |   |   |   |
| <b>MTH950</b> | 15678968 | uncharacterized protein MTH950  | 1 |   |   | 1 |
| <b>MTH952</b> | 15678970 | conserved methanogen-specific ATPase-operon protein (COG1417, DUF22)                              | 1 | 1 |   | 1 |
| <b>MTH953</b> | 15678971 | ATP synthase, subunit D (delta)   | 1 | 1 | 1 | 1 |
| <b>MTH954</b> | 15678972 | ATP synthase, subunit B (beta)  | 1 | 1 | 1 | 1 |
| <b>MTH955</b> | 15678973 | ATP synthase, subunit A (alfa)  | 1 | 1 | 1 | 1 |
| <b>MTH956</b> | 15678974 | ATP synthase, subunit F   | 1 |   |   | 1 |
| <b>MTH957</b> | 15678975 | ATP synthase, subunit C (gamma)   | 1 | 1 |   | 1 |
| <b>MTH958</b> | 15678976 | ATP synthase, subunit E (epsilon)   | 1 | 1 | 1 | 1 |
| <b>MTH960</b> | 15678978 | ATP synthase, subunit I   | 1 | 1 | 1 | 1 |
| <b>MTH969</b> | 15678987 | conserved methanogen-specific protein MTH969  | 1 |   |   |   |
| <b>MTH970</b> | 15678988 | D-3-phosphoglycerate dehydrogenase (SerA) (EC 1.1.1.95) containing regulatory ACT domain          | 1 | 1 | 1 | 1 |
| <b>MTH972</b> | 15678990 | conserved protein (COG4021, DUF549), predicted tRNA(His) guanylyltransferase                      |   |   |   | 1 |
| <b>MTH973</b> | 15678991 | NAD(P)-dependent aspartate dehydrogenase (NadB)   | 1 |   |   |   |
| <b>MTH974</b> | 15678992 | conserved methanogen-specific protein (COG1873) implicated in RNA metabolism                      | 1 | 1 | 1 | 1 |
| <b>MTH975</b> | 15678993 | phenylalanine--tRNA ligase (EC 6.1.1.20) beta chain; Tyrosyl-tRNA synthetase (EC 6.1.1.1)         | 1 |   |   | 1 |
| <b>MTH977</b> | 15678995 | membrane-bound cell surface glycoprotein (s-layer protein)  | 1 | 1 |   | 1 |
| <b>MTH978</b> | 15678996 | NADP-dependent glyceraldehyde-3-phosphate dehydrogenase (gapN), lactaldehyde dehydrogenase (CofA) | 1 | 1 |   |   |
| <b>MTH980</b> | 15678998 | type II secretion system protein F, GspF (COG1459)  | 1 |   |   |   |
| <b>MTH984</b> | 15679002 | 1,3-propanediol dehydrogenase/ iron-containing alcohol dehydrogenase (COG1454)                    | 1 |   |   |   |
| <b>MTH993</b> | 15679011 | universal stress protein (UspA); chaperone (ATP-dependent)  | 1 |   |   | 1 |
| <b>MTH996</b> | 15679014 | carbamoyl-phosphate synthase, large subunit (carB)  | 1 | 1 | 1 | 1 |

|                |          |   |   |   |   |   |
|----------------|----------|---|---|---|---|---|
| <b>MTH997</b>  | 15679015 | carbamoyl-phosphate synthase, large subunit (carB)  | 1 | 1 | 1 | 1 |
| <b>MTH998</b>  | 15679016 | carbamoyl-phosphate synthase, small subunit (carB)  |   |   |   | 1 |
| <b>MTH1001</b> | 15679019 | ATPase, E1-E2 type: calcium-translocating P-type ATPase, PMCA-type  | 1 | 1 | 1 | 1 |
| <b>MTH1003</b> | 15679021 | molybdenum cofactor biosynthesis protein MoeA   |   |   |   | 1 |
| <b>MTH1005</b> | 15679023 | serine/threonine protein kinase (Rio1 family)   |   | 1 |   | 1 |
| <b>MTH1006</b> | 15679024 | RNA-binding protein; hydratase (S1 and KH domains) (COG1094)  |   | 1 |   | 1 |
| <b>MTH1007</b> | 15679025 | type II DNA topoisomerase VI subunit B (EC 5.99.1.3)  | 1 | 1 | 1 | 1 |
| <b>MTH1008</b> | 15679026 | type II DNA topoisomerase VI subunit A (EC 5.99.1.3)  | 1 | 1 | 1 | 1 |
| <b>MTH1009</b> | 15679027 | glyceraldehyde 3-phosphate dehydrogenase (gapA)   | 1 | 1 | 1 | 1 |
| <b>MTH1014</b> | 15679032 | predicted methanogen-specific metal-binding transcription factor (COG4008)  | 1 | 1 | 1 | 1 |
| <b>MTH1015</b> | 15679033 | methyl coenzyme M reductase system, component A2; ATPase subunit of an ABC-type Ni <sup>2+</sup> transport system   | 1 | 1 | 1 | 1 |
| <b>MTH1020</b> | 15679038 | IMP cyclohydrolase (PurO)   |   | 1 |   | 1 |
| <b>MTH1022</b> | 15679040 | biopolymer transport protein, MotA/TolQ/ExbB family   | 1 | 1 |   | 1 |
| <b>MTH1024</b> | 15679042 | rod shape-determining protein (MreB protein)  | 1 | 1 | 1 | 1 |
| <b>MTH1025</b> | 15679043 | uncharacterized conserved protein MTH1025   |   | 1 | 1 | 1 |
| <b>MTH1028</b> | 15679046 | conserved archaeal membrane-spanning protein MTH1028 (COG1627, DUF515)  |   | 1 |   | 1 |
| <b>MTH1030</b> | 15679048 | sortase (surface protein transpeptidase), SrtA involved in cell wall protein attachment (PF04203)   |   | 1 |   |   |
| <b>MTH1033</b> | 15679051 | 2-oxoglutarate synthase subunit korA (EC 1.2.7.3) (2-ketoglutarate oxidoreductase alpha chain) (KOR) (2-oxoglutarate-ferredoxin oxidoreductase subunit alpha) | 1 | 1 |   |   |
| <b>MTH1034</b> | 15679052 | 2-oxoglutarate synthase subunit korB (EC 1.2.7.3) (2-ketoglutarate oxidoreductase beta chain) (KOR) (2-oxoglutarate-ferredoxin oxidoreductase subunit beta)   |   | 1 |   | 1 |
| <b>MTH1035</b> | 15679053 | 2-oxoglutarate synthase subunit korC (EC 1.2.7.3) (2-ketoglutarate oxidoreductase gamma chain) (KOR) (2-oxoglutarate-ferredoxin oxidoreductase subunit gamma) |   | 1 |   | 1 |
| <b>MTH1036</b> | 15679054 | succinyl-CoA synthetase, beta subunit (sucD)  | 1 | 1 | 1 | 1 |
| <b>MTH1037</b> | 15679055 | conserved methanogen-specific ABC transporter, permease   |   | 1 |   |   |
| <b>MTH1038</b> | 15679056 | conserved membrane-spanning protein MTH1038 (COG4086, DUF1002)  |   |   |   | 1 |
| <b>MTH1040</b> | 15679058 | transglutaminase/protease-like protein  |   | 1 |   | 1 |
| <b>MTH1041</b> | 15679059 | triosephosphate isomerase (tpi)   | 1 | 1 | 1 |   |
| <b>MTH1042</b> | 15679060 | 3-phosphoglycerate kinase (pgk)   |   | 1 |   | 1 |
| <b>MTH1049</b> | 15679062 | DNA-dependent RNA polymerase, subunit B" (RpoB")  | 1 | 1 | 1 | 1 |
| <b>MTH1050</b> | 15679063 | DNA-dependent RNA polymerase, subunit B' (RpoB')  | 1 | 1 | 1 | 1 |
| <b>MTH1051</b> | 15679064 | DNA-dependent RNA polymerase, subunit A' (RpoA')  | 1 | 1 | 1 | 1 |
| <b>MTH1052</b> | 15679065 | DNA-dependent RNA polymerase, subunit A" (RpoA")  | 1 | 1 | 1 | 1 |
| <b>MTH1053</b> | 15679066 | 50S ribosomal protein L30e  |   | 1 |   | 1 |
| <b>MTH1054</b> | 15679067 | transcription termination factor NusA   | 1 | 1 | 1 | 1 |
| <b>MTH1055</b> | 15679068 | 30S ribosomal protein S23 (E.coli S12P)   |   | 1 | 1 | 1 |
| <b>MTH1056</b> | 15679069 | 30S ribosomal protein S5 (E.coli S7P)   | 1 | 1 | 1 | 1 |
| <b>MTH1057</b> | 15679070 | translation elongation factor, EF-2   | 1 | 1 | 1 | 1 |
| <b>MTH1058</b> | 15679071 | translation elongation factor, EF-1 alpha   | 1 | 1 | 1 | 1 |
| <b>MTH1059</b> | 15679072 | 30S ribosomal protein S20 (E.coli S10P)   |   | 1 |   | 1 |
| <b>MTH1062</b> | 15679073 | N5-methyl-tetrahydromethanopterin:coenzyme M methyltransferase, subunit A homolog   |   | 1 |   |   |
| <b>MTH1064</b> | 15679075 | conserved methanogen-specific protein MTH1064 (COG1432, DUF88)  |   | 1 |   | 1 |
| <b>MTH1065</b> | 15679076 | universal stress protein (UspA); chaperone (ATP-dependent)  |   | 1 | 1 |   |
| <b>MTH1066</b> | 15679077 | predicted transcriptional activator (COG4987)   |   |   |   | 1 |
| <b>MTH1068</b> | 15679079 | conserved (UPF0334) kinase-like protein/ ATPase-kinase involved in pili biogenesis (pilT) (COG1618, COG0630)  |   | 1 |   |   |
| <b>MTH1070</b> | 15679081 | zinc metalloprotease (U62 family), modulator of DNA gyrase  |   | 1 |   |   |
| <b>MTH1072</b> | 15679083 | hydrogenase expression/formation protein HypD (HypD)  |   | 1 |   | 1 |
| <b>MTH1080</b> | 15679091 | CRISPR-associated RAMP protein Csm3 (COG1337)   |   | 1 | 1 |   |
| <b>MTH1081</b> | 15679092 | CRISPR-associated protein Csm2 (COG1421, DUF310)  |   | 1 |   | 1 |
| <b>MTH1082</b> | 15679093 | CRISPR-associated protein, Csm1, metal-dependent hydrolase HD superfamily/ possibly novel polymerase (COG1353, PF01966)                                       |   |   |   | 1 |
| <b>MTH1086</b> | 15679097 | CRISPR-associated protein Cas3, DNA-helicase (COG1203) (acquired virus resistance system)   |   | 1 |   |   |
| <b>MTH1094</b> | 15679105 | circadian clock protein KaiC, RecA/ Rad55 superfamily ATPase involved in homologous recombination   |   | 1 |   |   |
| <b>MTH1097</b> | 15679108 | conserved protein (COG3467), pyridoxamine 5'-phosphate oxidase-related (FMN-binding) (crystal structure known)  |   | 1 |   |   |
| <b>MTH1104</b> | 15679115 | partially conserved membrane-bound protein MTH1104  |   | 1 |   |   |
| <b>MTH1105</b> | 15679116 | 1L-myo-inositol-1-phosphate synthase  | 1 | 1 | 1 | 1 |

|                |          |   |   |   |   |   |
|----------------|----------|---|---|---|---|---|
| <b>MTH1107</b> | 15679118 | pyruvate carboxylase subunit B (EC 6.4.1.1)(PycB)   | 1 | 1 |   |   |
| <b>MTH1108</b> | 15679119 | archaeosine biosynthesis protein queC (EC 3.5.-.-).   | 1 |   | 1 |   |
| <b>MTH1110</b> | 15679121 | conserved methanogen-specific protein (COG4075); nitrogen regulatory protein PII homolog                                | 1 |   | 1 |   |
| <b>MTH1113</b> | 15679124 | conserved archaeal protein (COG1303, UPF0106); SpoU-like RNA methylase, archaeal tRNA-methylase for position 56 (Trm56) | 1 |   | 1 |   |
| <b>MTH1117</b> | 15679128 | phosphoenolpyruvate synthase, C-terminal part (ppsA)  | 1 | 1 | 1 |   |
| <b>MTH1118</b> | 15679129 | phosphoenolpyruvate synthase (ppsA)   | 1 | 1 | 1 | 1 |
| <b>MTH1119</b> | 15679130 | 50S ribosomal protein L10e  | 1 | 1 | 1 |   |
| <b>MTH1121</b> | 15679132 | conserved Methanobacteriaceae-specific protein MTH1121  | 1 |   |   |   |
| <b>MTH1122</b> | 15679133 | type-2 seryl-tRNA synthetase (EC 6.1.1.11) (Seryl-tRNA(Ser/Sec) synthetase) (SerRS)                                     | 1 | 1 | 1 |   |
| <b>MTH1123</b> | 15679134 | conserved protein, putative ATPase, glucocorticoid receptor-like DNA-binding domain                                     | 1 |   | 1 |   |
| <b>MTH1125</b> | 15679136 | fkbp-type peptidyl-prolyl cis-trans isomerase   | 1 |   | 1 |   |
| <b>MTH1129</b> | 15679140 | methyl coenzyme M reductase II, alpha subunit   | 1 | 1 | 1 | 1 |
| <b>MTH1130</b> | 15679141 | methyl coenzyme M reductase II, gamma subunit   | 1 | 1 | 1 | 1 |
| <b>MTH1131</b> | 15679142 | methyl coenzyme M reductase II, D protein   | 1 | 1 | 1 |   |
| <b>MTH1132</b> | 15679143 | methyl coenzyme M reductase II, beta subunit  | 1 | 1 | 1 | 1 |
| <b>MTH1133</b> | 15679144 | polyferredoxin (MvhB)   | 1 | 1 | 1 | 1 |
| <b>MTH1134</b> | 15679145 | methyl viologen-reducing hydrogenase, alpha subunit   | 1 | 1 | 1 | 1 |
| <b>MTH1135</b> | 15679146 | methyl viologen-reducing hydrogenase, gamma subunit   | 1 | 1 |   |   |
| <b>MTH1136</b> | 15679147 | methyl viologen-reducing hydrogenase, delta subunit   | 1 | 1 | 1 | 1 |
| <b>MTH1137</b> | 15679148 | conserved methanogen-specific protein (FlpA) (COG4018)  | 1 | 1 |   |   |
| <b>MTH1138</b> | 15679149 | methyl viologen-reducing hydrogenase, delta subunit homolog FlpD  | 1 |   |   |   |
| <b>MTH1139</b> | 15679150 | formate dehydrogenase, beta subunit (F420-reducing) related protein FlpB  | 1 | 1 |   |   |
| <b>MTH1140</b> | 15679151 | formate dehydrogenase, alpha subunit related protein/ nitrate reductase catalytic subunit, FlpC                         | 1 | 1 |   |   |
| <b>MTH1142</b> | 15679153 | H(2)-dependent N5,N10-methylenetetrahydromethanopterin dehydrogenase  | 1 | 1 | 1 | 1 |
| <b>MTH1144</b> | 15679155 | conserved methanogen-specific hypothetical protein MTH1144 (COG4019)  | 1 |   |   |   |
| <b>MTH1146</b> | 15679157 | conserved hypothetical protein MTH1146 (COG0323); NIF3-related protein (NGG1p interacting factor 3)                     | 1 |   | 1 |   |
| <b>MTH1147</b> | 15679158 | conserved methanogen-specific hypothetical protein (COG4015)/ UBA/THIF-type NAD/FAD binding fold                        | 1 |   |   |   |
| <b>MTH1149</b> | 15679160 | ABC transporter involved in Fe-S cluster assembly, ATPase component (SufC)  | 1 | 1 | 1 | 1 |
| <b>MTH1150</b> | 15679161 | ABC transporter involved in Fe-S cluster assembly, permease component (SufBD)   | 1 | 1 | 1 | 1 |
| <b>MTH1153</b> | 15679164 | conserved methanogen-specific protein MTH1153 (COG4065)   | 1 |   | 1 |   |
| <b>MTH1154</b> | 15679165 | universal stress protein (UspA); chaperone (ATP-dependent)  | 1 | 1 | 1 | 1 |
| <b>MTH1156</b> | 15679167 | N5-methyl-tetrahydromethanopterin:coenzyme M methyltransferase, subunit H   | 1 | 1 | 1 | 1 |
| <b>MTH1157</b> | 15679168 | N5-methyl-tetrahydromethanopterin:coenzyme M methyltransferase, subunit G   | 1 | 1 | 1 |   |
| <b>MTH1158</b> | 15679169 | N5-methyl-tetrahydromethanopterin:coenzyme M methyltransferase, subunit F   | 1 | 1 |   | 1 |
| <b>MTH1159</b> | 15679170 | N5-methyl-tetrahydromethanopterin:coenzyme M methyltransferase, subunit A   | 1 | 1 | 1 | 1 |
| <b>MTH1161</b> | 15679172 | N5-methyl-tetrahydromethanopterin:coenzyme M methyltransferase, subunit C   | 1 | 1 | 1 | 1 |
| <b>MTH1162</b> | 15679173 | N5-methyl-tetrahydromethanopterin:coenzyme M methyltransferase, subunit D   | 1 | 1 |   | 1 |
| <b>MTH1163</b> | 15679174 | N5-methyl-tetrahydromethanopterin:coenzyme M methyltransferase, subunit E   | 1 | 1 | 1 |   |
| <b>MTH1164</b> | 15679175 | methyl coenzyme M reductase I, alpha subunit  | 1 | 1 | 1 | 1 |
| <b>MTH1165</b> | 15679176 | methyl coenzyme M reductase I, gamma subunit  | 1 | 1 | 1 | 1 |
| <b>MTH1166</b> | 15679177 | methyl coenzyme M reductase I, C protein  | 1 |   | 1 |   |
| <b>MTH1167</b> | 15679178 | methyl coenzyme M reductase I, D protein  | 1 | 1 | 1 | 1 |
| <b>MTH1168</b> | 15679179 | methyl coenzyme M reductase I, beta subunit   | 1 | 1 | 1 | 1 |
| <b>MTH1175</b> | 15679186 | dinitrogenase iron-molybdenum cofactor biosynthesis protein (NifB/ NifX/ NifY family)                                   | 1 |   | 1 |   |
| <b>MTH1180</b> | 15679191 | conserved methanogen-specific protein related to methyl coenzyme M reductase II operon protein C (mtrC) (COG4052)       | 1 | 1 |   |   |
| <b>MTH1182</b> | 15679193 | 2-phosphosulfolactate phosphatase (EC 3.1.3.-) (ComB)   | 1 |   | 1 |   |
| <b>MTH1193</b> | 15679204 | transcriptional regulator (AsnC-HTH), leucine regulator (Lrp)   | 1 | 1 | 1 | 1 |
| <b>MTH1196</b> | 15679207 | type 1 GTP cyclohydrolase (FolE2, MptA) (COG1469, UPF0343, DUF198); archaeosine (7-deazaguanosine) biosynthesis protein | 1 | 1 |   |   |
| <b>MTH1199</b> | 15679210 | conserved archaeal protein (COG2410, DUF429), ribosomal protein S7  | 1 |   |   |   |

|                |          |   |   |   |   |   |
|----------------|----------|---|---|---|---|---|
| <b>MTH1201</b> | 15679212 | 5-formaminoimidazole-4-carboxamide-1-beta-D-ribofuranosyl 5'-monophosphate synthetase (FAICAR) (PurP)   | 1 | 1 | 1 | 1 |
| <b>MTH1202</b> | 15679213 | proteasome, beta subunit  | 1 | 1 | 1 | 1 |
| <b>MTH1203</b> | 15679214 | mbI-RNase (metallo beta lactamase), mRNA 3'-end processing factor   | 1 | 1 | 1 | 1 |
| <b>MTH1204</b> | 15679215 | phosphoribosylformylglycinamide cyclo-ligase (AIR synthase) (PurM)  | 1 | 1 |   | 1 |
| <b>MTH1205</b> | 15679216 | L-sulfolactate dehydrogenase/ 2-ketoglutarate reductase involved in HS-CoM and methanopterin biosynthesis   |   | 1 | 1 |   |
| <b>MTH1210</b> | 15679221 | 5-methylcytosine-specific restriction enzyme (mrr)  |   | 1 |   |   |
| <b>MTH1212</b> | 15679223 | dihydroorotate dehydrogenase electron transfer subunit (PyrK)   |   | 1 |   |   |
| <b>MTH1216</b> | 15679227 | phosphopantothenoilcysteine synthase/decarboxylase (PPCS/PPCDC; CoaBC)  |   | 1 |   |   |
| <b>MTH1217</b> | 15679228 | archaeal transcription terminator NusA (COG0195)  | 1 | 1 | 1 | 1 |
| <b>MTH1219</b> | 15679230 | conserved Methanobacteriaceae-specific membrane-spanning protein MTH1219 putatively involved in cell wall metabolism                              |   | 1 |   |   |
| <b>MTH1221</b> | 15679232 | archaeal intramolecular RNA (single-stranded DNA) ligase  |   | 1 |   |   |
| <b>MTH1222</b> | 15679233 | inosine-5'-monophosphate dehydrogenase related protein I containing signal transduction CBS-domain (4x)   | 1 | 1 | 1 |   |
| <b>MTH1223</b> | 15679234 | inosine-5'-monophosphate dehydrogenase related protein II containing signal transduction CBS-domain (4x)  | 1 | 1 | 1 | 1 |
| <b>MTH1224</b> | 15679235 | inosine-5'-monophosphate dehydrogenase related protein III containing signal transduction CBS-domain (4x)   | 1 | 1 | 1 | 1 |
| <b>MTH1225</b> | 15679236 | inosine-5'-monophosphate dehydrogenase related protein IV containing signal transduction CBS-domain (4x)  | 1 | 1 | 1 | 1 |
| <b>MTH1226</b> | 15679237 | inosine-5'-monophosphate dehydrogenase related protein V containing signal transduction CBS-domain (2x) fused to a Zn-ribbon (rubredoxin) domain  | 1 | 1 | 1 |   |
| <b>MTH1229</b> | 15679240 | conserved methano-archaeal protein MTH1229 (COG2029, DUF366)  |   | 1 |   |   |
| <b>MTH1234</b> | 15679245 | uncharacterized protein MTH1234   |   | 1 |   |   |
| <b>MTH1237</b> | 15679248 | NADH dehydrogenase (ubiquinone), subunit 1 related protein (EhbO) ('quinone binding')   |   | 1 |   | 1 |
| <b>MTH1238</b> | 15679249 | formate hydrogenlyase, subunit 5 (EhbN); large (alfa) subunit NiFe H2ase  |   | 1 |   | 1 |
| <b>MTH1239</b> | 15679250 | formate hydrogenlyase, subunit 7 (EhbM); small subunit NiFe H2ase   |   | 1 |   |   |
| <b>MTH1240</b> | 15679251 | ferredoxin-like protein (EhbL)  |   | 1 |   | 1 |
| <b>MTH1241</b> | 15679252 | polyferredoxin (EhbK)   |   | 1 |   |   |
| <b>MTH1254</b> | 15679265 | argininosuccinate synthase (EC 6.3.4.5), citrulline-aspartate ligase (ArgG)   | 1 | 1 | 1 |   |
| <b>MTH1256</b> | 15679267 | conserved protein; N-terminal YjeF related protein fused to C-terminal sugar kinase (COG0063, COG0062)  |   | 1 |   |   |
| <b>MTH1259</b> | 15679270 | formylmethanofuran:tetrahydromethanopterin formyltransferase  | 1 | 1 | 1 | 1 |
| <b>MTH1260</b> | 15679271 | sensory transduction histidine kinase   |   | 1 |   |   |
| <b>MTH1263</b> | 15679274 | conserved protein (SAM-dependent methyltransferase); Trm2-RNA methylase (TRAM domain)   |   | 1 |   |   |
| <b>MTH1280</b> | 15679284 | Gln/asn-dependent aspartyl-tRNA(Asn) amidotransferase subunit B (EC 6.3.5.-) (Asp/Glu-ADT subunit B).   | 1 | 1 |   | 1 |
| <b>MTH1282</b> | 15679286 | inosine-5'-monophosphate dehydrogenase related protein VI; signal transduction CBS-domain (2x) associated with a ParBc (ParB-nuclease) HTH domain |   | 1 |   | 1 |
| <b>MTH1287</b> | 15679291 | hydrogenase maturation factor, HypF   |   | 1 |   |   |
| <b>MTH1289</b> | 15679293 | heat shock protein GrpE   |   | 1 |   |   |
| <b>MTH1290</b> | 15679294 | DnaK protein (Hsp70)  | 1 | 1 | 1 | 1 |
| <b>MTH1291</b> | 15679295 | DnaJ protein  |   | 1 |   |   |
| <b>MTH1294</b> | 15679296 | conserved methanogen-specific membrane-spanning protein MTH1294   |   | 1 |   | 1 |
| <b>MTH1295</b> | 15679297 | conserved methanogen-specific membrane-spanning protein MTH1295 (COG1196)   |   | 1 |   | 1 |
| <b>MTH1297</b> | 15679299 | coenzyme F420-reducing hydrogenase, beta subunit  | 1 | 1 |   |   |
| <b>MTH1298</b> | 15679300 | coenzyme F420-reducing hydrogenase, gamma subunit   | 1 | 1 |   |   |
| <b>MTH1300</b> | 15679302 | coenzyme F420-reducing hydrogenase, alpha subunit   | 1 | 1 |   | 1 |
| <b>MTH1301</b> | 15679303 | conserved Methanobacteriaceae-specific membrane-spanning protein; peptidase propeptide (PepSY) surface prot.                                      | 1 | 1 |   | 1 |
| <b>MTH1302</b> | 15679304 | archaeal ATP-Grasp superfamily protein (COG1938)/ HS-CoB biosynthesis protein (AksE)  | 1 | 1 |   | 1 |
| <b>MTH1306</b> | 15679306 | probable 3-isopropylmalate dehydratase (LeuD)/ HS-CoB biosynthesis protein (AksE)   | 1 | 1 | 1 | 1 |
| <b>MTH1308</b> | 15679308 | translation initiation factor eIF-2, alpha subunit  | 1 | 1 | 1 | 1 |
| <b>MTH1309</b> | 15679309 | 30S ribosomal protein S27E  |   | 1 |   | 1 |
| <b>MTH1310</b> | 15679310 | 50S ribosomal protein L36a ( L44E)  |   | 1 |   |   |
| <b>MTH1312</b> | 15679312 | proliferating-cell nuclear antigen (PCNA); DNA polymerase sliding clamp   | 1 | 1 | 1 | 1 |
| <b>MTH1314</b> | 15679314 | transcription elongation factor TFIIS; DNA-directed RNA polymerase subunit M (EC 2.7.7.6) (RpoM)  |   | 1 |   |   |
| <b>MTH1316</b> | 15679316 | conserved protein (COG1628, DUF99, UPF0215); predicted endonuclease   |   | 1 |   | 1 |

|                |          |   |   |   |   |   |
|----------------|----------|---|---|---|---|---|
|                |          | V homolog   |   |   |   |   |
| <b>MTH1317</b> | 15679317 | DNA-dependent RNA polymerase, subunit L (RpoL), exosome subunit RPC19   | 1 |   | 1 |   |
| <b>MTH1318</b> | 15679318 | RNA-binding protein, exonuclease, Csl4  | 1 | 1 | 1 | 1 |
| <b>MTH1319</b> | 15679319 | diphthamide synthase, subunit DPH2, translation factor EF-2 modification  | 1 |   |   |   |
| <b>MTH1320</b> | 15679320 | adenine/ (verified) hypoxanthine phosphoribosyltransferase (APRT) (EC 2.4.2.8)  | 1 | 1 |   |   |
| <b>MTH1321</b> | 15679321 | signal recognition particle protein SRP54   | 1 |   | 1 |   |
| <b>MTH1322</b> | 15679322 | 55-pseudouridylate synthetase (pus10)   | 1 |   |   |   |
| <b>MTH1324</b> | 15679324 | RNA polymerase Rpb4 (RpoH)  | 1 |   | 1 |   |
| <b>MTH1325</b> | 15679325 | conserved protein, predicted RNA-binding protein (COG1491)  | 1 | 1 | 1 | 1 |
| <b>MTH1326</b> | 15679326 | dimethyladenosine transferase (EC 2.1.1.-), S-adenosylmethionine-6-N',N'-adenosyl(rRNA)dimethyltransferase) (16S rRNA dimethylase)                      | 1 |   |   |   |
| <b>MTH1329</b> | 15679329 | methyltransferase related protein (SAM-dependent methyltransferase)/ methylase of polypeptide chain release factors (HemK)/r/rRNA cytosine-C5 methylase | 1 |   | 1 |   |
| <b>MTH1334</b> | 15679334 | diaminopimelate epimerase (DapF)  | 1 |   | 1 |   |
| <b>MTH1335</b> | 15679335 | diaminopimelate decarboxylase (EC 4.1.1.20) (DAP decarboxylase)   | 1 |   | 1 | 1 |
| <b>MTH1336</b> | 15679336 | mutator MutT protein homolog; A,G-mismatch DNA glycosylase  | 1 |   |   |   |
| <b>MTH1337</b> | 15679337 | N-acetylornithine aminotransferase (ArgD)   | 1 | 1 | 1 | 1 |
| <b>MTH1343</b> | 15679343 | imidazoleglycerol-phosphate synthase (cyclase) (HisF)   | 1 |   |   |   |
| <b>MTH1345</b> | 15679344 | conserved protein (molybdopterin binding domain), formylmethanofuran dehydrogenase subunit E homolog  | 1 |   | 1 |   |
| <b>MTH1346</b> | 15679345 | conserved methanogen-specific membrane-bound protein MTH1346 (COG5643)  | 1 | 1 |   |   |
| <b>MTH1347</b> | 15679346 | ATP-dependent helicase (RAD3, XPD)  | 1 |   |   |   |
| <b>MTH1348</b> | 15679347 | precorrin-2 methyltransferase (CbiL)  | 1 |   | 1 |   |
| <b>MTH1349</b> | 15679348 | transcription regulator (ArsR/ MarR-HTH5 family)  | 1 |   |   |   |
| <b>MTH1350</b> | 15679349 | flavoprotein Al; F420H2 oxidase (fprA)  | 1 | 1 | 1 | 1 |
| <b>MTH1351</b> | 15679350 | rubrerythrin (fprB)   | 1 | 1 | 1 | 1 |
| <b>MTH1352</b> | 15679351 | rubredoxin (fprC)   | 1 | 1 | 1 | 1 |
| <b>MTH1354</b> | 15679353 | NADH: rubredoxin oxidoreductase (NPOR)  | 1 | 1 | 1 | 1 |
| <b>MTH1361</b> | 15679360 | ferrous iron transport protein B (FeoB)   | 1 | 1 | 1 | 1 |
| <b>MTH1362</b> | 15679361 | ferrous iron transport protein A (FeoA)   | 1 |   | 1 |   |
| <b>MTH1369</b> | 15679368 | molybdenum cofactor biosynthesis MoeA   | 1 |   |   |   |
| <b>MTH1370</b> | 15679369 | ABC transporter (ATP-binding protein)   | 1 |   | 1 |   |
| <b>MTH1371</b> | 15679370 | ABC-type Na <sup>+</sup> efflux pump, permease component  | 1 |   |   |   |
| <b>MTH1372</b> | 15679371 | ABC-type Na <sup>+</sup> efflux pump, permease component  | 1 |   |   |   |
| <b>MTH1374</b> | 15679373 | phosphoribosylformylglycinamide synthase II (PurL)  | 1 | 1 | 1 | 1 |
| <b>MTH1375</b> | 15679374 | isoleucyl-tRNA synthetase   | 1 | 1 | 1 | 1 |
| <b>MTH1376</b> | 15679375 | S-adenosylmethionine synthetase (EC 2.5.1.6) (MetK)   | 1 | 1 | 1 | 1 |
| <b>MTH1377</b> | 15679376 | conserved protein MTH1377 (COG1430, DUF192, UPF0127)  | 1 |   |   |   |
| <b>MTH1378</b> | 15679377 | PBS lyase HEAT domain protein repeat-containing protein/ phycoyanin alpha phycoyanobilin lyase CpcE   | 1 |   |   |   |
| <b>MTH1380</b> | 15679379 | serine hydroxymethyltransferase (GlyA)  | 1 |   | 1 |   |
| <b>MTH1381</b> | 15679380 | CoB--CoM heterodisulfide reductase iron-sulfur subunit A (EC 1.8.98.1)  | 1 | 1 | 1 | 1 |
| <b>MTH1383</b> | 15679382 | DNA repair protein RadA (RadA, RecA, Rad51)   | 1 | 1 | 1 | 1 |
| <b>MTH1384</b> | 15679383 | replication factor A related protein (C-terminal part), ssDNA-binding replication initiation  | 1 | 1 | 1 | 1 |
| <b>MTH1385</b> | 15679384 | replication factor A related protein, ssDNA-binding replication initiation  | 1 | 1 | 1 | 1 |
| <b>MTH1386</b> | 15679385 | 3-isopropylmalate dehydratase large subunit 1 (EC 4.2.1.33) (Isopropylmalate isomerase 1)   | 1 | 1 | 1 | 1 |
| <b>MTH1387</b> | 15679386 | 3-isopropylmalate dehydratase large subunit 2 (EC 4.2.1.33) (Isopropylmalate isomerase 2)   | 1 | 1 | 1 | 1 |
| <b>MTH1388</b> | 15679387 | 3-isopropylmalate dehydrogenase, NAD-dependent (LeuB)   | 1 | 1 | 1 | 1 |
| <b>MTH1389</b> | 15679388 | nifS protein;cysteine desulfurase (EC 4.4.1.-)  | 1 | 1 | 1 | 1 |
| <b>MTH1390</b> | 15679389 | riboflavin synthase beta subunit; 6,7-dimethyl-8-ribityllumazine synthase (EC 2.5.1.9) (RibH)   | 1 |   | 1 |   |
| <b>MTH1391</b> | 15679390 | conserved protein (COG1571, DUF1743), predicted DNA binding protein (Zn-ribbon)/ archaeal-specific RecJ-like exonuclease                                | 1 |   | 1 |   |
| <b>MTH1392</b> | 15679391 | glycosyl transferase (GT2 family); dolichyl-phosphate mannosyltransferase related protein   | 1 |   | 1 |   |
| <b>MTH1393</b> | 15679392 | phosphoribosylaminoimidazole carboxylase (AIR carboxylase) fused to phosphoribosylcarboxyaminoimidazole (NCAIR) mutase (PurE)                           | 1 |   |   |   |
| <b>MTH1394</b> | 15679393 | putative 3-octaprenyl-4-hydroxybenzoate carboxylase, 4-hydroxybenzoate decarboxylase (UbiD)   | 1 |   | 1 |   |
| <b>MTH1395</b> | 15679394 | pyruvate formate-lyase activating enzyme related protein/ radical SAM protein   | 1 |   |   |   |
| <b>MTH1397</b> | 15679396 | sirohydrochlorin cobaltochelate (EC 4.99.1.3) (CbiXS)   | 1 |   |   |   |

|                |          |  |   |   |   |   |
|----------------|----------|--|---|---|---|---|
| <b>MTH1398</b> | 15679397 | conserved protein MTH1398 (COG1545, DUF35); putative nucleide binding protein (Zn-ribbon)  | 1 | 1 | 1 | 1 |
| <b>MTH1402</b> | 15679401 | potassium ion transport protein (TrkA-C domain) fused to PhoU regulatory domain; ATP binding   | 1 | 1 | 1 | 1 |
| <b>MTH1404</b> | 15679403 | conserved Methanobacteriaceae-specific membrane-spanning protein MTH1404   | 1 |   |   |   |
| <b>MTH1406</b> | 15679405 | fucose-1-phosphate aldolase, class II aldolase/adducin family  | 1 |   |   |   |
| <b>MTH1410</b> | 15679409 | conserved archaea-specific hypothetical protein MTH1410 (COG5440)  | 1 | 1 | 1 | 1 |
| <b>MTH1412</b> | 15679411 | cell division control protein 6 homolog 1 (CDC6 homolog 1) (ORC1)  | 1 |   |   |   |
| <b>MTH1413</b> | 15679412 | aspartate carbamoyltransferase (EC 2.1.3.2) (PyrB)   | 1 |   |   |   |
| <b>MTH1414</b> | 15679413 | tRNA(1-methyladenosine) methyltransferase (m1A57A58) (complex GCD14 subunit protein)   | 1 |   |   |   |
| <b>MTH1415</b> | 15679414 | ATP-dependent ss-DNA endonuclease (XPF; RAD1), eIF-4A family   | 1 | 1 |   |   |
| <b>MTH1417</b> | 15679416 | peroxiredoxin, predicted regulator of disulfide bond formation conserved protein (DorE/DsrF)   | 1 | 1 | 1 | 1 |
| <b>MTH1418</b> | 15679417 | conserved protein MTH1418 (COG2043, DUF169)  | 1 | 1 | 1 | 1 |
| <b>MTH1423</b> | 15679422 | 30S ribosomal protein S13 (E.coli S15); S15P/S13E  | 1 |   |   |   |
| <b>MTH1425</b> | 15679424 | Kae1 protein, DNA-binding protein with apurinic (AP)-endonuclease activity (AP-lyase) fused with protein kinase Bud32  | 1 |   |   |   |
| <b>MTH1430</b> | 15679429 | branched-chain amino-acid aminotransferase (IlvE)  | 1 | 1 | 1 |   |
| <b>MTH1434</b> | 15679431 | type II restriction endonuclease   | 1 |   |   | 1 |
| <b>MTH1442</b> | 15679439 | ketol-acid reductoisomerase (EC 1.1.1.86), acetohydroxy-acid isomeroreductase (IlvC)   | 1 | 1 | 1 | 1 |
| <b>MTH1443</b> | 15679440 | acetolactate synthase, small subunit (IlvH) (regulatory ACT domain)  | 1 | 1 | 1 | 1 |
| <b>MTH1444</b> | 15679441 | acetolactate synthase, large subunit (IlvB)  | 1 | 1 | 1 | 1 |
| <b>MTH1445</b> | 15679442 | glycinamide ribonucleotide synthetase; phosphoribosylamine-glycine ligase (EC 6.3.4.13) (GARS) (PurD)  | 1 |   |   |   |
| <b>MTH1447</b> | 15679444 | arginyl-tRNA synthetase (ArgRS)  | 1 |   |   | 1 |
| <b>MTH1448</b> | 15679445 | signal peptidase I   | 1 |   |   |   |
| <b>MTH1449</b> | 15679446 | dihydroxy-acid dehydratase (EC 4.2.1.9) (DAD) (IlvD)   | 1 |   |   | 1 |
| <b>MTH1452</b> | 15679449 | conserved barrel domain protein (Cupin-2) (COG1917)  | 1 |   |   | 1 |
| <b>MTH1453</b> | 15679450 | hybrid cluster (6Fe-6S, prismane)-containing protein; hydroxylamine reductase (COG1151)  | 1 | 1 |   | 1 |
| <b>MTH1455</b> | 15679452 | threonyl-tRNA synthetase   | 1 |   |   | 1 |
| <b>MTH1460</b> | 15679457 | cobyrinic acid a,c-diamide synthase (glutamine-hydrolyzing) (CbiA/CbiP/cobB)   | 1 | 1 |   |   |
| <b>MTH1464</b> | 15679461 | coenzyme F420-dependent N5,N10-methylene tetrahydromethanopterin dehydrogenase   | 1 | 1 | 1 | 1 |
| <b>MTH1467</b> | 15679464 | imidazoleglycerol-phosphate dehydratase (HisB, TrpB2)  | 1 |   |   |   |
| <b>MTH1474</b> | 15679471 | bifunctional enzyme fae/hps [Includes: Formaldehyde-activating enzyme (E4C.3.-.-) (Fae); 3-hexulose-6-phosphate synthase (EC 4.1.2.-) (HPS) (D-arabino-3-hexulose-6-osphate formaldehyde lyase)] | 1 | 1 | 1 | 1 |
| <b>MTH1476</b> | 15679473 | tryptophan synthase, beta 2 subunit (TrpB2)  | 1 | 1 | 1 | 1 |
| <b>MTH1479</b> | 15679476 | conserved metal-dependent phosphoesterase (PHP family, C terminal part) (COG0613, PF02231)   | 1 |   |   |   |
| <b>MTH1481</b> | 15679478 | 2-isopropylmalate synthase (EC 2.3.3.13)   | 1 | 1 |   | 1 |
| <b>MTH1483</b> | 15679480 | DNA/RNA-binding protein Alba (dsDNA binding protein, exponential growth)   | 1 | 1 | 1 |   |
| <b>MTH1485</b> | 15679482 | membrane-bound serine/threonine protein kinase related protein containing Class III signal sequence  | 1 |   |   |   |
| <b>MTH1486</b> | 15679483 | conserved ABC-transporter (permease)   | 1 |   |   | 1 |
| <b>MTH1487</b> | 15679484 | ABC-type multidrug transport system, ATPase component  | 1 |   |   | 1 |
| <b>MTH1489</b> | 15679486 | AP endonuclease family 2 endonuclease IV   | 1 |   |   |   |
| <b>MTH1493</b> | 15679490 | cation transporting P-type ATPase related protein  | 1 |   |   |   |
| <b>MTH1496</b> | 15679493 | Gln/asn-dependent aspartyl-tRNA(Asn) amidotransferase subunit A (EC 6.3.5.-) (Glu-ADT subunit A)   | 1 | 1 |   | 1 |
| <b>MTH1499</b> | 15679496 | GTP cyclohydrolase II;3,4-dihydroxy-2-butanone 4-phosphate synthase (DHBP synthase) (RibB)   | 1 |   |   |   |
| <b>MTH1501</b> | 15679498 | O-phosphoserine-tRNA synthetase (SepRS)  | 1 |   |   | 1 |
| <b>MTH1502</b> | 15679499 | thiol:fumarate reductase subunit A protein/ succinate dehydrogenase flavoprotein subunit   | 1 |   |   | 1 |
| <b>MTH1505</b> | 15679502 | N-ethylammelane chlorohydrolase homolog (COG0402); 5-methylthioadenosine/S-adenosylhomocysteine deaminase  | 1 |   |   |   |
| <b>MTH1506</b> | 15679503 | ATP phosphoribosyltransferase (EC 2.4.2.17) (HisG)   | 1 |   |   | 1 |
| <b>MTH1508</b> | 15679505 | leucyl-tRNA synthetase (LeuS)  | 1 | 1 | 1 | 1 |
| <b>MTH1510</b> | 15679507 | NH(3)-dependent NAD+ synthetase (NadE)   | 1 |   |   |   |
| <b>MTH1511</b> | 15679508 | arsenical pump-driving ATPase  | 1 |   |   | 1 |
| <b>MTH1512</b> | 15679509 | H(2)-dependent N5,N10-methylenetetrahydromethanopterin dehydrogenase homolog (II)  | 1 | 1 | 1 | 1 |

|                |          |   |   |   |   |   |
|----------------|----------|---|---|---|---|---|
| <b>MTH1514</b> | 15679511 | precorrin-6Y methylase (CbiE)   |   |   |   | 1 |
| <b>MTH1520</b> | 15679517 | calcium-gated potassium channel mthK (ATP binding)  |   |   |   | 1 |
| <b>MTH1523</b> | 15679520 | glucose-1-phosphate adenylyltransferase related protein/ sugar phosphate nucleotidyl transferase                    | 1 | 1 | 1 |   |
| <b>MTH1524</b> | 15679521 | imidazoleglycerol-phosphate synthase; amidotransferase hisH (EC 2.4.2.-) (HisH)                                     |   |   |   | 1 |
| <b>MTH1525</b> | 15679522 | hydrogenase expression/formation protein HypE related protein (HypE)  |   |   |   | 1 |
| <b>MTH1528</b> | 15679524 | coenzyme F390 synthetase I  | 1 | 1 |   | 1 |
| <b>MTH1534</b> | 15679530 | aryldialkylphosphatase related protein/ Pro-Hyp metallo dipeptidase (MEROPS family M38) (COG1228)                   |   |   |   | 1 |
| <b>MTH1535</b> | 15679531 | heavy-metal (Zn, Cu+) transporting CPX-type ATPase (zntA, CopA)   |   |   |   | 1 |
| <b>MTH1536</b> | 15679532 | DNA polymerase II large subunit (EC 2.7.7.7) (Pol II)   |   |   |   | 1 |
| <b>MTH1537</b> | 15679533 | adenylosuccinate lyase (PurB)   | 1 | 1 | 1 | 1 |
| <b>MTH1538</b> | 15679534 | Na+ dependent nucleoside/dicarboxylate transporter (COG0609)  | 1 | 1 |   | 1 |
| <b>MTH1539</b> | 15679535 | anaerobic ribonucleoside-triphosphate reductase   |   |   |   | 1 |
| <b>MTH1541</b> | 15679537 | partially conserved protein MTH1541   |   |   |   | 1 |
| <b>MTH1542</b> | 15679538 | lysyl-tRNA synthetase (EC 6.1.1.6) (Lysine--tRNA ligase) (LysRS)  | 1 | 1 | 1 | 1 |
| <b>MTH1543</b> | 15679539 | thiamine biosynthesis protein (thiC1)   | 1 | 1 | 1 | 1 |
| <b>MTH1544</b> | 15679540 | ribokinase/ broad-substrate nucleoside kinase   | 1 | 1 |   | 1 |
| <b>MTH1546</b> | 15679542 | 6-phospho-3-hexulose isomerase (PHI) (HTH-RpiR family)  | 1 | 1 |   | 1 |
| <b>MTH1547</b> | 15679543 | nitrate reductase (NarQ)/ formate dehydrogenase (FdhD) accessory protein  |   |   |   | 1 |
| <b>MTH1549</b> | 15679545 | NADH dehydrogenase I chain F (nuoF)   |   |   |   | 1 |
| <b>MTH1550</b> | 15679546 | molybdenum cofactor biosynthesis MoaA   |   |   |   | 1 |
| <b>MTH1551</b> | 15679547 | molybdopterin-guanine dinucleotide biosynthesis protein B (MobB) related  |   |   |   | 1 |
| <b>MTH1552</b> | 15679548 | formate dehydrogenase, alpha subunit homolog  | 1 | 1 |   | 1 |
| <b>MTH1554</b> | 15679550 | tungsten formylmethanofuran dehydrogenase, subunit F  | 1 | 1 | 1 | 1 |
| <b>MTH1555</b> | 15679551 | tungsten formylmethanofuran dehydrogenase, subunit G  |   |   | 1 | 1 |
| <b>MTH1556</b> | 15679552 | tungsten formylmethanofuran dehydrogenase, subunit D  |   |   | 1 | 1 |
| <b>MTH1557</b> | 15679553 | tungsten formylmethanofuran dehydrogenase, subunit A  | 1 | 1 | 1 | 1 |
| <b>MTH1558</b> | 15679554 | tungsten formylmethanofuran dehydrogenase, subunit C  | 1 | 1 | 1 | 1 |
| <b>MTH1559</b> | 15679555 | tungsten formylmethanofuran dehydrogenase, subunit B  | 1 | 1 | 1 | 1 |
| <b>MTH1568</b> | 15679564 | conserved methanogen-specific protein MTH1568 (COG1413)   |   |   |   | 1 |
| <b>MTH1569</b> | 15679565 | repressor nitrogen metabolism (gln, nif) (NrpR)   |   |   |   | 1 |
| <b>MTH1570</b> | 15679566 | glutamine synthetase (EC 6.3.1.2) (Glutamate--ammonia ligase) (GS)  | 1 | 1 | 1 | 1 |
| <b>MTH1571</b> | 15679567 | molybdopterin biosynthesis protein MoeB homolog   |   |   |   | 1 |
| <b>MTH1575</b> | 15679570 | inosine-5'-monophosphate dehydrogenase related protein X containing (2x) signal transduction CBS-domain             |   |   |   | 1 |
| <b>MTH1577</b> | 15679572 | glutaredoxin, NrdH-redoxin (NrdH)   |   |   |   | 1 |
| <b>MTH1580</b> | 15679575 | DNA ligase Cdc9 (EC 6.5.1.1) (ADP-dependent)  |   |   |   | 1 |
| <b>MTH1584</b> | 15679579 | phosphomannomutase/ phosphoglucomutase homolog  |   |   |   | 1 |
| <b>MTH1588</b> | 15679583 | ferrityochelin/ siderophore-binding protein/ transacetylase (COG0663)   |   |   |   | 1 |
| <b>MTH1589</b> | 15679584 | bifunctional acetylating glucosamine-1-phosphate uridylyltransferase  |   |   |   | 1 |
| <b>MTH1591</b> | 15679586 | 2,3-bisphosphoglycerate-independent phosphoglycerate mutase 1   |   |   |   | 1 |
| <b>MTH1593</b> | 15679588 | 30S ribosomal protein S3Ae  | 1 | 1 | 1 | 1 |
| <b>MTH1595</b> | 15679590 | NADP-dependent FMN oxidoreductase/ multimeric flavodoxin (WrbA)   |   |   | 1 | 1 |
| <b>MTH1597</b> | 15679592 | conserved protein (COG1690, UPF0027); RtcB family protein implicated in RNA metabolism                              | 1 | 1 | 1 | 1 |
| <b>MTH1601</b> | 15679596 | phosphoserine aminotransferase (SerC)/ archaeal aspartate aminotransferase (AspC)                                   | 1 | 1 | 1 | 1 |
| <b>MTH1608</b> | 15679603 | signal recognition particle protein SRP54 (SRP alpha, docking protein; ftsY)  |   |   |   | 1 |
| <b>MTH1609</b> | 15679604 | prefoldin subunit alpha (GimC subunit alpha)  |   |   |   | 1 |
| <b>MTH1611</b> | 15679606 | translation initiation factor 6 (EIF6)  |   |   |   | 1 |
| <b>MTH1612</b> | 15679607 | 50S ribosomal protein L31; translation initiation factor 6 (eIF-6)  |   |   |   | 1 |
| <b>MTH1614</b> | 15679609 | predicted subunit tRNA(5-aminomethyl-2-thiouridylate)methyltransferase  |   |   |   | 1 |
| <b>MTH1616</b> | 15679611 | 30S ribosomal protein S19 (S19E)  | 1 | 1 | 1 | 1 |
| <b>MTH1620</b> | 15679615 | thiamine (thiazole) biosynthetic enzyme (Thi4)/ ribulose-1,5-biphosphate synthetase                                 | 1 | 1 |   | 1 |
| <b>MTH1621</b> | 15679616 | GTP-binding protein, GTP1/OBG family; GTPase putatively involved in cell cycle control                              | 1 | 1 |   | 1 |
| <b>MTH1622</b> | 15679617 | conserved protein contain regulatory signal transduction CBS-domain (2x)  |   |   |   | 1 |
| <b>MTH1623</b> | 15679618 | membrane-bound oligosaccharyl transferase STT3 subunit related protein; archaeal oligosaccharide transferase (AglB) |   |   | 1 | 1 |
| <b>MTH1624</b> | 15679619 | DNA topoisomerase I   |   |   |   | 1 |
| <b>MTH1626</b> | 15679621 | phosphoserine phosphatase (SerB) fused with chromosome segregation ATPase smc                                       | 1 | 1 |   | 1 |

|                 |          |  |   |   |   |
|-----------------|----------|--|---|---|---|
| <b>MTH1627</b>  | 15679622 | TATA-binding transcription initiation factor   | 1 | 1 | 1 |
| <b>MTH1629</b>  | 15679624 | adenylate cyclase, class 2 (thermophilic) CyaB (COG1437, PF01928)  | 1 |   |   |
| <b>MTH1630</b>  | 15679625 | 2-isopropylmalate synthase (IeuA) (EC 2.3.3.13); HS-CoB and MFR biosynthesis (AksA)  | 1 |   | 1 |
| <b>MTH1631</b>  | 15679626 | 3-isopropylmalate dehydratase (LeuC) large subunit (EC 4.2.1.33) (Isopropylmalate isomerase); HS-CoB and MFR biosynthesis (AksD)   | 1 |   |   |
| <b>MTH1632</b>  | 15679627 | conserved protein (COG0316, DUF98); chorismate-pyruvate lyase/ beta-ribofuranosylaminobenzene 5'-phosphate synthase family   | 1 |   | 1 |
| <b>MTH1634</b>  | 15679629 | transcriptional control factor (enhancer-binding protein); DNA2/NAM7 helicase family   | 1 |   |   |
| <b>MTH1636</b>  | 15679631 | S-adenosylhomocysteine hydrolase   | 1 |   | 1 |
| <b>MTH1639</b>  | 15679634 | cell division control protein Cdc48 (AAA-ATPase)   | 1 | 1 | 1 |
| <b>MTH1645</b>  | 15679640 | ABC1-type protein kinase (AarF-related)  | 1 |   |   |
| <b>MTH1646</b>  | 15679641 | UDP-N-acetylglucosamine--N-acetylmuramyl-(pentapeptide) pyrophosphoryl-undecaprenol N-acetylglucosamine transferase (Undecaprenyl-PP-MurNAc-pentapeptide-UDPGlcNAc GlcNAc transferase) (N-terminal part) | 1 |   | 1 |
| <b>MTH1647</b>  | 15679642 | UDP-N-acetylglucosamine--N-acetylmuramyl-(pentapeptide) pyrophosphoryl-undecaprenol N-acetylglucosamine transferase (Undecaprenyl-PP-MurNAc-pentapeptide-UDPGlcNAc GlcNAc transferase) (C-terminal part) | 1 |   |   |
| <b>MTH1649</b>  | 15679644 | hydrogenase expression/formation protein HypC (HypC)   | 1 |   |   |
| <b>MTH1657</b>  | 15679652 | indole-3-glycerol phosphate synthase (TrpC)  | 1 |   | 1 |
| <b>MTH1659</b>  | 15679654 | tryptophan synthase, beta subunit 1 (TrpB1)  | 1 |   |   |
| <b>MTH1660</b>  | 15679655 | tryptophan synthase, subunit alpha (TrpA)  | 1 |   |   |
| <b>MTH1664</b>  | 15679658 | conserved protein (COG2151, DUF59); predicted Suf system metal-sulfur cluster biosynthetic enzyme  | 1 |   | 1 |
| <b>MTH1666</b>  | 15679660 | glutamate synthase (NADPH), alpha subunit related protein  | 1 |   |   |
| <b>MTH1669</b>  | 15679663 | transcription initiation factor IIE, alpha subunit   | 1 |   |   |
| <b>MTH1671</b>  | 15679665 | conserved methanogen-specific Fe-S protein (COG2000) related to carbon monoxide dehydrogenase subunit gamma (cdhE)   | 1 |   | 1 |
| <b>MTH1672</b>  | 15679666 | Ni <sup>2+</sup> -binding GTPase involved in regulation of expression and maturation of hydrogenase HypB (COG0378)   | 1 | 1 | 1 |
| <b>MTH1673</b>  | 15679667 | SN-glycerol-3-phosphate transport ATP-binding protein (ugpC)   | 1 | 1 | 1 |
| <b>MTH1674</b>  | 15679668 | (2R)-phospho-3-sulfolactate synthase (ComA)  | 1 |   | 1 |
| <b>MTH1675</b>  | 15679669 | conserved FMN-binding protein (COG1751, DUF1867)   | 1 | 1 | 1 |
| <b>MTH1676</b>  | 15679670 | cell division protein FtsZ   | 1 | 1 | 1 |
| <b>MTH1678</b>  | 15679672 | transcription termination factor NusG  | 1 | 1 | 1 |
| <b>MTH1679</b>  | 15679673 | 50S ribosomal protein L12 (E.coli L11P)  | 1 | 1 | 1 |
| <b>MTH1680</b>  | 15679674 | 50S ribosomal protein L10a (E.coli L1P)  | 1 | 1 | 1 |
| <b>MTH1681</b>  | 15679675 | 50S ribosomal protein Lp0 (E.coli L10) (acidic ribosomal protein P0) homolog (L10E)  | 1 | 1 | 1 |
| <b>MTH1682</b>  | 15679676 | 50S ribosomal protein Lp1;L12P ('A' type)  | 1 | 1 | 1 |
| <b>MTH1683</b>  | 15679677 | alanyl-tRNA synthetase   | 1 | 1 | 1 |
| <b>MTH1686</b>  | 15679680 | fructose-1,6-bisphosphatase  | 1 | 1 | 1 |
| <b>MTH1689</b>  | 15679683 | conserved protein (COG1392, DUF47); phosphate transport regulator (distinct to PhoU)   | 1 |   |   |
| <b>MTH1694</b>  | 15679688 | aspartate aminotransferase related protein   | 1 |   |   |
| <b>MTH1695</b>  | 15679689 | RNase L inhibitor/ ATPase RIL  | 1 | 1 | 1 |
| <b>MTH1696</b>  | 15679690 | histone HMTA2  | 1 |   | 1 |
| <b>MTH1698</b>  | 15679692 | delta 1-pyrroline-5-carboxylate synthetase; aspartate/glutamate/uridylylate kinase (COG2054)   | 1 |   |   |
| <b>MTH1698a</b> | 15679901 | Zn-ribbon RNA-binding protein involved in translation  | 1 |   | 1 |
| <b>MTH1699</b>  | 15679693 | translation elongation factor EF-1b  |   |   | 1 |
| <b>MTH1702</b>  | 15679696 | secretory protein kinase/ type II secretion system protein E   | 1 | 1 | 1 |
| <b>MTH1705</b>  | 15679699 | cobalt transport membrane protein (Cbi )/ predicted nickel transport protein NikQ  | 1 |   |   |
| <b>MTH1707</b>  | 15679701 | cobalamin biosynthesis protein M (CbiM)/ predicted nickel transport protein NikM   | 1 |   |   |
| <b>MTH1708</b>  | 15679702 | acetyl-CoA decarboxylase/synthase complex, alpha subunit (AcsB)  | 1 | 1 | 1 |
| <b>MTH1709</b>  | 15679703 | acetyl-CoA decarboxylase/synthase complex, epsilon subunit (AcsE)  | 1 | 1 |   |
| <b>MTH1710</b>  | 15679704 | acetyl-CoA decarboxylase/synthase complex, beta subunit (AcsA)   | 1 | 1 | 1 |
| <b>MTH1712</b>  | 15679706 | acetyl-CoA decarboxylase/synthase complex, delta subunit (AcsD); corrinoid/iron-sulfur protein, small subunit  | 1 | 1 | 1 |
| <b>MTH1713</b>  | 15679707 | acetyl-CoA decarboxylase/synthase complex, gamma subunit (AcsC); corrinoid/iron-sulfur protein, large subunit  | 1 | 1 | 1 |
| <b>MTH1714</b>  | 15679708 | formate hydrogenlyase, iron-sulfur subunit 2   | 1 |   | 1 |
| <b>MTH1722</b>  | 15679714 | transcriptional regulator 3',5'-cyclic-nucleotide phosphodiesterase (lcc)  | 1 |   |   |

|                |                     |   |   |   |   |   |
|----------------|---------------------|---|---|---|---|---|
|                |                     | related protein   |   |   |   |   |
| <b>MTH1727</b> | 15679719            | periplasmic phosphate-binding protein PstS  | 1 | 1 | 1 | 1 |
| <b>MTH1728</b> | 15679720            | periplasmic phosphate-binding protein PstS homolog  | 1 | 1 | 1 | 1 |
| <b>MTH1729</b> | 15679721            | phosphate transporter permease PstC   |   | 1 |   |   |
| <b>MTH1730</b> | 15679722            | phosphate transporter permease PstC homolog   |   | 1 |   | 1 |
| <b>MTH1731</b> | 15679723            | phosphate transport system ATP-binding  | 1 | 1 | 1 | 1 |
| <b>MTH1732</b> | 15679724            | phosphate transport system regulator  | 1 | 1 |   | 1 |
| <b>MTH1733</b> | 15679725            | conserved archaeal protein MTH1733 (COG1667)  |   | 1 |   | 1 |
| <b>MTH1734</b> | 15679726            | phosphate transport system regulator phoU homolog   | 1 | 1 | 1 | 1 |
| <b>MTH1735</b> | 15679727            | fumarate hydratase, class I (fumA)  |   | 1 |   |   |
| <b>MTH1737</b> | 15679729            | formate hydrogenlyase, iron-sulfur subunit I/ pyruvate oxidoreductase complex subunit   |   | 1 |   | 1 |
| <b>MTH1738</b> | 15679730            | pyruvate oxidoreductase, beta subunit   | 1 |   | 1 |   |
| <b>MTH1739</b> | 15679731            | pyruvate oxidoreductase, alpha subunit  | 1 | 1 | 1 | 1 |
| <b>MTH1740</b> | 15679732            | pyruvate oxidoreductase, gamma + delta subunit  | 1 | 1 | 1 |   |
| <b>MTH1741</b> | 15679733            | methanopterin biosynthesis protein; dihydropteroate synthase  | 1 | 1 |   | 1 |
| <b>MTH1742</b> | 15679734            | conserved protein/ P-loop ATPase involved in RNA modification (thiouridine synthesis)   | 1 | 1 |   |   |
| <b>MTH1745</b> | 15679737            | protein disulfide-isomerase, thioredoxin-related (DsbD/CcdA)/ chaperonine (COG0785)   |   | 1 |   | 1 |
| <b>MTH1752</b> | 15679744            | coenzyme F420-dependent N5,N10-methylene tetrahydromethanopterin reductase  | 1 | 1 | 1 | 1 |
| <b>MTH1757</b> | 5183324<br>15679745 | alpha,alpha-trehalose-phosphate synthase  |   | 1 |   |   |
| <b>MTH1764</b> | 15679752            | sensory transduction regulatory protein (PAS/PAC/GAF domain, cGMP phosphodiesterase)  |   | 1 |   | 1 |
| <b>MTH1767</b> | 15679755            | tyrosyl-tRNA synthetase (TyrRS)   |   | 1 |   | 1 |
| <b>MTH1768</b> | 15679756            | NMD protein affecting ribosome stability and mRNA decay (COG1499)   |   | 1 |   | 1 |
| <b>MTH1769</b> | 15679757            | translation initiation factor eIF-2, beta subunit   |   | 1 |   | 1 |
| <b>MTH1770</b> | 15679758            | DNA replication initiator (Cdc21/Cdc54/minichromosome maintenance), MCM helicase  |   | 1 | 1 | 1 |
| <b>MTH1772</b> | 15679760            | conserved Methanobacteriaceae-specific membrane-spanning protein MTH1772  |   | 1 | 1 | 1 |
| <b>MTH1773</b> | 15679761            | cell division protein J; ribosomal RNA methyltransferase (EC 2.1.1.-) (rRNA (uridine-2'-O-)-methyltransferase)                  | 1 | 1 | 1 |   |
| <b>MTH1774</b> | 15679762            | conserved protein (COG0622, UPF0025)/ predicted phosphoesterase, YfcE   |   | 1 |   |   |
| <b>MTH1777</b> | 15679765            | conserved methanogen-specific protein MTH1777   |   | 1 |   |   |
| <b>MTH1782</b> | 15679770            | uncharacterized membrane-bound protein MTH1782  |   | 1 |   |   |
| <b>MTH1783</b> | 15679771            | uncharacterized proten MTH1783  |   | 1 |   |   |
| <b>MTH1789</b> | 15679777            | dTDP-glucose 4,6-dehydratase RfbB   | 1 |   | 1 |   |
| <b>MTH1790</b> | 15679778            | dTDP-4-dehydrorhamnose 3,5-epimerase RfbC   |   | 1 |   | 1 |
| <b>MTH1791</b> | 15679779            | glucose-1-phosphate thymidyltransferase RfbA  |   | 1 |   | 1 |
| <b>MTH1792</b> | 15679780            | dTDP-4-dehydrorhamnose reductase RfbD   |   | 1 |   |   |
| <b>MTH1798</b> | 15679786            | flavodoxin, fldA (COG0716) C-terminal part  |   | 1 |   |   |
| <b>MTH1799</b> | 15679787            | flavodoxin, fldA (COG0716) N-terminal part  | 1 | 1 |   | 1 |
| <b>MTH1806</b> | 15679794            | phycocyanin alpha phycocyanobilin lyase CpcE related protein; PBS lyase HEAT domain protein repeat-containing protein (COG1413) | 1 | 1 | 1 |   |
| <b>MTH1807</b> | 15679795            | phytoene dehydrogenase/ desaturase  | 1 | 1 |   |   |
| <b>MTH1824</b> | 15679812            | Dps-family bacterioferritin protein (COG1633)/ rubrerythrin   |   | 1 |   | 1 |
| <b>MTH1826</b> | 15679814            | conserved protein with 4Fe-4S ferredoxin domain (COG1633)   |   | 1 |   |   |
| <b>MTH1827</b> | 15679815            | quinolinate synthetase (NadA)   |   | 1 |   | 1 |
| <b>MTH1830</b> | 15679818            | mechanosensitive channel protein MscS   |   | 1 |   |   |
| <b>MTH1833</b> | 15679821            | conserved hypothetical protein MTH1833 (COG1196)  | 1 | 1 | 1 | 1 |
| <b>MTH1834</b> | 15679822            | ZPR1-like zinc finger protein (COG1779)   | 1 | 1 | 1 | 1 |
| <b>MTH1836</b> | 15679824            | conserved protein (COG2018) with regulatory roadblock-LC7 domain  |   | 1 |   | 1 |
| <b>MTH1837</b> | 15679825            | P-loop containing nucleoside triphosphate hydrolase (COG3367, DUF1611), predicted HypB/UreG family                              | 1 |   |   |   |
| <b>MTH1838</b> | 15679826            | conserved Methanobacteriaceae-specific protein MTH1838 (COG2450)  |   | 1 |   | 1 |
| <b>MTH1840</b> | 15679828            | cell division ATPase MinD   | 1 | 1 | 1 | 1 |
| <b>MTH1842</b> | 15679830            | TatD-related protein export protein (COG1099)   |   | 1 |   |   |
| <b>MTH1846</b> | 15679834            | glycyl-tRNA synthetase  | 1 | 1 |   | 1 |
| <b>MTH1847</b> | 15679835            | bifunctional deoxycytidine triphosphate deaminase/dephosphatase   |   | 1 |   | 1 |
| <b>MTH1850</b> | 15679838            | fumarate reductase (frdB); thiol:fumarate reductase subunit B protein   | 1 | 1 | 1 |   |
| <b>MTH1852</b> | 15679840            | indolepyruvate oxidoreductase, alpha subunit (Indolepyruvate ferredoxin oxidoreductase alpha subunit)                           |   | 1 |   |   |
| <b>MTH1854</b> | 15679842            | regulatory subunit (ACT domain family) linked with coenzyme F390 synthetase II  | 1 | 1 | 1 |   |

|                |          |  |   |   |   |
|----------------|----------|--|---|---|---|
| <b>MTH1855</b> | 15679843 | coenzyme F390 synthetase II  | 1 | 1 | 1 |
| <b>MTH1858</b> | 15679846 | phage infection protein homolog/ ABC-2 type transporter, permease (ATP-dependent Na <sup>+</sup> efflux)                           | 1 | 1 | 1 |
| <b>MTH1859</b> | 15679847 | conserved methanogen-specific protein (COG1873) implicated in RNA metabolism   | 1 | 1 | 1 |
| <b>MTH1860</b> | 15679848 | orotate phosphoribosyltransferase (EC 2.4.2.10) (OPRT) (OPRTase); orotidine 5'-monophosphate synthase                              | 1 | 1 | 1 |
| <b>MTH1861</b> | 15679849 | molybdenum cofactor biosynthesis MoaB  | 1 | 1 | 1 |
| <b>MTH1865</b> | 15679853 | predicted methanogen-specific peptidyl-prolyl cis-trans isomerase (UPF0288)  | 1 | 1 |   |
| <b>MTH1866</b> | 15679854 | conserved methanogen-specific protein MTH1866 (COG4029)  |   | 1 |   |
| <b>MTH1867</b> | 15679855 | conserved methanogen-specific protein MTH1867 (COG4048)  |   | 1 | 1 |
| <b>MTH1868</b> | 15679856 | conserved methanogen-specific protein MTH1868 (COG4050)  | 1 | 1 | 1 |
| <b>MTH1869</b> | 15679857 | activator of (R)-2-hydroxyglutaryl-CoA dehydratase; CoA-substrate-specific enzyme activase   | 1 | 1 | 1 |
| <b>MTH1870</b> | 15679858 | conserved methanogen-specific protein MTH1870 (COG4051)  | 1 |   |   |
| <b>MTH1871</b> | 15679859 | nitrogenase iron-molybdenum cofactor biosynthesis protein NifB (NifB) (radical SAM protein)  |   | 1 |   |
| <b>MTH1872</b> | 15679860 | translation initiation factor eIF-2B, alpha subunit  |   | 1 |   |
| <b>MTH1878</b> | 15679866 | CoB--CoM heterodisulfide reductase iron-sulfur subunit C (EC 1.8.98.1)   | 1 | 1 | 1 |
| <b>MTH1879</b> | 15679867 | CoB--CoM heterodisulfide reductase subunit B (EC 1.8.98.1)   | 1 | 1 | 1 |
| <b>MTH1880</b> | 15679868 | conserved methanogen-specific protein (COG4009, DUF749)  |   | 1 | 1 |
| <b>MTH1881</b> | 15679869 | conserved methanogen-specific protein MTH1881 (COG4010)  |   | 1 | 1 |
| <b>MTH1882</b> | 15679870 | conserved protein (COG2191); probable phosphoesterase (ICC related)  | 1 | 1 | 1 |
| <b>MTH1884</b> | 15679872 | conserved protein; signal transduction CBS-domain (2x); cyclic nucleotide-binding domain protein                                   |   | 1 | 1 |
| <b>MTH1894</b> | 15679876 | putative L-threonine-O-3-phosphate decarboxylase, cobalamin biosynthesis protein D (CobD)  |   | 1 |   |
| <b>MTH1900</b> | 15679882 | uncharacterized protein MTH1900  | 1 | 1 | 1 |
| <b>MTH1901</b> | 15679883 | membrane-bound partially conserved protein (COG0810); phosphatidylserine/phosphatidylglycerophosphate/cardiolipin related synthase |   | 1 | 1 |
| <b>MTH1902</b> | 15679884 | conserved protein; Zn-dependent hydrolase (beta lactamase fold) (COG2220, UPF0173))  | 1 | 1 | 1 |
| <b>MTH1903</b> | 15679885 | GTP-binding protein E.coli Ras-family (Era)  | 1 | 1 | 1 |
| <b>MTH1904</b> | 15679886 | conserved archaea-specific protein MTH1904 (COG3365)   |   | 1 |   |
| <b>MTH1907</b> | 15679889 | conserved protein (COG1293, DUF814), predicted RNA-binding protein, eukaryotic snRNP-like protein                                  |   | 1 |   |
| <b>MTH1910</b> | 15679892 | fumarate hydratase, class I related protein, beta subunit  | 1 | 1 | 1 |
| <b>MTH1911</b> | 15679893 | conserved protein MTH1911 (COG0800); TIM barrel protein/ metal-dependent phosphoesterase (PHP family)                              |   | 1 |   |
| <b>MTH1912</b> | 15679894 | conserved Methanobacteriaceae-specific protein MTH1912   |   | 1 | 1 |
| <b>MTH1913</b> | 15679895 | conserved protein MTH1913 (COG1432, DUF88)   | 1 | 1 | 1 |
| <b>MTH1914</b> | 15679896 | pyridoxal phosphate-dependent protein MTH1914 (COG1921, UPF0425)   |   | 1 | 1 |
| <b>MTH1916</b> | 15679898 | biotin acetyl-CoA carboxylase ligase; biotin operon repressor bifunctional protein   |   | 1 |   |
| <b>MTH1917</b> | 15679899 | pyruvate carboxylase subunit A (EC 6.4.1.1) (Pyruvic carboxylase A) (PycA)   | 1 | 1 | 1 |
| <b>MTH1918</b> | 15679900 | protein methyltransferas/ RNA methylase  |   | 1 |   |